MOX-Report No. 36/2026

A nonconforming method for a generalized Darcy-Forchheimer model

Botti, M.; Mascotto, L.; Mosconi, M.

MOX, Dipartimento di Matematica
Politecnico di Milano, Via Bonardi 9 - 20133 Milano (Italy)

mox-dmat@polimi.it https://mox.polimi.it

A nonconforming method for a generalized Darcy–Forchheimer model

Michele Botti[*], Lorenzo Mascotto[†], Marialetizia Mosconi [‡]

Abstract

We analyze a dual mixed nonconforming discretization of a generalized Darcy–Forchheimer model. Compared to the analogous scheme proposed in [23], we consider general, i.e., non-quadratic, Forchheimer nonlinearities; we admit mixed, inhomogeneous boundary conditions; we allow for more general, i.e., with lower Lebesgue regularity, permeability tensors; we construct general-order schemes; we prove convergence to the exact solution under low regularity assumptions, based on novel Sobolev-trace inequalities for broken spaces; we derive error estimates of general-order assuming extra regularity of the exact solution and data; we present numerical results assessing the performance of the proposed schemes for different types of nonlinearity and nonlinear solvers.

AMS subject classification: 76S05; 65N12; 65N30.

Keywords: generalized Darcy–Forchheimer law; Sobolev-trace inequalities; Crouzeix-Raviart elements; high-order schemes.

1 Introduction

State-of-the-art. The Darcy–Forchheimer's law models the fluid flow in porous media [21]. It is a nonlinear extension of Darcy's law and provides a more accurate description of high-velocity flow behaviours. Numerical discretizations of Darcy–Forchheimer equations pose extra theoretical and computational challenges compared to their linear counterpart; as such, they have received increasing attention over the last three decades. In [19], existence and uniqueness are established for a semi-discrete formulation of the standard (quadratic) Darcy–Forchheimer model. Well-posedness of the fully discrete scheme and corresponding error estimates are provided in [26]; see also [28]; more general nonlinearities are considered in [24]. In these works, the problem is formulated in the standard mixed setting, and Raviart-Thomas/piecewise-polynomial pairs are employed. A different approach is undertaken in [23], where a lowest order mixed dual formulation based on piecewise-constant/lowest order Crouzeix-Raviart (CR in what follows) pairs is introduced: convergence to the exact solution of discrete solution sequences under mesh refinements is proved and the analysis of a nonlinear solver is also provided. Numerical results for this scheme are presented in [25]; see also [30] for results concerning the standard mixed formulation. We also mention [35], where, compared to [23], additional stabilization in the normal direction for the fluxes are considered, following ideas from [14] for the linear case. More recent contributions include [2–4, 9, 16, 17, 29, 31, 34, 36, 37].

Goals of the paper. The main objective of this work is to design a general-order dual mixed formulation for a generalized Darcy–Forchheimer problem. The starting point is the work [23] of Girault and Wheeler, which we extend along several directions.

[*]MOX, Department of Mathematics, Politecnico di Milano, 20133 Milano, Italy (michele.botti@polimi.it)

[†]Department of Mathematics and Applications, University of Milano-Bicocca, 20125 Milan, Italy (lorenzo.mascotto@unimib.it); Faculty of Mathematics, University of Vienna, 1090 Vienna, Austria; IMATI-CNR, 27100 Pavia, Italy

[‡]Department of Mathematics and Applications, University of Milano-Bicocca, 20125 Milan, Italy (m.mosconi@campus.unimib.it)

- We consider more general nonlinearities, replacing the quadratic Darcy–Forchheimer nonlinearity with an $(\alpha - 2)$-type law, which boils down to the classical one when $\alpha = 3$; see problem (7) below.
- We admit inhomogeneous, mixed boundary conditions.
- We allow for permeability tensors $\underline{\mathbf{K}}$ with lower Lebesgue regularity; cf. (9) below.
- We introduce a general-order scheme employing piecewise-polynomial spaces of order $p - 1$ for the fluxes and Crouzeix-Raviart spaces of order p for the potentials.
- We prove convergence under low-regularity assumptions on the solution and data, based on novel Sobolev-trace inequalities in broken spaces, with constants independent of the type of discretization spaces (in particular, independent of the polynomial degree in our case).
- We derive general-order error estimates under additional regularity assumptions on the solution and data.
- We present numerical experiments assessing the performance of the scheme for different values of the nonlinearity parameter α and for different nonlinear solvers.

The use of high-order schemes for nonlinear problems may appear counterintuitive, as solutions can exhibit singular behavior even for regular data and smooth domains; our motivation is the prospective development of hp-adaptive strategies, which are particularly well suited for the efficient discretization of such problems. As in [23], we adopt a dual mixed formulation and discretize the potential with nonconforming (Crouzeix-Raviart) elements. Using nonconforming methods in the discretization of more complex nonlinear problems is important, as standard conforming discretization might not converge to the exact solution; cf. [5].

Outline of the remainder of the paper. While in Section 1.1 we set some standard spaces, their properties, and assumptions on the problem domain, Section 2 is devoted to introduce the general nonlinear Darcy–Forchheimer model problem and prove its well-posedness. In Section 3, we introduce admissible sequences of meshes, broken Sobolev spaces, and finite element (piecewise-polynomial and Crouzeix-Raviart) spaces; we also discuss known and novel Sobolev-Poincaré and Sobolev-trace inequalities for functions in piecewise Sobolev spaces. The method is introduced in Section 4; its convergence for low-regularity solution and data is detailed in Section 5, while error estimates under extra regularity assumptions are derived in Section 6. Numerical experiments are given in Section 7, while some conclusions are drawn in Section 8. Appendix A is concerned with the proof of technical results needed for the well-posedness of the continuous problem.

1.1 Functional setting

We consider a domain Ω in $\mathbb{R}^d$, $d = 2, 3$, with boundary Γ, which we split into $\Gamma = \Gamma_{\mathrm{D}} \cup \Gamma_{\mathrm{N}}$. We assume that either

$$\Omega \text{ is star-shaped with respect to a ball } B_{\mathfrak{R}} \text{ of radius } \mathfrak{R} \tag{1}$$

or

$$\Omega \text{ admits a shape-regular decomposition into } \mathfrak{N} \text{ simplices.} \tag{2}$$

These two options are relevant to establish some inequalities in Section 3.2 below, with constants that are explicit with respect to the geometric parameters in (1) and (2). The simplicial subdivision in (2) is not related to the discretization meshes in Section 3.1 below.

The diameter of Ω is h_Ω; $\mathbf{n}_\Omega$ is the outward unit normal vector to Γ. We denote scalars in standard font; vector fields in boldface font; tensors in underlined boldface font. Greek letters in boldface font denote multi-indices in $\mathbb{N}^d$; the lengths are $|\boldsymbol{\beta}| := \sum_{i=1}^d \boldsymbol{\beta}_i$ for $\boldsymbol{\beta}$ in $\mathbb{N}^d$. For a generic subset X of Ω with diameter h_X, and for all p in $[1, \infty)$ and k in $\mathbb{N}$, we consider the Lebesgue and Sobolev spaces $\mathrm{L}^p(X)$ and $\mathrm{W}^{k,p}(X)$, which we endow with norm, and seminorm and norm, respectively,

$$\|v\|_{\mathrm{L}^p(X)}^p := \int_X |v|^p,$$

and

$$|v|_{\mathrm{W}^{k,p}(X)} := \Big(\sum_{|\boldsymbol{\alpha}|=k} \|D^{\boldsymbol{\alpha}} v\|_{\mathrm{L}^p(X)} \Big)^{\frac{1}{p}}, \qquad \|v\|_{\mathrm{W}^{k,p}(X)} := \Big(\sum_{\ell=0}^{k} \big(\mathrm{h}_X^{\ell-k} |v|_{\mathrm{W}^{\ell,p}(X)} \big)^p \Big)^{\frac{1}{p}}.$$

Sobolev spaces of noninteger order are constructed by interpolation. The subspace of functions in $\mathrm{L}^p(X)$ with zero average over X is $\mathrm{L}^p_0(X)$. Sobolev norms and seminorms applied to vector fields are denoted by $\|\cdot\|_{\mathbf{W}^{k,p}(X)}$ and $|\cdot|_{\mathbf{W}^{k,p}(X)}$; Lebesgue norms applied to tensors are denoted by $\|\cdot\|_{\underline{\mathbf{L}}^p(X)}$. We recall the following Sobolev embeddings [20, Sect. 2.3]:

- if $kp < d$, $\mathrm{W}^{k,p}(X) \hookrightarrow \mathrm{L}^q(X)$ for all q in $[p, \frac{pd}{d-kp}]$;
- if $kp = d$, $\mathrm{W}^{k,p}(X) \hookrightarrow \mathrm{L}^q(X)$ for all q in $[p, \infty)$.

We spell out the generic Sobolev embedding bound: for k, p, and q as above, there exists a positive constant C_{Sob} depending on q, k, p, and X, such that

$$\|v\|_{\mathrm{L}^q(X)} \le C_{\mathrm{Sob}}\, \mathrm{h}_X^{\frac{d}{q}-\frac{d}{p}+k} \|v\|_{\mathrm{W}^{k,p}(X)} \qquad \forall v \in \mathrm{W}^{k,p}(X). \tag{3}$$

Given an index p in $[1,\infty)$, we define (with $1 \le p \le p^\sharp \le p^*$)

$$p' := \frac{p}{p-1}; \qquad p^\sharp := \begin{cases} \frac{p(d-1)}{d-p} & \text{if } p < d \\ \infty & \text{otherwise;} \end{cases} \qquad p^* := \begin{cases} \frac{pd}{d-p} & \text{if } p < d \\ \infty & \text{otherwise.} \end{cases} \tag{4}$$

We have the following trace theorem [20, Ch. 3.2]: given $\widetilde{\Gamma}$ a subset of the boundary of X, there exists a positive constant C_{Trc} such that

$$\|v\|_{\mathrm{L}^{p^\sharp}(\widetilde{\Gamma})} \le \|v\|_{\mathrm{L}^{p^\sharp}(\partial X)} \overset{(3)}{\le} C_{\mathrm{Sob}} \|v\|_{\mathrm{W}^{\frac{1}{p'},p}(\partial X)} \le C_{\mathrm{Trc}} \|v\|_{\mathrm{W}^{1,p}(X)} \qquad \forall v \in \mathrm{W}^{1,p}(X). \tag{5}$$

The trace operator is surjective from $\mathrm{W}^{1,p}(X)$ to $\mathrm{W}^{\frac{1}{p'},p}(\Gamma)$. We consider the subspace of functions in $\mathrm{W}^{1,p}(X)$ with trace g in $\mathrm{W}^{\frac{1}{p'},p}(\widetilde{\Gamma})$

$$\mathrm{W}^{1,p}_{\widetilde{\Gamma},g}(X) := \{ v \in \mathrm{W}^{1,p}(X) \mid v_{|\widetilde{\Gamma}} = g \}.$$

A Poincaré-Steklov inequality holds true [20, Ch. 3.3]: there exists a positive constant C_{PS} depending only on p and X such that

$$\|v\|_{\mathrm{L}^p(X)} \le C_{\mathrm{PS}}\, \mathrm{h}_X |v|_{\mathrm{W}^{1,p}(X)} \qquad \forall v \in \begin{cases} \mathrm{W}^{1,p}_{\widetilde{\Gamma}}(X) & \widetilde{\Gamma} \subseteq \partial X \\ \mathrm{W}^{1,p}(X) \cap \mathrm{L}^p_0(\Omega). \end{cases} \tag{6}$$

Inequality (6) holds true also for functions with zero average over a subset of X and/or ∂X with nonzero measure. We denote the Euclidean vector norm by $|\mathbf{v}| = \sqrt{\mathbf{v}^T \cdot \mathbf{v}}$. For generic Banach spaces X and Y, $Y \subset X$, we consider the quotient space X/Y endowed with quotient norm

$$\|x\|_{X/Y} := \inf_{y \in Y} \|x - y\|_X.$$

Moreover, X^* denotes the dual space of X, which we endow with the norm $\|z\|_{X^*} = \sup_{x \in X} \frac{\langle z, x\rangle}{\|x\|_X}$, where $\langle z, x\rangle$ denotes the action of the functional z on the elements x in X.

2 The model problem

Given $\alpha > 2$, $b : \Omega \to \mathbb{R}$, $g_N : \Gamma_N \to \mathbb{R}$, and $g_D : \Gamma_D \to \mathbb{R}$, we consider the generalized Darcy–Forchheimer problem: find a flux $\mathbf{u} : \Omega \to \mathbb{R}^d$ and a potential $\mathrm{p} : \Omega \to \mathbb{R}$ such that

$$\begin{cases} \boldsymbol{\nabla} \mathrm{p} + \frac{\mu}{\rho} \underline{\mathbf{K}}^{-1} \mathbf{u} + \frac{\beta}{\rho} |\mathbf{u}|^{\alpha-2} \mathbf{u} = 0 & \text{in } \Omega \\ \boldsymbol{\nabla} \cdot \mathbf{u} = b & \text{in } \Omega \\ \mathbf{u} \cdot \mathbf{n} = g_N & \text{on } \Gamma_N \\ \mathrm{p} = g_D & \text{on } \Gamma_D. \end{cases} \tag{7}$$

If $\Gamma_N = \Gamma$, then b and g_N must satisfy the compatibility conditions

$$\int_\Omega b \,\mathrm{d}\mathbf{x} = \int_\Gamma g_N \,\mathrm{d}s. \tag{8}$$

The permeability tensor $\underline{\mathbf{K}}^{-1}$ is positive definite; let $\lambda_{\min} > 0$ be its smallest eigenvalue over Ω. The density ρ, the viscosity μ, and the Darcy–Forchheimer coefficient β are positive constants. With the notation as in (4), we assume that

$$\begin{aligned} &\underline{\mathbf{K}}^{-1} \in \underline{\mathbf{L}}^{\frac{\alpha}{\alpha-2}}(\Omega), && b \in \mathcal{B} := \mathrm{L}^{((\alpha')^*)'}(\Omega) = \mathrm{L}^{\frac{\alpha d}{d+\alpha}}(\Omega), \\ &g_N \in \mathcal{G}_N := \mathrm{L}^{((\alpha')^\sharp)'}(\Gamma_N) = \mathrm{L}^{\alpha\frac{d-1}{d}}(\Gamma_N), && g_D \in \mathcal{G}_D := \mathrm{W}^{\frac{1}{\alpha},\alpha'}(\Gamma_D), \end{aligned} \tag{9}$$

and, for a generic g in $\mathcal{G}_D$, we define the spaces

$$\boldsymbol{\mathcal{V}} := \mathbf{L}^\alpha(\Omega), \qquad \mathcal{Q}_g := \begin{cases} \mathrm{W}^{1,\alpha'}(\Omega) \cap \mathrm{L}^2_0(\Omega) & \text{if } \Gamma_N = \Gamma \\ \mathrm{W}^{1,\alpha'}_{\Gamma_D,g}(\Omega) & \text{if } \Gamma_N \neq \Gamma. \end{cases}$$

On the continuous level, we may also take $\mathcal{G}_N$ equal to $[\mathrm{W}^{\frac{1}{\alpha},\alpha'}(\Gamma_N)]^*$; however, this choice would not be fine on the discrete level, since we shall be using nonconforming spaces.

We consider the following variational formulation: find $(\mathbf{u}, \mathrm{p}) \in \boldsymbol{\mathcal{V}} \times \mathcal{Q}_{g_D}$ such that

$$\frac{\mu}{\rho}\int_\Omega (\underline{\mathbf{K}}^{-1})\mathbf{u}\cdot\mathbf{v}\,\mathrm{d}\mathbf{x} + \frac{\beta}{\rho}\int_\Omega |\mathbf{u}|^{\alpha-2}\mathbf{u}\cdot\mathbf{v}\,\mathrm{d}\mathbf{x} + \int_\Omega \boldsymbol{\nabla}\,\mathrm{p}\cdot\mathbf{v}\,\mathrm{d}\mathbf{x} = 0 \qquad \forall\,\mathbf{v}\in\boldsymbol{\mathcal{V}} \tag{10a}$$

$$\int_\Omega \mathbf{u}\cdot\boldsymbol{\nabla}\,\mathrm{q}\,\mathrm{d}\mathbf{x} = -\int_\Omega b\,\mathrm{q}\,\mathrm{d}\mathbf{x} + \int_{\Gamma_N} g_N\,\mathrm{q}\,\mathrm{d}s \qquad \forall\,\mathrm{q}\in\mathcal{Q}_0. \tag{10b}$$

Introduce

$$\boldsymbol{\mathcal{H}} := \{\mathbf{v}\in\boldsymbol{\mathcal{V}} \mid \boldsymbol{\nabla}\cdot\mathbf{v}\in \mathrm{L}^{((\alpha')^*)'}(\Omega)\}$$

and

$$\boldsymbol{\mathcal{D}} := \{\mathbf{v}\in\boldsymbol{\mathcal{H}} \mid \mathbf{v}\cdot\mathbf{n}_{|\Gamma_N} = 0,\ \boldsymbol{\nabla}\cdot\mathbf{v} = 0 \text{ in } \Omega\}. \tag{11}$$

An integration by parts reveals that $\mathbf{v}$ in $\boldsymbol{\mathcal{V}}$ belongs to $\boldsymbol{\mathcal{D}}$ if and only if $\mathbf{v}$ satisfies

$$\int_\Omega \boldsymbol{\nabla}\,\mathrm{q}\cdot\mathbf{v}\,\mathrm{d}\mathbf{x} = 0 \qquad \forall\,\mathrm{q}\in\mathcal{Q}_0. \tag{12}$$

Lemma 2.1. *If $\Gamma_N \neq \Gamma$, for any $\mathfrak{a}$ in $(1,\infty)$ and g in $\mathcal{G}_D$, we have the inf-sup condition*

$$\inf_{\mathrm{q}\in\mathrm{W}^{1,\mathfrak{a}'}_{\Gamma_D,g}(\Omega)}\ \sup_{\mathbf{v}\in\mathbf{L}^{\mathfrak{a}}(\Omega)} \frac{\int_\Omega \mathbf{v}\cdot\boldsymbol{\nabla}\,\mathrm{q}\,\mathrm{d}\mathbf{x}}{\|\boldsymbol{\nabla}\,\mathrm{q}\|_{\mathbf{L}^{\mathfrak{a}'}(\Omega)}\|\mathbf{v}\|_{\mathbf{L}^{\mathfrak{a}}(\Omega)}} = 1. \tag{13}$$

If $\Gamma_N = \Gamma$, then the inf-sup condition holds true by replacing $\mathrm{W}^{1,\mathfrak{a}'}_{\Gamma_D,g}(\Omega)$ with $\mathrm{W}^{1,\mathfrak{a}'}(\Omega)\cap\mathrm{L}^2_0(\Omega)$.

Proof. A duality argument reveals

$$1 = \frac{\|\boldsymbol{\nabla}\,\mathrm{q}\|_{\mathbf{L}^{\mathfrak{a}'}(\Omega)}}{\|\boldsymbol{\nabla}\,\mathrm{q}\|_{\mathbf{L}^{\mathfrak{a}'}(\Omega)}} = \sup_{\mathbf{v}\in\mathbf{L}^{\mathfrak{a}}(\Omega)} \frac{\int_\Omega \mathbf{v}\cdot\boldsymbol{\nabla}\,\mathrm{q}\,\mathrm{d}\mathbf{x}}{\|\boldsymbol{\nabla}\,\mathrm{q}\|_{\mathbf{L}^{\mathfrak{a}'}(\Omega)}\|\mathbf{v}\|_{\mathbf{L}^{\mathfrak{a}}(\Omega)}} \qquad \forall\,\mathrm{q}\in\mathrm{W}^{1,\mathfrak{a}'}_{\Gamma_D,g}(\Omega).$$

Taking the infimum over all q on both sides yields (13). □

Next, we show that there exists solution to (10b) for given b and g_N.

Proposition 2.2. *Given b and g_N as in (9), there exist $\mathbf{u}_\ell$ in $\boldsymbol{\mathcal{V}}/\boldsymbol{\mathcal{D}}$ satisfying*

$$\int_\Omega \mathbf{u}_\ell\cdot\boldsymbol{\nabla}\,\mathrm{q}\,\mathrm{d}\mathbf{x} = -\int_\Omega b\,\mathrm{q}\,\mathrm{d}\mathbf{x} + \int_{\Gamma_N} g_N\,\mathrm{q}\,\mathrm{d}s \qquad \forall\,\mathrm{q}\in\mathcal{Q}_0 \tag{14}$$

and a positive constant C_ℓ only depending on α and Ω such that

$$\|\mathbf{u}_\ell\|_{\mathbf{L}^\alpha(\Omega)} \le C_\ell\big(\|b\|_{\mathrm{L}^{((\alpha')^*)'}(\Omega)} + \|g_N\|_{\mathrm{L}^{((\alpha')^\sharp)'}(\Gamma_N)}\big). \tag{15}$$

Proof. For $\alpha = 3$ and pure Neumann boundary conditions, the proof can be found in [23, Prop. 1]. Here, we consider general $\alpha > 2$ and mixed boundary conditions. We consider two cases.

Case 1: mixed/Dirichlet boundary conditions. Triangle's inequality, Cauchy-Schwarz' inequality, the continuous Sobolev embedding theorem (3), and the continuous trace theorem (5) yield, for a hidden constant only depending on α and Ω,

$$\left| - \int_\Omega b \text{ q } \mathrm{d}\mathbf{x} + \int_{\Gamma_N} g \text{ q } \mathrm{d}s \right| \lesssim \left(\|b\|_{\mathrm{L}^{((\alpha')^*)'}(\Omega)} + \|g_N\|_{\mathrm{L}^{((\alpha')^\sharp)'}(\Gamma_N)} \right) |\mathrm{q}|_{\mathrm{W}^{1,\alpha'}(\Omega)} \qquad \forall\, \mathrm{q} \in \mathcal{Q}_0,$$

i.e., the mapping $\mathrm{q} \to -\int_\Omega b \text{ q } \mathrm{d}\mathbf{x} + \int_{\Gamma_N} g \text{ q } \mathrm{d}s$ belongs to $(\mathcal{Q}_0)^*$. The assertion follows from the inf-sup condition (13).

Case 2: pure Neumann boundary conditions. The compatibility condition (8), triangle's inequality, Cauchy-Schwarz' inequality, the continuous Sobolev embedding theorem (3), the continuous trace theorem (5), and Poincaré-Steklov's inequality yield, for a hidden constant only depending on α and Ω,

$$\begin{aligned}
\left| - \int_\Omega b \text{ q } \mathrm{d}\mathbf{x} + \int_{\Gamma_N} g \text{ q } \mathrm{d}s \right| &\le \inf_{c \in \mathbb{R}} \left(\left| \int_\Omega b\,(\mathrm{q} - c)\,\mathrm{d}\mathbf{x} \right| + \left| \int_{\Gamma_N} g\,(\mathrm{q} - c)\,\mathrm{d}s \right| \right) \\
&\le \left(\|b\|_{\mathrm{L}^{((\alpha')^*)'}(\Omega)} + \|g_N\|_{\mathrm{L}^{((\alpha')^\sharp)'}(\Gamma_N)} \right) \inf_{c \in \mathbb{R}} \left(\|\mathrm{q} - c\|_{\mathrm{L}^{(\alpha')^*}(\Omega)} + \|\mathrm{q} - c\|_{\mathrm{L}^{(\alpha')^\sharp}(\Gamma_N)} \right) \\
&\lesssim \left(\|b\|_{\mathrm{L}^{((\alpha')^*)'}(\Omega)} + \|g_N\|_{\mathrm{L}^{((\alpha')^\sharp)'}(\Gamma_N)} \right) |\mathrm{q}|_{\mathrm{W}^{1,\alpha'}(\Omega)}.
\end{aligned}$$

The mapping $\mathrm{q} \to -\int_\Omega b \text{ q } \mathrm{d}\mathbf{x} + \int_{\Gamma_N} g \text{ q } \mathrm{d}s$ belongs to $(\mathcal{Q}_0)^*$. The assertion follows from the inf-sup condition (13). □

We consider the reduced problem on the kernel $\boldsymbol{\mathcal{D}}$: given $\mathbf{u}_\ell$ as in (14), find $\mathbf{u}_0$ in $\boldsymbol{\mathcal{D}}$ such that

$$\frac{\mu}{\rho} \int_\Omega (\underline{\mathbf{K}}^{-1})(\mathbf{u}_0 + \mathbf{u}_\ell) \cdot \mathbf{v}\,\mathrm{d}\mathbf{x} + \frac{\beta}{\rho} \int_\Omega |\mathbf{u}_0 + \mathbf{u}_\ell|^{\alpha-2}((\mathbf{u}_0 + \mathbf{u}_\ell) \cdot \mathbf{v})\,\mathrm{d}\mathbf{x} = 0 \qquad \forall \mathbf{v} \in \boldsymbol{\mathcal{D}}. \tag{16}$$

We denote by $\boldsymbol{\mathcal{A}}(\cdot) : \mathbf{L}^\alpha(\Omega) \to \mathbf{L}^{\alpha'}(\Omega)$ the mapping

$$\boldsymbol{\mathcal{A}}(\mathbf{v}) := \frac{\mu}{\rho} \underline{\mathbf{K}}^{-1} \mathbf{v} + \frac{\beta}{\rho} |\mathbf{v}|^{\alpha-2} \mathbf{v}. \tag{17}$$

Since

$$\begin{aligned}
\left\| |\mathbf{v}|^{\alpha-2} \mathbf{v} \right\|_{\mathbf{L}^{\alpha'}(\Omega)} &= \left(\int_\Omega ||\mathbf{v}|^{\alpha-2} \mathbf{v}|^{\alpha'}\,\mathrm{d}\mathbf{x} \right)^{\frac{1}{\alpha'}} \\
&= \left(\int_\Omega |\mathbf{v}|^{(\alpha-1)\alpha'}\,\mathrm{d}\mathbf{x} \right)^{\frac{1}{\alpha'}} = \left(\int_\Omega |\mathbf{v}|^{\alpha}\,\mathrm{d}\mathbf{x} \right)^{\frac{\alpha-1}{\alpha}} = \|\mathbf{v}\|^{\alpha-1}_{\mathbf{L}^\alpha(\Omega)},
\end{aligned}$$

we have

$$\|\boldsymbol{\mathcal{A}}(\mathbf{v})\|_{\mathbf{L}^{\alpha'}(\Omega)} \le \left[\frac{\mu}{\rho} \|\underline{\mathbf{K}}^{-1}\|_{\underline{\mathbf{L}}^{\frac{\alpha}{\alpha-2}}(\Omega)} + \frac{\beta}{\rho} \right] \|\mathbf{v}\|^{\alpha-1}_{\mathbf{L}^\alpha(\Omega)} \tag{18}$$

The following result extends [23, Prop. 2] from $\alpha = 3$ to $\alpha > 2$ and mixed boundary conditions. The proof is omitted for brevity and is essentially based on the inf-sup condition (13).

Proposition 2.3. *The solution* $\mathbf{u} = \mathbf{u}_0 + \mathbf{u}_\ell$ *to* (16) *is also solution to* (10) *and vice-versa. Moreover, given* $\mathbf{u}$ *solution to* (16)*, there exists a unique* p *in* $\mathcal{Q}_{g_D}$ *solution to* (10b)*, i.e.,*

$$\boldsymbol{\mathcal{A}}(\mathbf{u}) = \boldsymbol{\nabla}\,\mathrm{p}\,. \tag{19}$$

We now show an algebraic inequality involving $\boldsymbol{\mathcal{A}}(\cdot)$.

Lemma 2.4. *For all* $\mathbf{v}$ *and* $\mathbf{w}$ *in* $\boldsymbol{\mathcal{V}}$*, the following inequality holds true: there exists a positive constant* $\mathrm{C_{BL}}$ *depending on* α *such that*

$$|\boldsymbol{\mathcal{A}}(\mathbf{v}) - \boldsymbol{\mathcal{A}}(\mathbf{w})| \le \frac{\mu}{\rho} |\underline{\mathbf{K}}^{-1}|\; |\mathbf{v} - \mathbf{w}| + \mathrm{C_{BL}} \frac{\beta}{\rho} |\mathbf{v} - \mathbf{w}| (|\mathbf{v}|^{\alpha-2} + |\mathbf{w}|^{\alpha-2}) \qquad \forall \alpha > 2. \tag{20}$$

Proof. Triangle's inequality yields

$$|\boldsymbol{\mathcal{A}}(\mathbf{v}) - \boldsymbol{\mathcal{A}}(\mathbf{w})| \le \frac{\mu}{\rho}|\underline{\mathbf{K}}^{-1}|\ |\mathbf{v}-\mathbf{w}| + \frac{\beta}{\rho}\big||\mathbf{v}|^{\alpha-2}\mathbf{v} - |\mathbf{w}|^{\alpha-2}\mathbf{w}\big|.$$

Using [7, Lemma 2.1], there exists a positive constant $\mathrm{C_{BL}}$ such that

$$\big||\mathbf{v}|^{\alpha-2}\mathbf{v} - |\mathbf{w}|^{\alpha-2}\mathbf{w}\big| \le \mathrm{C_{BL}}\,|\mathbf{v}-\mathbf{w}|\left(|\mathbf{v}|^{\alpha-2} + |\mathbf{w}|^{\alpha-2}\right).$$

The assertion follows combining the two bounds above. □

Based on [23, Sect. 2], in order to show the well-posedness of (16), it suffices to prove the following three properties of $\boldsymbol{\mathcal{A}}(\cdot)$:

1. monotonicity, i.e., recalling that $\lambda_{\min}$ is the smallest eigenvalue of $\underline{\mathbf{K}}^{-1}$, we have

$$\frac{\mu}{\rho}\lambda_{\min}\|\mathbf{w}-\mathbf{v}\|^2_{\mathbf{L}^2(\Omega)} \le \int_\Omega (\boldsymbol{\mathcal{A}}(\mathbf{w}+\mathbf{y}) - \boldsymbol{\mathcal{A}}(\mathbf{v}+\mathbf{y}))\cdot(\mathbf{w}-\mathbf{v})\,\mathrm{d}\mathbf{x} \qquad \forall\, \mathbf{y},\mathbf{v},\mathbf{w} \in \boldsymbol{\mathcal{V}}; \tag{21a}$$

2. coercivity, i.e., we have

$$\lim_{\|\mathbf{v}\|_{\mathbf{L}^\alpha(\Omega)}\to+\infty}\Big(\frac{1}{\|\mathbf{v}\|_{\mathbf{L}^\alpha(\Omega)}}\int_\Omega \boldsymbol{\mathcal{A}}(\mathbf{v}+\mathbf{y})\cdot\mathbf{v}\Big) = +\infty \qquad \forall \mathbf{y}\in\boldsymbol{\mathcal{V}}; \tag{21b}$$

3. hemi-continuity, i.e., given $\mathbf{y}$, $\mathbf{v}$, and $\mathbf{w}$ in $\boldsymbol{\mathcal{V}}$, the mapping

$$t \to \int_\Omega \boldsymbol{\mathcal{A}}(\mathbf{y}+\mathbf{v}+t\,\mathbf{w})\cdot\mathbf{w}\,\mathrm{d}\mathbf{x} \tag{21c}$$

is continuous from $\mathbb{R}$ into $\mathbb{R}$.

The proofs of these properties are postponed to Appendix A. We are in a position to show the well-posedness of (16) and hence, due to Proposition 2.3, of (10).

Proposition 2.5. *Given b and g_N as in* (9)*, problem* (10) *admits a unique solution* $(\mathbf{u},\mathrm{p})$ *in* $\boldsymbol{\mathcal{V}}\times\mathcal{Q}_{g_D}$*. Moreover, given C_ℓ as in* (15)*, we have*

$$\|\mathbf{u}\|_{\mathbf{L}^\alpha(\Omega)} \le \Big(\frac{2^{\alpha'}(\alpha-1)\mu^{\alpha'}}{\beta^{\alpha'}}\|\underline{\mathbf{K}}^{-1}\|^{\alpha'-1}_{\underline{\mathbf{L}}^{\frac{\alpha}{\alpha-2}}} + 2\Big)^{\frac{1}{\alpha}} C_\ell^{\alpha'-1}\big(\|b\|_{\mathrm{L}((\alpha')^*)'(\Omega)} + \|g_N\|_{\mathrm{L}((\alpha')^\sharp)'(\Gamma_N)}\big)^{\alpha'-1} \tag{22a}$$

and

$$\begin{aligned}\|\boldsymbol{\nabla}\mathrm{p}\|_{\mathbf{L}^{\alpha'}(\Omega)} \le \Big(\frac{\mu}{\rho}\|\underline{\mathbf{K}}^{-1}\|_{\underline{\mathbf{L}}^{\frac{\alpha}{\alpha-2}}(\Omega)} + \frac{\beta}{\rho}\Big)\Big(\frac{2^{\alpha'}(\alpha-1)\mu^{\alpha'}}{\beta^{\alpha'}}\|\underline{\mathbf{K}}^{-1}\|^{\alpha'-1}_{\underline{\mathbf{L}}^{\frac{\alpha}{\alpha-2}}} + 2\Big)^{\frac{1}{\alpha'}}\cdot \\ \cdot\, C_\ell\big(\|b\|_{\mathrm{L}((\alpha')^*)'(\Omega)} + \|g_N\|_{\mathrm{L}((\alpha')^\sharp)'(\Gamma_N)}\big).\end{aligned} \tag{22b}$$

Proof. Based on [32, Chapt. I], properties (21a), (21b), and (21c) yield the existence and uniqueness of a solution $\mathbf{u}$ to (16). Proposition 2.3 yields the existence and uniqueness of p solution to (10). As in Proposition 2.3, we split $\mathbf{u}$ as $\mathbf{u}_0+\mathbf{u}_\ell$. Since $\mathbf{u}_0$ belongs to $\boldsymbol{\mathcal{D}}$, we have

$$0 \overset{(12)}{=} \int_\Omega \boldsymbol{\nabla}\mathrm{p}\cdot\mathbf{u}_0 \overset{(19)}{=} \int_\Omega \boldsymbol{\mathcal{A}}(\mathbf{u})\cdot\mathbf{u}_0\,\mathrm{d}\mathbf{x}.$$

Estimates (103) with $\widetilde{\mathbf{v}}$ equal to $\mathbf{u}$, and (105) with $\widetilde{\mathbf{v}}$ and $\mathbf{y}$ equal to $\mathbf{u}$ and $\mathbf{u}_\ell$ entail

$$\begin{aligned}0 = \int_\Omega \boldsymbol{\mathcal{A}}(\mathbf{u})\cdot\mathbf{u}\,\mathrm{d}\mathbf{x} - \int_\Omega \boldsymbol{\mathcal{A}}(\mathbf{u})\cdot\mathbf{u}_\ell\,\mathrm{d}\mathbf{x} \ge \frac{\mu}{\rho}\lambda_{\min}\|\mathbf{u}\|^2_{\mathbf{L}^2(\Omega)} + \frac{\beta}{\rho}\|\mathbf{u}\|^\alpha_{\mathbf{L}^\alpha(\Omega)} \\ - \frac{\mu}{\rho}\|\underline{\mathbf{K}}^{-1}\|_{\underline{\mathbf{L}}^{\frac{\alpha}{\alpha-2}}(\Omega)}\|\mathbf{u}\|_{\mathbf{L}^\alpha(\Omega)}\|\mathbf{u}_\ell\|_{\mathbf{L}^\alpha(\Omega)} - \frac{\beta}{\rho}\|\mathbf{u}\|^{\alpha-1}_{\mathbf{L}^\alpha(\Omega)}\|\mathbf{u}_\ell\|_{\mathbf{L}^\alpha(\Omega)}.\end{aligned}$$

Applying Young's inequality twice gives

$$\frac{\mu}{\rho}\lambda_{\min}\|\mathbf{u}\|^2_{\mathbf{L}^2(\Omega)} + \frac{\beta}{\rho}\|\mathbf{u}\|^\alpha_{\mathbf{L}^\alpha(\Omega)} \le \frac{\mu}{\rho}\big\|\underline{\mathbf{K}}^{-1}\big\|_{\underline{\mathbf{L}}^{\frac{\alpha}{\alpha-2}}(\Omega)}\Big(\frac{\varepsilon}{\alpha}\|\mathbf{u}\|^\alpha_{\mathbf{L}^\alpha(\Omega)} + \frac{1}{\varepsilon^{\alpha'-1}\alpha'}\|\mathbf{u}_\ell\|^{\alpha'}_{\mathbf{L}^\alpha(\Omega)}\Big) + \frac{\beta}{\rho}\left(\frac{1}{\alpha'}\|\mathbf{u}\|^\alpha_{\mathbf{L}^\alpha(\Omega)} + \frac{1}{\alpha}\|\mathbf{u}_\ell\|^\alpha_{\mathbf{L}^\alpha(\Omega)}\right),$$

whence

$$\Big(\frac{\beta}{\rho} - \frac{\beta}{\alpha'\rho} - \frac{\varepsilon\mu}{\alpha\rho}\big\|\underline{\mathbf{K}}^{-1}\big\|_{\underline{\mathbf{L}}^{\frac{\alpha}{\alpha-2}}}\Big)\|\mathbf{u}\|^\alpha_{\mathbf{L}^\alpha(\Omega)} = \frac{1}{\alpha}\Big(\frac{\beta}{\rho} - \frac{\varepsilon\mu}{\rho}\big\|\underline{\mathbf{K}}^{-1}\big\|_{\underline{\mathbf{L}}^{\frac{\alpha}{\alpha-2}}}\Big)\|\mathbf{u}\|^\alpha_{\mathbf{L}^\alpha(\Omega)}$$
$$\le -\frac{\mu}{\rho}\lambda_{\min}\|\mathbf{u}\|^2_{\mathbf{L}^2(\Omega)} + \frac{\mu}{\varepsilon^{\alpha'-1}}\alpha'\rho\big\|\underline{\mathbf{K}}^{-1}\big\|_{\underline{\mathbf{L}}^{\frac{\alpha}{\alpha-2}}(\Omega)}\|\mathbf{u}_\ell\|^{\alpha'}_{\mathbf{L}^\alpha(\Omega)} + \frac{\beta}{\alpha\rho}\|\mathbf{u}_\ell\|^\alpha_{\mathbf{L}^\alpha(\Omega)}.$$

Estimate (22a) follows from applying (15) and taking

$$\varepsilon = \frac{\beta}{2\mu}\big\|\underline{\mathbf{K}}^{-1}\big\|^{-1}_{\underline{\mathbf{L}}^{\frac{\alpha}{\alpha-2}}(\Omega)}.$$

Estimate (22b) follows from combining (19), (18), and (22a).

□

3 Finite element spaces and functional inequalities

This section is devoted to introduce the basic setting for a nonconforming discretization of problem (10). More precisely, sequences of regular meshes, and corresponding broken Sobolev and finite element spaces are introduced in Section 3.1; important inequalities (Poincaré- and trace-type) for broken Sobolev and Crouzeix-Raviart spaces are exhibited in Section 3.2. While the tools developed in Section 3.2 below remain valid in arbitrary dimension, henceforth we fix $d = 2$. This choice allows us to characterize the Crouzeix-Raviart space in (26) in two equivalent ways; see Section 3.1 below for more details.

3.1 Meshes, and broken Sobolev and finite element spaces

Meshes. We consider mesh sequences $\{\mathcal{T}_h\}$, where each $\mathcal{T}_h$ is a finite collection of disjoint, closed, simplicial elements such that $\overline{\Omega} = \bigcup_{K\in\mathcal{T}_h} K$. For each K in $\mathcal{T}_h$, ∂K, h_K, and $\mathfrak{R}_K$ denote the boundary of, the diameter of, and the radius of the largest ball contained in K, respectively. We assume that the sequence of meshes is shape-regular, i.e., there exists a positive constant γ such that $h_K \le \gamma\mathfrak{R}_K$ for all K in $\mathcal{T}_h$, for all meshes $\mathcal{T}_h$. The piecewise L^2-projector $\Pi_s^{0,\mathcal{T}_h}$ onto the space of polynomials of order s, s in $\mathbb{N}$, is given by

$$\int_K \Pi_s^{0,\mathcal{T}_h} v\, q_s\,\mathrm{d}\mathbf{x} := \int_K v\, q_s\,\mathrm{d}\mathbf{x} \qquad \forall v \in L^2(\Omega), \quad \forall q_s \in P_s(K), \quad \forall K \in \mathcal{T}_h; \tag{23}$$

the vector version of this projection operator is $\boldsymbol{\Pi}_s^{0,\mathcal{T}_h}$.

We associate each $\mathcal{T}_h$ with the set $\mathcal{F}_h$ of facets. With each facet F in $\mathcal{F}_h$, we associate its diameter h_F and a unit normal vector $\mathbf{n}_F$, and

- either there exist distinct $K_{1,F}$ and $K_{2,F}$ in $\mathcal{T}_h$ such that $F = \partial K_{1,F} \cap \partial K_{2,F}$ and F is called an *internal facet*,
- or there exists K_F in $\mathcal{T}_h$ such that $F \subseteq \partial K_F \cap \Gamma$ and F is called a *boundary facet*.

Interfaces and boundary facets are collected in the subsets $\mathcal{F}_h^I$ and $\mathcal{F}_h^B$, respectively; we assume that it is possible to split the boundary facets into Dirichlet $\mathcal{F}_h^D$ and Neumann $\mathcal{F}_h^N$ boundary facets, i.e., F is in $\mathcal{F}_h^D$ if it belongs to $\mathcal{F}_h^B$ and F is contained in Γ_D (similar for the Neumann case); we also introduce $\mathcal{F}_h^{ID} := \mathcal{F}_h^I \cup \mathcal{F}_h^D$ and $\mathcal{F}_h^{IN} := \mathcal{F}_h^I \cup \mathcal{F}_h^N$. The set of facets of an element K

is $\mathcal{F}^K$; we also define $\mathcal{F}^{KD} := \mathcal{F}^K \cap \mathcal{F}_{\mathrm{h}}^D$ and $\mathcal{F}^{KI} := \mathcal{F}^K \cap \mathcal{F}_{\mathrm{h}}^I$. For F in $\mathcal{F}_{\mathrm{h}}$, we define the facet patches

$$\omega_F := \bigcup \{K \in \mathcal{T}_{\mathrm{h}} \mid F \in \mathcal{F}^K\}.$$

The piecewise L^2-projector $\Pi_s^{0,\mathcal{F}_{\mathrm{h}}}$ onto the space of facet polynomials of order s, s in $\mathbb{N}$, reads

$$\int_F \Pi_s^{0,\mathcal{F}_{\mathrm{h}}} v \; q_s \,\mathrm{d}s := \int_F v \; q_s \,\mathrm{d}s \qquad \forall v \in \mathrm{W}^{1,1}(\Omega), \quad \forall q_s \in \mathrm{P}_s(F) \quad \forall F \in \mathcal{F}_{\mathrm{h}};$$

the vector version of this projection operator is $\boldsymbol{\Pi}_s^{0,\mathcal{F}_{\mathrm{h}}}$.

We associate each $\mathcal{T}_{\mathrm{h}}$ with the set of its vertices $\mathcal{V}_{\mathrm{h}}$; the set of vertices of a given element K is $\mathcal{V}^K$. The vertices of K are denoted by $\nu_{i,K}$, $i = 1, 2, 3$, and the corresponding barycentric coordinates by $\lambda_{K,i}$; when convenient, we shall replace $\lambda_{K,i}$ with $\lambda_{K,F}$ where F is the facet opposite to the i-th vertex and we shall omit the subscript K when no confusion occurs.

Consider now an element K in $\mathcal{T}_{\mathrm{h}}$. A local continuous trace inequality holds true [11, Corollary 1.3]: if p is in $[1, d)$, there exists a positive constant $C_{\mathrm{TR}}^\sharp$ depending only on p and γ such that

$$\|v\|_{\mathrm{L}^{p^\sharp}(\partial K)} \leq C_{\mathrm{TR}}^\sharp \big(\|v\|_{\mathrm{L}^{p^*}(K)} + \|\boldsymbol{\nabla} v\|_{\mathbf{L}^p(K)} \big). \tag{24}$$

Broken Sobolev spaces. For p larger than or equal to 1, we define

$$\mathrm{W}^{1,p}(\mathcal{T}_{\mathrm{h}}) := \left\{ u \in \mathrm{L}^p(\Omega) \;\middle|\; u_{|K} \in \mathrm{W}^{1,p}(K) \qquad \forall K \in \mathcal{T}_{\mathrm{h}} \right\}.$$

For every v in $\mathrm{W}^{1,p}(\mathcal{T}_{\mathrm{h}})$ and F in $\mathcal{F}_{\mathrm{h}}$, the jump operator on F is well-defined thanks to the trace theorem and is given by

$$[\![v]\!]_F := \begin{cases} v_{|K_{1,F}} \mathbf{n}_{K_{1,F}} \cdot \mathbf{n}_F + v_{|K_{2,F}} \mathbf{n}_{K_{2,F}} \cdot \mathbf{n}_F & \text{if } F \subset \mathcal{F}_{\mathrm{h}}^I, \ F = \partial K_{1,F} \cap \partial K_{2,F} \\ v_{|F} \mathbf{n}_{K_F} \cdot \mathbf{n}_\Omega & \text{if } F \in \mathcal{F}_{\mathrm{h}}^B, \ F \subset \partial K_F \cap \Gamma. \end{cases}$$

We further define the normal jump operator on F of a vector field $\mathbf{v}$ in $\mathbf{W}^{1,p}(\mathcal{T}_{\mathrm{h}})$ as

$$[\![\mathbf{v}]\!]_{F,\mathbf{n}} := \begin{cases} \mathbf{v}_{|K_{1,F}} \cdot \mathbf{n}_{K_{1,F}} + \mathbf{v}_{|K_{2,F}} \cdot \mathbf{n}_{K_{2,F}} & \text{if } F \subset \mathcal{F}_{\mathrm{h}}^I, \ F = \partial K_{1,F} \cap \partial K_{2,F} \\ \mathbf{v}_{|F} \cdot \mathbf{n}_{K_F} & \text{if } F \in \mathcal{F}_{\mathrm{h}}^B, \ F \subset \partial K_F \cap \Gamma. \end{cases}$$

We omit the subscript F whenever it is clear from the context. For k in $\mathbb{N}$, we introduce

$$\mathrm{W}_k^{1,p}(\mathcal{T}_{\mathrm{h}}) := \left\{ v \in \mathrm{W}^{1,p}(\mathcal{T}_{\mathrm{h}}) \,\middle|\, ([\![v]\!], q_{k-1}^F)_{0,F} = 0 \quad \forall q_{k-1}^F \in \mathrm{P}_{k-1}(F), \forall F \in \mathcal{F}_{\mathrm{h}}^I \right\},$$

and, for v_D in $\mathrm{L}^1(\widetilde{\Gamma})$, $\widetilde{\Gamma} \subseteq \Gamma$ such that each F in $\mathcal{F}_{\mathrm{h}}^B$ is either fully contained in $\widetilde{\Gamma}$ or not,

$$\mathrm{W}_{k,v_D}^{1,p}(\mathcal{T}_{\mathrm{h}}, \widetilde{\Gamma}) := \Big\{ v \in \mathrm{W}_k^{1,p}(\mathcal{T}_{\mathrm{h}}) \,\Big|\, ([\![v]\!] - v_D, q_{k-1}^F)_{0,F} = 0 \qquad \forall q_{k-1}^F \in \mathrm{P}_{k-1}(F), \forall F \in \mathcal{F}_{\mathrm{h}}^B \text{ with } F \subset \widetilde{\Gamma} \Big\}.$$

Vector valued and tensor valued broken Sobolev spaces are denoted using the boldface and underlined-boldface fonts, respectively.

Finite element spaces. We denote the space of polynomials of order smaller than or equal to a nonnegative integer k over an element K and an edge F by $\mathrm{P}_k(K)$ and $\mathrm{P}_k(F)$, respectively. If k is a negative integer, we set $\mathrm{P}_k(K) = \mathrm{P}_k(F) = \emptyset$. We introduce the Lagrangian finite element space of order k:

$$\mathcal{L}_k(\mathcal{T}_{\mathrm{h}}) := \{ \mathrm{q_h} \in \mathcal{C}^0(\overline{\Omega}) \mid \mathrm{q_h}_{|K} \in \mathrm{P}_k(K) \quad \forall K \in \mathcal{T}_{\mathrm{h}} \}.$$

Given an element K in $\mathcal{T}_{\mathrm{h}}$, basis functions of each local space can be split into

- vertex basis functions denoted by $\{\varphi^{\nu_i}\}_{i=1}^3$; (25a)
- facet modal basis functions associated with each facet F of $\mathcal{F}^K$, denoted by $\{\varphi_j^F\}_{j=1}^{k-1}$; (25b)
- bulk modal basis functions denoted by $\{\varphi_\ell^K\}_{\ell=1}^{(k-1)(k-2)/2}$. (25c)

We introduce the piecewise-polynomial space of order k

$$\mathrm{P}_k(\mathcal{T}_\mathrm{h}) := \left\{ q_k \in \mathrm{L}^2(\Omega) \,\middle|\, q_{k|K} \in \mathrm{P}_k(K) \quad \forall K \in \mathcal{T}_\mathrm{h} \right\};$$

vector valued piecewise-polynomial spaces are denoted by $\mathbf{P}_k(\mathcal{T}_\mathrm{h})$. Given g in $\mathcal{G}_D$, we further define the Crouzeix-Raviart (CR) spaces [18, 27]

$$\mathrm{CR}_k(\mathcal{T}_\mathrm{h}) := \{\mathrm{q_h} \in \mathrm{P}_k(\mathcal{T}_\mathrm{h}) \,|\, (\llbracket \mathrm{q_h} \rrbracket, q^F_{k-1})_{0,F} = 0 \quad \forall q^F_{k-1} \in \mathrm{P}_{k-1}(F), \forall F \in \mathcal{F}^I_\mathrm{h}\}, \tag{26a}$$

$$\mathrm{CR}_{k,g}(\mathcal{T}_\mathrm{h}, \mathcal{F}^D_\mathrm{h}) := \{\mathrm{q_h} \in \mathrm{CR}_k(\mathcal{T}_\mathrm{h}) \,|\, (\llbracket \mathrm{q_h} \rrbracket - g, q^F_{k-1})_{0,F} = 0 \; \forall q^F_{k-1} \in \mathrm{P}_{k-1}(F), \forall F \in \mathcal{F}^D_\mathrm{h}\}. \tag{26b}$$

We have the inclusions

$$\mathrm{CR}_k(\mathcal{T}_\mathrm{h}) \subset \mathrm{W}^{1,p}_k(\mathcal{T}_\mathrm{h}), \qquad \mathrm{CR}_{k,g}(\mathcal{T}_\mathrm{h}, \mathcal{F}^D_\mathrm{h}) \subset \mathrm{W}^{1,p}_{k,g}(\mathcal{T}_\mathrm{h}, \Gamma_D).$$

Next, we introduce a basis for the Crouzeix-Raviart spaces. We denote the univariate Legendre polynomials of degree k over $\hat{I} := [-1,1]$ by $\widehat{S}_k(\cdot)$. With each facet F in $\mathcal{F}_\mathrm{h}$, we associate the facet nonconforming bubble function [15, Def. 3.2] (which is extended by zero outside ω_F)

$$b^F_k := \begin{cases} \widehat{S}_k\,(1 - 2\lambda_{K,F}) & \forall K \in \mathcal{T}_\mathrm{h},\ K \subset \omega_F \\ 0 & \text{otherwise.} \end{cases} \tag{27}$$

We first detail a set of unisolvent degrees of freedom for the **odd degree** Crouzeix-Raviart spaces $\mathrm{CR}_{k,g}(\mathcal{T}_\mathrm{h}, \mathcal{F}^D_\mathrm{h})$. Given an element K, consider for all F in $\mathcal{F}^K$ the mapped Legendre polynomials S^F_j on F, j non-negative integer, and a basis $\{m^K_{\boldsymbol{\beta}}\}^{k-3}_{|\boldsymbol{\beta}|=0}$ of $\mathrm{P}_{k-3}(K)$ consisting of elements such that $\left\| m^K_{\boldsymbol{\beta}} \right\|_{\mathrm{L}^\infty(\Omega)} = 1$. We introduce a set of linear functionals: given v in $\mathrm{W}^{1,1}(\Omega)$,

$$|F|^{-1} \int_F v\, S^F_j \,\mathrm{d}s \qquad \forall j = 0, \dots, k-1, \quad \forall F \in \mathcal{F}^{IN}_\mathrm{h}; \tag{28a}$$

$$|K|^{-1} \int_K v\, m^K_{\boldsymbol{\beta}} \,\mathrm{d}\mathbf{x} \qquad \forall |\boldsymbol{\beta}| = 0, \dots, k-3, \quad \forall K \in \mathcal{T}_\mathrm{h}. \tag{28b}$$

The functionals in (28) are a set of unisolvent degrees of freedom (DoFs) for $\mathrm{CR}_{k,g}(\mathcal{T}_\mathrm{h}, \mathcal{F}^D_\mathrm{h})$; see, e.g., [1, Lemma 2.1].

We detail next a set of unisolvent degrees of freedom for **even degree** Crouzeix-Raviart spaces. With each element K in $\mathcal{T}_\mathrm{h}$, we associate the bulk nonconforming bubble function [33, Rem. 2] (which is extended by zero outside K)

$$b^K_k := \begin{cases} \frac{1}{2}(-1 + \sum_{i=1}^3 \widehat{S}_k(1 - 2\lambda_i)) & \text{on } K \\ 0 & \text{otherwise,} \end{cases} \tag{29}$$

and we consider the linear functionals

$$|K|^{-1} \int_K v\, b^K_k \,\mathrm{d}s. \tag{30}$$

The functionals in (28) and (30) are a set of unisolvent DoFs for $\mathrm{CR}_{k,g}(\mathcal{T}_\mathrm{h}, \mathcal{F}^D_\mathrm{h})$ if and only if, cf. [1, Lemma 2.2], v satisfies the compatibility condition

$$\sum_{F \in \partial K} \int_F v \sum_{\substack{1 \le j \le k-1 \\ j \text{ odd}}} \frac{S^F_j}{\left\| S^F_j \right\|^2_{\mathrm{L}^2(F)}} \,\mathrm{d}s = 0 \qquad \forall K \in \mathcal{T}_\mathrm{h}.$$

The Crouzeix-Raviart spaces in (26) are spanned by modal and nonconforming bubble functions [6]. This characterization depends on the order of the scheme:

- *odd order* Crouzeix-Raviart elements are spanned by the modal functions (25b) and (25c) and the facet nonconforming bubbles (27), i.e.,

$$\mathrm{CR}_k(\mathcal{T}_\mathrm{h}) = \mathrm{span}\left(b^F_k \text{ and } \{\varphi^F_j\}^{k-1}_{j=1} \quad \forall F \subset \mathcal{F}_\mathrm{h}; \quad \{\varphi^K_\ell\}^{(k-1)(k-2)/2}_{\ell=1} \quad \forall K \in \mathcal{T}_\mathrm{h} \right); \tag{31}$$

- *even degree* Crouzeix-Raviart elements are spanned by the modal functions (25) and the bulk nonconforming bubbles, i.e.,

$$\mathrm{CR}_k(\mathcal{T}_\mathrm{h}) = \mathrm{span}\Big(\varphi^\nu\ \forall\nu\subset\mathcal{V}_\mathrm{h};\quad \{\varphi_j^F\}_{j=1}^{k-1}\ \forall F\subset\mathcal{F}_\mathrm{h};\quad b_k^K \text{ and } \{\varphi_\ell^K\}_{\ell=1}^{(k-2)(k-1)/2}\ \forall K\in\mathcal{T}_\mathrm{h}\Big). \tag{32}$$

The spaces in (31)-(32) and (26) coincide; see, e.g., [13, Lem. 1.2, 1.3] and [33]. For even k, the functions in (32) are linearly dependent, cf. [22] for the second order case, since the piecewise nonconforming bubble function, which on each element is given by b_k^K, is globally continuous. As such, in order to obtain a basis, it is necessary to remove one bulk nonconforming bubble function.

Seminorms in broken Sobolev spaces. We add a subscript h to all differential operators to denote corresponding operators defined piecewise over $\mathcal{T}_\mathrm{h}$; for instance, $\boldsymbol{\nabla}_\mathrm{h}$ is the broken gradient over $\mathcal{T}_\mathrm{h}$.

Given p and q larger than or equal to 1, we endow, whenever it makes sense for the above choices of p and q, the space $\mathrm{W}^{1,p}(\mathcal{T}_\mathrm{h})$ with the seminorms, for $d=2$,

$$\|v\|_{\mathrm{W}^{1,p;q}_{\Gamma_D}(\mathcal{T}_\mathrm{h})} := \|\boldsymbol{\nabla}_\mathrm{h}\, v\|_{\mathbf{L}^p(\Omega)} + \Big(\sum_{F\in\mathcal{F}_\mathrm{h}^{ID}} \mathrm{h}_F^{-\frac{p}{q'}-d\frac{p}{p'}+d\frac{p}{q'}} \|[\![v]\!]\|^p_{\mathrm{L}^q(F)}\Big)^{\frac1p}, \tag{33a}$$

$$|\!|\!|v|\!|\!|_{\mathrm{W}^{1,p;q}_{\Gamma_D}(\mathcal{T}_\mathrm{h})} := \|\boldsymbol{\nabla}_\mathrm{h}\, v\|_{\mathbf{L}^p(\Omega)} + \Big(\sum_{F\in\mathcal{F}_\mathrm{h}^{ID}} \mathrm{h}_F^{-\frac{p}{q'}-d\frac{p}{p'}+d\frac{p}{q'}} \Big\|\Pi_0^{0,\mathcal{F}_\mathrm{h}}\, [\![v]\!]\Big\|^p_{\mathrm{L}^q(F)}\Big)^{\frac1p}. \tag{33b}$$

Both seminorms are stronger than the seminorm $\|\boldsymbol{\nabla}_\mathrm{h}\, v\|_{\mathbf{L}^p(\Omega)}$.

3.2 Inequalities in broken Sobolev and Crouzeix-Raviart spaces

We recall the following technical, preliminary result, cf. [11, Theorem 1.7] and [10, Theorem 3.4]. Amongst other things, it states that the seminorms in (33) are norms. Recall that the spatial dimension d is 2.

Lemma 3.1 (Sobolev-Poincaré and -trace inequalities in broken Sobolev spaces)**.** *Let Ω satisfy either* (1) *or* (2)*. Let $\{\mathcal{T}_\mathrm{h}\}$ be a family of meshes as in Section 3.1 and p be in $[1,d)$. There exist positive constants C^*_{SP} and $C^\sharp_{\mathrm{ST}}$ depending on p, Γ_D, Ω through either $\mathfrak{R}$ or $\mathfrak{N}$ in* (1) *and* (2)*, d, and the shape-regularity parameter γ such that, for all $v\in\mathrm{W}^{1,p}_{\Gamma_D}(\mathcal{T}_\mathrm{h})$,*

$$\|v\|_{\mathrm{L}^q(\Omega)} \le C^*_{\mathrm{SP}}\|v\|_{\mathrm{W}^{1,p;p^\sharp}_{\Gamma_D}(\mathcal{T}_\mathrm{h})} \qquad \forall\, \mathrm{q}\in[1,p^*], \tag{34a}$$

$$\|v\|_{\mathrm{L}^q(\Gamma)} \le C^\sharp_{\mathrm{ST}}\|v\|_{\mathrm{W}^{1,p;p^\sharp}_{\Gamma_D}(\mathcal{T}_\mathrm{h})} \qquad \forall q\in[1,p^\sharp]. \tag{34b}$$

The explicit dependence of C^*_{SP} and $C^\sharp_{\mathrm{ST}}$ on the parameters highlighted above is discussed in [11, Theorem 1.7] and [10, Theorem 3.4].

Now, we establish a variant of Lemma 3.1, where weaker norms on the right-hand sides of (34) are employed, notably, we replace $\|v\|_{\mathrm{W}^{1,p;q}_{\Gamma_D}(\mathcal{T}_\mathrm{h})}$ by $|\!|\!|\cdot|\!|\!|_{\mathrm{W}^{1,p;q}_{\Gamma_D}(\mathcal{T}_\mathrm{h})}$.

Proposition 3.2 (Improved Sobolev-Poincaré and -trace inequalities in broken Sobolev spaces)**.** *Let Ω satisfy either* (1) *or* (2)*. Let $\{\mathcal{T}_\mathrm{h}\}$ be a family of meshes as in Section 3.1 and p be in $[1,d)$. There exist positive constants $\widetilde{C}^*_{\mathrm{SP}}$ and $\widetilde{C}^\sharp_{\mathrm{ST}}$ depending on p, Γ_D, Ω through either $\mathfrak{R}$ or $\mathfrak{N}$ in* (1) *and* (2)*, d, and the shape-regularity parameter γ such that, for all $v\in\mathrm{W}^{1,p}_{\Gamma_D}(\mathcal{T}_\mathrm{h})$,*

$$\|v\|_{\mathrm{L}^q(\Omega)} \le \widetilde{C}^*_{\mathrm{SP}}|\!|\!|v|\!|\!|_{\mathrm{W}^{1,p;p^\sharp}_{\Gamma_D}(\mathcal{T}_\mathrm{h})} \qquad \forall q\in[1,p^*], \tag{35a}$$

$$\|v\|_{\mathrm{L}^q(\Gamma)} \le \widetilde{C}^\sharp_{\mathrm{ST}}|\!|\!|v|\!|\!|_{\mathrm{W}^{1,p;p^\sharp}_{\Gamma_D}(\mathcal{T}_\mathrm{h})} \qquad \forall q\in[1,p^\sharp]. \tag{35b}$$

Proof. A proof of (35a) is given in [11, Corollary 1.10]. Therefore, we focus on (35b). We assume that $q=p^\sharp$, since the assertion for smaller values of q follows from Hölder's inequality.

Recall that $\Pi_0^{0,\mathcal{T}_{\mathrm{h}}}$ denotes the piecewise average operator over $\mathcal{T}_{\mathrm{h}}$. Triangle's inequality gives

$$\|v\|_{\mathrm{L}^{p^\sharp}(\Gamma)} \leq \left\| v - \Pi_0^{0,\mathcal{T}_{\mathrm{h}}} v \right\|_{\mathrm{L}^{p^\sharp}(\Gamma)} + \left\| \Pi_0^{0,\mathcal{T}_{\mathrm{h}}} v \right\|_{\mathrm{L}^{p^\sharp}(\Gamma)}. \tag{36}$$

As for the first term on the right-hand side, an elementwise trace inequality on the elements abutting Γ (constant $C_{\mathrm{TR}}^\sharp$ depending on the shape-regularity parameter γ), cf. (24), an elementwise Sobolev embedding inequality (constant C_{Sob} depending on the shape-regularity parameter γ), cf. (3), and an elementwise Poincaré-Steklov inequality (constant C_{PS} depending on the shape-regularity parameter γ), cf. (6), lead to

$$\left\| v - \Pi_0^{0,\mathcal{T}_{\mathrm{h}}} v \right\|_{\mathrm{L}^{p^\sharp}(\Gamma)} \leq C_{\mathrm{TR}}^\sharp (1 + C_{\mathrm{PS}} C_{\mathrm{Sob}}) \| \boldsymbol{\nabla}_{\mathrm{h}}\, v \|_{\mathbf{L}^p(\Omega)}.$$

Inserting this inequality in (36) yields

$$\|v\|_{\mathrm{L}^{p^\sharp}(\Gamma)} \leq C_{\mathrm{TR}}^\sharp (1 + C_{\mathrm{PS}} C_{\mathrm{Sob}}) \| \boldsymbol{\nabla}_{\mathrm{h}}\, v \|_{\mathbf{L}^p(\Omega)} + \left\| \Pi_0^{0,\mathcal{T}_{\mathrm{h}}} v \right\|_{\mathrm{L}^{p^\sharp}(\Gamma)}. \tag{37}$$

The assertion follows by estimating the second term on the right-hand side. We apply Lemma 3.1 and get, for $C_{\mathrm{ST}}^\sharp$ as in (34b),

$$\left\| \Pi_0^{0,\mathcal{T}_{\mathrm{h}}} v \right\|_{\mathrm{L}^{p^\sharp}(\Omega)} \leq C_{\mathrm{ST}}^\sharp \Big(\sum_{F \in \mathcal{F}_{\mathrm{h}}^{ID}} \left\| \left[\!\left[\Pi_0^{0,\mathcal{T}_{\mathrm{h}}} v \right]\!\right] \right\|_{\mathrm{L}^{p^\sharp}(F)}^p \Big)^{\frac{1}{p}}. \tag{38}$$

Recall that $\Pi_0^{0,\mathcal{F}_{\mathrm{h}}}$ is the piecewise average operator over $\mathcal{F}_{\mathrm{h}}$. We estimate each jump term separately:

$$\left\| \left[\!\left[\Pi_0^{0,\mathcal{T}_{\mathrm{h}}} v \right]\!\right] \right\|_{\mathrm{L}^{p^\sharp}(F)} \leq \left\| \left[\!\left[\Pi_0^{0,\mathcal{T}_{\mathrm{h}}} v \right]\!\right] - \Pi_0^{0,\mathcal{F}_{\mathrm{h}}} [\![v]\!] \right\|_{\mathrm{L}^{p^\sharp}(F)} + \left\| \Pi_0^{0,\mathcal{F}_{\mathrm{h}}} [\![v]\!] \right\|_{\mathrm{L}^{p^\sharp}(F)}. \tag{39}$$

The second term on the right-hand side is good to go. As for the first one, proceeding exactly as in the proof of [11, Corollary 1.10], standard manipulations give the existence of a positive constant C depending only on γ and p such that

$$\Big(\sum_{F \in \mathcal{F}_{\mathrm{h}}^{ID}} \left\| \left[\!\left[v - \Pi_0^{0,\mathcal{T}_{\mathrm{h}}} v \right]\!\right] \right\|_{\mathrm{L}^{p^\sharp}(F)}^p \Big)^{\frac{1}{p}} \leq C \| \boldsymbol{\nabla}_{\mathrm{h}}\, v \|_{\mathbf{L}^p(\Omega)}.$$

Combining the above display, (37), (38), (39) entails the assertion. □

Due to definitions (26) and (33b), we note that

$$\begin{aligned} |\!|\!| \mathrm{q}_{\mathrm{h}} |\!|\!|_{\mathrm{W}^{1,p;q}_{\Gamma_D}(\mathcal{T}_{\mathrm{h}})} =& \| \boldsymbol{\nabla}_{\mathrm{h}}\, \mathrm{q}_{\mathrm{h}} \|_{\mathbf{L}^p(\Omega)} \\ &+ \Big(\sum_{F \in \mathcal{F}_{\mathrm{h}}^D} \mathrm{h}_F^{-\frac{p}{q'} - d\frac{p}{p'} + d\frac{p}{q'}} \left\| \Pi_0^{0,\mathcal{F}_{\mathrm{h}}} g \right\|_{\mathrm{L}^q(F)}^p \Big)^{\frac{1}{p}} \quad \forall\, \mathrm{q}_{\mathrm{h}} \in \mathrm{CR}_{k,g}(\mathcal{T}_{\mathrm{h}}, \mathcal{F}_{\mathrm{h}}^D). \end{aligned}$$

Thus, we have the following immediate consequence of Proposition 3.2.

Corollary 3.3 (Improved Sobolev-Poincaré and -trace inequalities in Crouzeix-Raviart spaces)**.** *Let Ω satisfy either* (1) *or* (2)*. Let $\{\mathcal{T}_{\mathrm{h}}\}$ be a family of meshes as in Section 3.1 and p be in* $[1,d)$*. Given $\widetilde{C}_{\mathrm{SP}}^*$ and $\widetilde{C}_{\mathrm{ST}}^\sharp$ as in* (35)*, for all q_{h} in $\mathrm{CR}_{k,g_D}(\mathcal{T}_{\mathrm{h}}, \mathcal{F}_{\mathrm{h}}^D)$, g_D in $\mathcal{G}_D$,*

$$\|\mathrm{q}_{\mathrm{h}}\|_{\mathrm{L}^q(\Omega)} \leq \widetilde{C}_{\mathrm{SP}}^* \Big[\| \boldsymbol{\nabla}_{\mathrm{h}}\, \mathrm{q}_{\mathrm{h}} \|_{\mathbf{L}^p(\Omega)} + \big(\sum_{F \in \mathcal{F}_{\mathrm{h}}^D} \left\| \Pi_0^{0,\mathcal{F}_{\mathrm{h}}} g_D \right\|_{\mathrm{L}^{p^\sharp}(F)}^p \big)^{\frac{1}{p}} \Big] \qquad \forall q \in [1, p^*], \tag{40a}$$

$$\|\mathrm{q}_{\mathrm{h}}\|_{\mathrm{L}^q(\Gamma)} \leq \widetilde{C}_{\mathrm{ST}}^\sharp \Big[\| \boldsymbol{\nabla}_{\mathrm{h}}\, \mathrm{q}_{\mathrm{h}} \|_{\mathbf{L}^p(\Omega)} + \Big(\sum_{F \in \mathcal{F}_{\mathrm{h}}^D} \left\| \Pi_0^{0,\mathcal{F}_{\mathrm{h}}} g_D \right\|_{\mathrm{L}^{p^\sharp}(F)}^p \Big)^{\frac{1}{p}} \Big] \qquad \forall q \in [1, p^\sharp]. \tag{40b}$$

Remark 1. Corollary 3.3 extends [23, Propositions 4 and 5] to the general-order case. The tools employed in the proof of Corollary 3.3 do not rely on any averaging operator. As such, the constants in (40) do not depend on the structure of the discretization space, with the exception of the zero moments up to order $p-1$ coming from the definition of the CR spaces in (26); this might be helpful in the proof of the convergence of the scheme, e.g., on a fixed mesh and increasing the polynomial degree. ■

4 A general-order method

For a generic g in $\mathcal{G}_D$, we introduce the finite element spaces,

$$\boldsymbol{\mathcal{V}}_{\mathrm{h}}^{k-1} := \mathbf{P}_{k-1}(\mathcal{T}_{\mathrm{h}}), \qquad \mathcal{Q}_{h,g}^{k} := \begin{cases} \mathrm{CR}_k(\mathcal{T}_{\mathrm{h}}) \cap \mathrm{L}_0^2(\Omega) & \text{if } \Gamma_N = \Gamma \\ \mathrm{CR}_{k,g}(\mathcal{T}_{\mathrm{h}}, \mathcal{F}_{\mathrm{h}}^D) & \text{if } \Gamma_N \neq \Gamma. \end{cases}$$

We consider the method: find $(\mathbf{u}_{\mathrm{h}}, \mathrm{p}_{\mathrm{h}}) \in \boldsymbol{\mathcal{V}}_{\mathrm{h}}^{k-1} \times \mathcal{Q}_{h,g_D}^{k}$ such that

$$\frac{\mu}{\rho}\int_\Omega (\underline{\mathbf{K}}^{-1})\mathbf{u}_{\mathrm{h}} \cdot \mathbf{v}_{\mathrm{h}}\,\mathrm{d}\mathbf{x} + \frac{\beta}{\rho}\int_\Omega |\mathbf{u}_{\mathrm{h}}|^{\alpha-2}\mathbf{u}_{\mathrm{h}} \cdot \mathbf{v}_{\mathrm{h}}\,\mathrm{d}\mathbf{x} + \int_\Omega \boldsymbol{\nabla}_{\mathrm{h}}\,\mathrm{p}_{\mathrm{h}} \cdot \mathbf{v}_{\mathrm{h}}\,\mathrm{d}\mathbf{x} = 0 \qquad \forall\, \mathbf{v}_{\mathrm{h}} \in \boldsymbol{\mathcal{V}}_{\mathrm{h}}^{k-1} \tag{41a}$$

$$\int_\Omega \mathbf{u}_{\mathrm{h}} \cdot \boldsymbol{\nabla}_{\mathrm{h}}\,\mathrm{q}_{\mathrm{h}}\,\mathrm{d}\mathbf{x} = -\int_\Omega b\,\mathrm{q}_{\mathrm{h}}\,\mathrm{d}\mathbf{x} + \int_{\Gamma_N} g_N\,\mathrm{q}_{\mathrm{h}}\,\mathrm{d}s \qquad \forall\,\mathrm{q}_{\mathrm{h}} \in \mathcal{Q}_{h,0}^{k}. \tag{41b}$$

The method (41) with $k = 1$, $\alpha = 3$, and pure Neumann boundary conditions was analyzed in [23]. This section is devoted to investigate the well-posedness of (Section 4.1) and error estimate for (Section 6) method (41).

4.1 Well-posedness

We define the discrete counterpart of the space $\boldsymbol{\mathcal{D}}$ in (11) as

$$\boldsymbol{\mathcal{D}}_{\mathrm{h}}^{k-1} := \left\{ \mathbf{v}_{\mathrm{h}} \in \boldsymbol{\mathcal{V}}_{\mathrm{h}}^{k-1} \,\middle|\, \int_\Omega \boldsymbol{\nabla}_{\mathrm{h}}\,\mathrm{q}_{\mathrm{h}} \cdot \mathbf{v}_{\mathrm{h}}\,\mathrm{d}\mathbf{x} = 0 \quad \forall\,\mathrm{q}_{\mathrm{h}} \in \mathcal{Q}_{h,0}^{k} \right\}$$

and its L^2-orthogonal in $\boldsymbol{\mathcal{V}}_{\mathrm{h}}^{k-1}$ as

$$\boldsymbol{\mathcal{D}}_{\mathrm{h}}^{k-1,\perp} := \left\{ \mathbf{w}_{\mathrm{h}} \in \boldsymbol{\mathcal{V}}_{\mathrm{h}}^{k-1} \,\middle|\, \int_\Omega \mathbf{w}_{\mathrm{h}} \cdot \mathbf{v}_{\mathrm{h}}\,\mathrm{d}\mathbf{x} = 0 \quad \forall \mathbf{v}_{\mathrm{h}} \in \boldsymbol{\mathcal{D}}_{\mathrm{h}}^{k-1} \right\}.$$

We prove a discrete inf-sup condition.

Lemma 4.1. *For all $\mathfrak{a}$ in $(1, \infty)$, there exists a positive constant $\mathfrak{b}_{\mathrm{h}}$ only depending on $\mathfrak{a}$, the shape-regularity parameter γ, and the order k, such that*

$$\inf_{\mathrm{q}_{\mathrm{h}} \in \mathcal{Q}_{h,g_D}^{k}} \sup_{\mathbf{v}_{\mathrm{h}} \in \boldsymbol{\mathcal{V}}_{\mathrm{h}}^{k-1}} \frac{\int_\Omega \mathbf{v}_{\mathrm{h}} \cdot \boldsymbol{\nabla}_{\mathrm{h}}\,\mathrm{q}_{\mathrm{h}}}{\|\boldsymbol{\nabla}_{\mathrm{h}}\,\mathrm{q}_{\mathrm{h}}\|_{\mathbf{L}^{\mathfrak{a}'}(\Omega)} \|\mathbf{v}_{\mathrm{h}}\|_{\mathbf{L}^{\mathfrak{a}}(\Omega)}} \geq \mathfrak{b}_{\mathrm{h}}. \tag{42}$$

Proof. Given q_{h} in $\mathcal{Q}_{h,g_D}^{k}$ and $\boldsymbol{\Pi}_{k-1}^{0,\mathcal{T}_{\mathrm{h}}}$ as in (23), an $\mathbf{L}^{\mathfrak{a}} - \mathbf{L}^2$ polynomial inverse inequality gives

$$\mathbf{w}_{\mathrm{h}} := |\,\boldsymbol{\nabla}_{\mathrm{h}}\,\mathrm{q}_{\mathrm{h}}\,|^{\mathfrak{a}'-2}\,\boldsymbol{\nabla}_{\mathrm{h}}\,\mathrm{q}_{\mathrm{h}}, \qquad \left\|\boldsymbol{\Pi}_{k-1}^{0,\mathcal{T}_{\mathrm{h}}}\mathbf{w}_{\mathrm{h}}\right\|_{\mathbf{L}^{\mathfrak{a}}(\Omega)} \leq \mathfrak{b}_{\mathrm{h}}^{-1}\|\mathbf{w}_{\mathrm{h}}\|_{\mathbf{L}^{\mathfrak{a}}(\Omega)} = \mathfrak{b}_{\mathrm{h}}^{-1}\|\boldsymbol{\nabla}_{\mathrm{h}}\,\mathrm{q}_{\mathrm{h}}\|_{\mathbf{L}^{\mathfrak{a}'}(\Omega)}^{\alpha'-1}. \tag{43}$$

A duality argument reveals

$$\begin{aligned}\|\boldsymbol{\nabla}_{\mathrm{h}}\,\mathrm{q}_{\mathrm{h}}\|_{\mathbf{L}^{\mathfrak{a}'}(\Omega)} &= \frac{\|\boldsymbol{\nabla}_{\mathrm{h}}\,\mathrm{q}_{\mathrm{h}}\|_{\mathbf{L}^{\mathfrak{a}'}(\Omega)}^{\mathfrak{a}'}}{\|\boldsymbol{\nabla}_{\mathrm{h}}\,\mathrm{q}_{\mathrm{h}}\|_{\mathbf{L}^{\mathfrak{a}'}(\Omega)}^{\mathfrak{a}'-1}} = \int_\Omega \boldsymbol{\nabla}_{\mathrm{h}}\,\mathrm{q}_{\mathrm{h}} \cdot \frac{|\,\boldsymbol{\nabla}_{\mathrm{h}}\,\mathrm{q}_{\mathrm{h}}\,|^{\mathfrak{a}'-2}\,\boldsymbol{\nabla}_{\mathrm{h}}\,\mathrm{q}_{\mathrm{h}}}{\|\boldsymbol{\nabla}_{\mathrm{h}}\,\mathrm{q}_{\mathrm{h}}\|_{\mathbf{L}^{\mathfrak{a}'}(\Omega)}^{\mathfrak{a}'-1}} \\ &\overset{(43)}{\leq} \mathfrak{b}_{\mathrm{h}}^{-1}\int_\Omega \boldsymbol{\nabla}_{\mathrm{h}}\,\mathrm{q}_{\mathrm{h}} \cdot \frac{\boldsymbol{\Pi}_{k-1}^{0,\mathcal{T}_{\mathrm{h}}}\mathbf{w}_{\mathrm{h}}}{\left\|\boldsymbol{\Pi}_{k-1}^{0,\mathcal{T}_{\mathrm{h}}}\mathbf{w}_{\mathrm{h}}\right\|_{\mathbf{L}^{\mathfrak{a}}(\Omega)}} \leq \mathfrak{b}_{\mathrm{h}}^{-1} \sup_{\mathbf{v}_{\mathrm{h}} \in \boldsymbol{\mathcal{V}}_{\mathrm{h}}^{k-1}} \int_\Omega \boldsymbol{\nabla}_{\mathrm{h}}\,\mathrm{q}_{\mathrm{h}} \cdot \frac{\mathbf{v}_{\mathrm{h}}}{\|\mathbf{v}_{\mathrm{h}}\|_{\mathbf{L}^{\mathfrak{a}}(\Omega)}}.\end{aligned}$$

Taking the infimum over q_{h} in $\mathcal{Q}_{g_D}$ on both sides of the above display yields (42). □

We prove the discrete version of Proposition 2.2.

Lemma 4.2. *Given b and g_N as in* (9)*, there exists* $\mathbf{u}_{\mathrm{h},\ell}$ *in* $\boldsymbol{\mathcal{D}}_{\mathrm{h}}^{k-1,\perp}$ *satisfying*

$$\int_\Omega \mathbf{u}_{\mathrm{h},\ell} \cdot \boldsymbol{\nabla}_{\mathrm{h}} \cdot \mathrm{q}_{\mathrm{h}} \, \mathrm{d}\mathbf{x} = -\int_\Omega b \, \mathrm{q}_{\mathrm{h}} \, \mathrm{d}\mathbf{x} + \int_{\Gamma_N} g_N \, \mathrm{q}_{\mathrm{h}} \, \mathrm{d}s \qquad \forall \, \mathrm{q}_{\mathrm{h}} \in \mathcal{Q}_{h,0}^k$$

and a positive constant $\widetilde{C}_\ell$ *depending on the order k through* $\mathfrak{b}_{\mathrm{h}}$ *in* (42)*,* Γ_D*,* Ω *through either* $\mathfrak{R}$ *or* $\mathfrak{N}$ *in* (1) *and* (2)*, and the shape-regularity parameter* γ *such that*

$$\|\mathbf{u}_{\mathrm{h},\ell}\|_{\mathbf{L}^\alpha(\Omega)} \leq \widetilde{C}_\ell \Big(\|b\|_{\mathrm{L}^{((\alpha')^*)'}(\Omega)} + \|g_N\|_{\mathrm{L}^{((\alpha')^\sharp)'}(\Gamma_N)} \Big). \tag{44}$$

Proof. We consider two cases.

Case 1: mixed/Dirichlet boundary conditions. Triangle's inequality, Cauchy-Schwarz' inequality, the broken Sobolev-Poincaré inequality (40a), and the broken trace inequality (40b) yield, for a hidden constant only depending on k, Γ_D, Ω through either $\mathfrak{R}$ or $\mathfrak{N}$ in (1) and (2), and γ,

$$\left| -\int_\Omega b \, \mathrm{q}_{\mathrm{h}} \, \mathrm{d}\mathbf{x} + \int_{\Gamma_N} g \, \mathrm{q}_{\mathrm{h}} \, \mathrm{d}s \right| \lesssim \Big(\|b\|_{\mathrm{L}^{((\alpha')^*)'}(\Omega)} + \|g_N\|_{\mathrm{L}^{((\alpha')^\sharp)'}(\Gamma_N)} \Big) \|\boldsymbol{\nabla}_{\mathrm{h}} \, \mathrm{q}_{\mathrm{h}}\|_{\mathbf{L}^{\alpha'}(\Omega)} \qquad \forall \, \mathrm{q}_{\mathrm{h}} \in \mathcal{Q}_{h,0}^k,$$

where the mapping $\mathrm{q}_{\mathrm{h}} \to -\int_\Omega b \, \mathrm{q}_{\mathrm{h}} \, \mathrm{d}\mathbf{x} + \int_{\Gamma_N} g \, \mathrm{q}_{\mathrm{h}} \, \mathrm{d}s$ belongs to $(\mathcal{Q}_{h,0}^k)^*$. The assertion follows from the discrete inf-sup condition (42).

Case 2: pure Neumann boundary conditions. For all c in $\mathbb{R}$, triangle's inequality, Cauchy-Schwarz' inequality, the compatibility condition (8), the broken Sobolev-Poincaré inequality (40a), and the discrete broken trace inequality (40b) yield, for a hidden constant only depending on k, Γ_D, Ω through either $\mathfrak{R}$ or $\mathfrak{N}$ in (1) and (2), and γ,

$$\begin{aligned}
\left| -\int_\Omega b \, \mathrm{q}_{\mathrm{h}} \, \mathrm{d}\mathbf{x} + \int_{\Gamma_N} g \, \mathrm{q}_{\mathrm{h}} \, \mathrm{d}s \right| &\leq \left| \int_\Omega b \, (\mathrm{q}_{\mathrm{h}} - c) \, \mathrm{d}\mathbf{x} \right| + \left| \int_{\Gamma_N} g \, (\mathrm{q}_{\mathrm{h}} - c) \, \mathrm{d}s \right| \\
&\leq \Big(\|b\|_{\mathrm{L}^{((\alpha')^*)'}(\Omega)} + \|g_N\|_{\mathrm{L}^{((\alpha')^\sharp)'}(\Gamma_N)} \Big) \Big(\|\mathrm{q}_{\mathrm{h}} - c\|_{\mathrm{L}^{(\alpha')^*}(\Omega)} + \|\mathrm{q}_{\mathrm{h}} - c\|_{\mathrm{L}^{(\alpha')^\sharp}(\Gamma_N)} \Big) \\
&\lesssim \Big(\|b\|_{\mathrm{L}^{((\alpha')^*)'}(\Omega)} + \|g_N\|_{\mathrm{L}^{((\alpha')^\sharp)'}(\Gamma_N)} \Big) \|\boldsymbol{\nabla}_{\mathrm{h}} \, \mathrm{q}_{\mathrm{h}}\|_{\mathbf{L}^{\alpha'}(\Omega)} \quad \forall \, \mathrm{q}_{\mathrm{h}} \in \mathcal{Q}_{h,0}^k.
\end{aligned}$$

The mapping $\mathrm{q}_{\mathrm{h}} \to -\int_\Omega b \, \mathrm{q}_{\mathrm{h}} \, \mathrm{d}\mathbf{x} + \int_{\Gamma_N} g \, \mathrm{q}_{\mathrm{h}} \, \mathrm{d}s$ belongs to $(\mathcal{Q}_{h,0}^k)^*$. The assertion follows from the discrete inf-sup condition (42). □

We now consider the discrete version of (16): find $\mathbf{u}_{\mathrm{h},0}$ in $\boldsymbol{\mathcal{D}}_{\mathrm{h}}^{k-1}$ such that

$$\frac{\mu}{\rho} \int_\Omega (\underline{\mathbf{K}}^{-1})(\mathbf{u}_{\mathrm{h},0} + \mathbf{u}_{\mathrm{h},\ell}) \cdot \mathbf{v}_{\mathrm{h}} \, \mathrm{d}\mathbf{x} + \frac{\beta}{\rho} \int_\Omega |\mathbf{u}_{\mathrm{h},0} + \mathbf{u}_{\mathrm{h},\ell}|^{\alpha-2} (\mathbf{u}_{\mathrm{h},0} + \mathbf{u}_{\mathrm{h},\ell}) \cdot \mathbf{v}_{\mathrm{h}} \, \mathrm{d}\mathbf{x} = 0 \quad \forall \mathbf{v}_{\mathrm{h}} \in \boldsymbol{\mathcal{D}}_{\mathrm{h}}^{k-1}. \tag{45}$$

A finite-dimensional modification of the arguments in Proposition 2.5 and the discrete inf-sup condition (42) entail the following result.

Proposition 4.3. *Given b and g_N as in* (9)*, problem* (41) *admits a unique solution* $(\mathbf{u}_{\mathrm{h}}, \mathrm{p}_{\mathrm{h}})$ *in* $\boldsymbol{\mathcal{V}}_{\mathrm{h}}^{k-1} \times \mathcal{Q}_{h,g_D}^k$*. Moreover, given* $\widetilde{C}_\ell$ *as in* (44)*, we have*

$$\|\mathbf{u}_{\mathrm{h}}\|_{\mathbf{L}^\alpha(\Omega)} \leq \Big(\frac{2^{\alpha'} (\alpha - 1) \mu^{\alpha'}}{\beta^{\alpha'}} \|\underline{\mathbf{K}}^{-1}\|_{\underline{\mathbf{L}}^{\frac{\alpha}{\alpha-2}}}^{\alpha'-1} + 2 \Big)^{\frac{1}{\alpha}} \widetilde{C}_\ell^{\alpha'-1} \big(\|b\|_{\mathrm{L}^{((\alpha')^*)'}(\Omega)} + \|g_N\|_{\mathrm{L}^{((\alpha')^\sharp)'}(\Gamma_N)} \big)^{\alpha'-1} \tag{46a}$$

and

$$\begin{aligned}
\|\boldsymbol{\nabla}_{\mathrm{h}} \, \mathrm{p}_{\mathrm{h}}\|_{\mathbf{L}^{\alpha'}(\Omega)} \leq \Big(\frac{\mu}{\rho} \|\underline{\mathbf{K}}^{-1}\|_{\underline{\mathbf{L}}^{\frac{\alpha}{\alpha-2}}(\Omega)} + \frac{\beta}{\rho} \Big) \Big(\frac{2^{\alpha'} (\alpha - 1) \mu^{\alpha'}}{\beta^{\alpha'}} \|\underline{\mathbf{K}}^{-1}\|_{\underline{\mathbf{L}}^{\frac{\alpha}{\alpha-2}}}^{\alpha'-1} + 2 \Big)^{\frac{1}{\alpha'}} \cdot \\
\cdot \, \widetilde{C}_\ell \big(\|b\|_{\mathrm{L}^{((\alpha')^*)'}(\Omega)} + \|g_N\|_{\mathrm{L}^{((\alpha')^\sharp)'}(\Gamma_N)} \big).
\end{aligned} \tag{46b}$$

Remark 2. Given $\mathbf{v}_\mathrm{h}$ in $\boldsymbol{\mathcal{D}}^0_\mathrm{h}$, we have

$$\int_{\mathcal{F}_\mathrm{h}} \Pi_0^{0,\mathcal{F}_\mathrm{h}} \mathrm{q}_\mathrm{h} \; [\![\mathbf{v}_\mathrm{h}]\!]_\mathbf{n} \, \mathrm{d}\mathbf{x} \overset{(\mathbf{v}_\mathrm{h}\in\boldsymbol{\mathcal{V}}^0_\mathrm{h})}{=} \int_{\mathcal{F}_\mathrm{h}} \Pi_0^{0,\mathcal{F}_\mathrm{h}} \mathrm{q}_\mathrm{h} \; [\![\mathbf{v}_\mathrm{h}]\!]_\mathbf{n} \, \mathrm{d}\mathbf{x} - \int_\Omega \mathrm{q}_\mathrm{h} \, \boldsymbol{\nabla}_\mathrm{h} \cdot \mathbf{v}_\mathrm{h}$$

$$\overset{(\mathrm{IBP})}{=} \int_\Omega \boldsymbol{\nabla}_\mathrm{h} \mathrm{q}_\mathrm{h} \cdot \mathbf{v}_\mathrm{h} \, \mathrm{d}\mathbf{x} \overset{(\mathbf{v}_\mathrm{h}\in\boldsymbol{\mathcal{D}}^0_\mathrm{h})}{=} 0 \qquad \forall \, \mathrm{q}_\mathrm{h} \in \mathcal{Q}^1_{h,0},$$

whence $[\![\mathbf{v}_\mathrm{h}]\!]_\mathbf{n} = 0$ on each F in $\mathcal{F}_\mathrm{h}$. As such, $\boldsymbol{\nabla} \cdot \mathbf{v}_\mathrm{h}$ belongs to $\mathbf{L}^\alpha(\Omega)$ and in particular we have

$$\boldsymbol{\mathcal{D}}^0_\mathrm{h} = \{\mathbf{v}_\mathrm{h} \in \boldsymbol{\mathcal{V}}^0_\mathrm{h} \mid \boldsymbol{\nabla} \cdot \mathbf{v}_\mathrm{h} = 0\}.$$

The characterization above is not valid for general k larger than 1. Indeed, the term $(\mathrm{q}_\mathrm{h}, \boldsymbol{\nabla}_\mathrm{h} \cdot \mathbf{v}_\mathrm{h})$ does not vanish in general; to see this, consider $\mathbf{v}_\mathrm{h}$ in $\boldsymbol{\mathcal{D}}^{k-1}_\mathrm{h}$, observe that $\boldsymbol{\nabla} \cdot \mathbf{v}_{\mathrm{h}|K}$ belongs to $\mathrm{P}_{k-2}(K)$ on each K in $\mathcal{T}_\mathrm{h}$ and the bulk moments of q_h in (28b) are up to order $k-3$. On the one hand, this fact does not undermine the well-posedness of the method as well as the derivation of error estimates of optimal order since in the dual-mixed formulation (41) the inclusion $\boldsymbol{\mathcal{D}}^{k-1}_\mathrm{h} \subset \boldsymbol{\mathcal{D}}$ is not necessary, while it would be essential in the standard mixed counterpart. ∎

5 Convergence analysis

In this section, we discuss the strong convergence in the natural norms of sequences of solutions $(\mathbf{u}_\mathrm{h}, \mathrm{p}_\mathrm{h})$ to method (41). To this aim, we proceed by showing the following intermediate steps:

- introduce $\mathbf{c}_\mathrm{h}$ in $\mathbf{L}^\alpha(\Omega)$, cf. (50), which represents a lifting of the discrete divergence of $\mathbf{u}$, and show its strong convergence in $\mathbf{L}^\alpha(\Omega)$ to $\mathbf{0}$, see Theorem 5.1;
- show strong convergence of several interpolation, projection, ... operators, see Lemma 5.2;
- show weak convergence in $\mathbf{L}^\alpha(\Omega)$ of the fluxes, see Lemma 5.3;
- show strong convergence in $\mathbf{L}^2(\Omega)$ of the fluxes, see Lemma 5.5;
- show weak convergence in $\mathbf{L}^{\alpha'}(\Omega)$ of the gradient of the potentials, see Proposition 5.6;
- show strong convergence in $\mathbf{L}^\alpha$ of the fluxes, see Theorem 5.7;
- show strong convergence in $\mathbf{L}^{\alpha'}(\Omega)$ of the gradient of the potentials, see Theorem 5.8.

Several of these results will be proven under an additional assumption:

$$\alpha \in (2, 4). \tag{47}$$

We preliminarily introduce the Crouzeix-Raviart interpolant $\mathcal{I}_k$; see, e.g., [1, 13, 22]; due to the intrinsic different nature of the spaces depending on the parity of the order k of the scheme, cf. Section 3.1, we distinguish two cases. For odd k and given q in $\mathrm{W}^{1,1}(\Omega)$, we consider the interpolant $\mathcal{I}_k$ defined such that the DoFs in (28) of q and $\mathcal{I}_k \,\mathrm{q}$ coincide. Instead, for even k and q in $\mathrm{W}^{1,t}(\Omega)$, $t > 2$, we consider the modal interpolant $\mathcal{I}_k$: $\mathcal{I}_k \,\mathrm{q}$ is the unique function in the Crouzeix-Raviart space such that

- $\mathcal{I}_k \,\mathrm{q}(\nu) := \mathrm{q}(\nu)$ for all ν in $\mathcal{V}_\mathrm{h}$;
- the facet (28a) and bulk (28b) moments of q and $\mathcal{I}_k \,\mathrm{q}$ coincide;
- the coefficients of the nonconforming bubbles in (29) in the expansion of $\mathcal{I}_k \,\mathrm{q}$ are set to 0.

For an arbitrary order (even or odd) k, the above definitions of $\mathcal{I}_k$ imply

$$\int_F (\mathrm{q} - \mathcal{I}_k \,\mathrm{q}) \, S^F_j \, \mathrm{d}s = 0 \qquad \forall j = 0, \dots, k-1, \quad \forall F \in \mathcal{F}^I_\mathrm{h}, \tag{48a}$$

$$\int_K (\mathrm{q} - \mathcal{I}_k \,\mathrm{q}) \, m^K_{\boldsymbol{\beta}} \, \mathrm{d}\mathbf{x} = 0 \qquad \forall |\boldsymbol{\beta}| = 0, \dots, k-3, \; \forall K \in \mathcal{T}_\mathrm{h}. \tag{48b}$$

For k, r, and m larger than or equal to 1, standard techniques [12] entail

$$\mathrm{h}^{-1} \|\mathrm{q} - \mathcal{I}_k \,\mathrm{q}\|_{\mathrm{L}^m(\Omega)} + \|\boldsymbol{\nabla}_\mathrm{h}(\mathrm{q} - \mathcal{I}_k \,\mathrm{q})\|_{\mathbf{L}^m(\Omega)} \lesssim \mathrm{h}^{s-1} \|\mathrm{q}\|_{\mathrm{W}^{s,m}(\Omega)} \quad \forall \,\mathrm{q} \in \mathrm{W}^{r,m}(\Omega), \; s := \min\{r, k+1\}. \tag{49}$$

5.1 Weak convergence in the natural norms

Given $\mathbf{w}$ in $\mathbf{L}^{\mathfrak{a}}(\Omega)$ with $\boldsymbol{\nabla}\cdot\mathbf{w}$ in $\mathrm{L}^{((\mathfrak{a}')^*)'}(\Omega)$, $\mathfrak{a}$ larger than 2, let $\mathbf{c}_{\mathrm{h}} = \mathbf{c}_{\mathrm{h}}(\mathbf{w})$ in $\boldsymbol{\mathcal{D}}_{\mathrm{h}}^{k-1,\perp}$ solve

$$\int_\Omega \mathbf{c}_{\mathrm{h}} \cdot \boldsymbol{\nabla}_{\mathrm{h}}\,\mathrm{q}_{\mathrm{h}}\;\mathrm{d}\mathbf{x} = -\int_\Omega \mathbf{w}\cdot\boldsymbol{\nabla}_{\mathrm{h}}\,\mathrm{q}_{\mathrm{h}}\;\mathrm{d}\mathbf{x} - \int_\Omega \boldsymbol{\nabla}\cdot\mathbf{w}\;\mathrm{q}_{\mathrm{h}}\;\mathrm{d}\mathbf{x} + \langle \mathbf{w}\cdot\mathbf{n}_\Omega, \mathrm{q}_{\mathrm{h}}\rangle_{\Gamma_N} \qquad \forall\,\mathrm{q}_{\mathrm{h}} \in \mathcal{Q}^k_{h,0}. \tag{50}$$

The existence of a solution to (50) follows from the discrete inf-sup condition (42) together with the fact that the right-hand side is a linear functional on $\mathcal{Q}^k_{h,0}$, as can be shown by arguments analogous to those of the proof of Lemma 4.2. We further set

$$\mathbf{P}_{\mathrm{h}}(\mathbf{w}) := \boldsymbol{\Pi}^{0,\mathcal{T}_{\mathrm{h}}}_{k-1}\mathbf{w} + \mathbf{c}_{\mathrm{h}}(\mathbf{w}). \tag{51}$$

The operator $\boldsymbol{\Pi}^{\mathbf{RT},\mathcal{T}_{\mathrm{h}}}_{k-1}$ denotes the Raviart-Thomas interpolant of order $k-1$. Given $\mathbb{1}_F$ the indicator function of F in ∂K (for a $K = K_F$ in $\mathcal{T}_{\mathrm{h}}$ with F in $\mathcal{F}^K$), $\boldsymbol{\Pi}^{\mathbf{RT},\mathcal{T}_{\mathrm{h}}}_{k-1}$ in particular satisfies

$$((\mathbf{w} - \boldsymbol{\Pi}^{\mathbf{RT},\mathcal{T}_{\mathrm{h}}}_{k-1}\mathbf{w}), \mathbf{q}^K_{k-2})_K = 0 \qquad \forall \mathbf{q}^K_{k-2} \in \mathbf{P}_{k-2}(K),\ \forall K \in \mathcal{T}_{\mathrm{h}}, \tag{52}$$

$$\boldsymbol{\nabla}\cdot(\boldsymbol{\Pi}^{\mathbf{RT},\mathcal{T}_{\mathrm{h}}}_{k-1}\mathbf{w}) = \Pi^{0,\mathcal{T}_{\mathrm{h}}}_{k-1}\,\boldsymbol{\nabla}\cdot\mathbf{w} \qquad \text{on each } K, \tag{53}$$

$$((\boldsymbol{\Pi}^{\mathbf{RT},\mathcal{T}_{\mathrm{h}}}_{k-1}\mathbf{w})\cdot\mathbf{n}_F), q^F_{k-1})_{0,F} = \langle \mathbf{w}\cdot\mathbf{n}_F, q^F_{k-1}\mathbb{1}_F\rangle_{\partial K} \qquad \forall q^F_{k-1} \in \mathrm{P}_{k-1}(F),\ \forall F \in \mathcal{F}_{\mathrm{h}}. \tag{54}$$

The right-hand side in (54) is well-posed due to the regularity of $\mathbf{w}$ and $\mathbb{1}_F$, which belongs to $\mathrm{W}^{\frac{1}{\mathfrak{a}},\mathfrak{a}'}(\partial K)$, $\mathfrak{a}$ larger than 2; cf. [20, Ch. 17].

Theorem 5.1. *Let $\mathfrak{a}$ be larger than 2. Let $\mathbf{c}_{\mathrm{h}}$ in $\boldsymbol{\mathcal{D}}_{\mathrm{h}}^{k-1,\perp}$ be solution to* (50) *for $\mathbf{w}$ in $\mathbf{L}^{\mathfrak{a}}(\Omega)$ with $\boldsymbol{\nabla}\cdot\mathbf{w}$ in $\mathrm{L}^{((\mathfrak{a}')^*)'}(\Omega)$. Then, for hidden constants only depending on the degree k and the shape-regularity parameter γ, we have*

$$\|\mathbf{c}_{\mathrm{h}}\|_{\mathbf{L}^{\mathfrak{a}}(\Omega)} \lesssim \left\|\mathbf{w} - \boldsymbol{\Pi}^{\mathbf{RT},\mathcal{T}_{\mathrm{h}}}_{k-1}\mathbf{w}\right\|_{\mathbf{L}^{\mathfrak{a}}(\Omega)} + \left\|\boldsymbol{\nabla}\cdot\mathbf{w} - \Pi^{0,\mathcal{T}_{\mathrm{h}}}_{k-1}\,\boldsymbol{\nabla}\cdot\mathbf{w}\right\|_{\mathrm{L}^{((\mathfrak{a}')^*)'}(\Omega)}. \tag{55}$$

Proof. For all q_{h} in $\mathcal{Q}^k_{h,0}$, we have

$$\begin{aligned}
\int_\Omega \mathbf{c}_{\mathrm{h}}(\mathbf{w})\cdot\boldsymbol{\nabla}_{\mathrm{h}}\,\mathrm{q}_{\mathrm{h}}\;\mathrm{d}\mathbf{x} &\overset{(50)}{=} -\int_\Omega \mathbf{w}\cdot\boldsymbol{\nabla}_{\mathrm{h}}\,\mathrm{q}_{\mathrm{h}}\;\mathrm{d}\mathbf{x} - \int_\Omega (\boldsymbol{\nabla}\cdot\mathbf{w})\,\mathrm{q}_{\mathrm{h}}\;\mathrm{d}\mathbf{x} + \int_{\Gamma_N} (\mathbf{w}\cdot\mathbf{n}_\Omega)\,\mathrm{q}_{\mathrm{h}}\;\mathrm{d}s \\
&\overset{\text{(IBP)}}{=} -\sum_{F\in\mathcal{F}_{\mathrm{h}}} \langle \mathbf{w}\cdot\mathbf{n}_F, [\![\mathrm{q}_{\mathrm{h}}]\!]\,\mathbb{1}_F\rangle_{\partial K_F} \\
&\overset{(\mathrm{q}_{\mathrm{h}}\in\mathcal{Q}^k_{h,0}),(54)}{=} -\sum_{F\in\mathcal{F}_{\mathrm{h}}} \Big\langle (\mathbf{w} - \boldsymbol{\Pi}^{\mathbf{RT},\mathcal{T}_{\mathrm{h}}}_{k-1}\mathbf{w})\cdot\mathbf{n}_F), \Big([\![\mathrm{q}_{\mathrm{h}}]\!] - \Big[\!\Big[\Pi^{0,\mathcal{T}_{\mathrm{h}}}_0\,\mathrm{q}_{\mathrm{h}}\Big]\!\Big]\Big)\mathbb{1}_F\Big\rangle_{\partial K_F} \\
&\leq \sum_{K\in\mathcal{T}_{\mathrm{h}}} \Big(\sum_{F\in\mathcal{F}^K} \left\|(\mathbf{w} - \boldsymbol{\Pi}^{\mathbf{RT},\mathcal{T}_{\mathrm{h}}}_{k-1}\mathbf{w})\cdot\mathbf{n}_K\right\|^{\mathfrak{a}}_{\left(\mathrm{W}^{\frac{1}{\mathfrak{a}},\mathfrak{a}'}(F)\right)^*}\Big)^{\frac{1}{\mathfrak{a}}} \left\|\mathrm{q}_{\mathrm{h}} - \Pi^{0,\mathcal{T}_{\mathrm{h}}}_0\,\mathrm{q}_{\mathrm{h}}\right\|_{\mathrm{W}^{\frac{1}{\mathfrak{a}},\mathfrak{a}'}(\partial K)}.
\end{aligned} \tag{56}$$

The dual norms on the right-hand side are well-posed since $\mathfrak{a}$ is larger than 2. We first derive a bound for the second term on the right-hand side of (56). The continuous trace inequality (5) and Poincaré-Steklov's inequality (6) entail

$$\left\|\mathrm{q}_{\mathrm{h}} - \Pi^{0,\mathcal{T}_{\mathrm{h}}}_0\,\mathrm{q}_{\mathrm{h}}\right\|_{\mathrm{W}^{\frac{1}{\mathfrak{a}},\mathfrak{a}'}(\partial K)} \lesssim \|\boldsymbol{\nabla}\,\mathrm{q}_{\mathrm{h}}\|_{\mathbf{L}^{\mathfrak{a}'}(K)}. \tag{57}$$

Next, we derive an upper bound for the first term on the right-hand side of (56). Given F in $\mathcal{F}^K$, K in $\mathcal{T}_{\mathrm{h}}$, a duality argument gives

$$\left\|(\mathbf{w} - \boldsymbol{\Pi}^{\mathbf{RT},\mathcal{T}_{\mathrm{h}}}_{k-1}\mathbf{w})\cdot\mathbf{n}_K\right\|_{(\mathrm{W}^{\frac{1}{\mathfrak{a}},\mathfrak{a}'}(F))^*} := \sup_{\varphi\in\mathrm{W}^{\frac{1}{\mathfrak{a}},\mathfrak{a}'}(F)} \frac{\langle(\mathbf{w} - \boldsymbol{\Pi}^{\mathbf{RT},\mathcal{T}_{\mathrm{h}}}_{k-1}\mathbf{w})\cdot\mathbf{n}_K, \varphi\rangle}{\|\varphi\|_{\mathrm{W}^{\frac{1}{\mathfrak{a}},\mathfrak{a}'}(F)}}. \tag{58}$$

There exists a stable facet-to-cell lifting operator $\mathcal{L}^K_F : \mathrm{W}^{\frac{1}{\mathfrak{a}},\mathfrak{a}'}(F) \to \mathrm{W}^{1,\mathfrak{a}'}(K)$, cf. [20, Lem. 17.1 and Eq. (17.8)], which requires $\mathfrak{a}$ larger than 2 and combines the zero-extension from an F in $\mathcal{F}^K$ to ∂K with the right-inverse of the trace operator over K. In particular, it holds true that

$$\mathcal{L}^K_F(\phi) = \phi\mathbb{1}_F \quad \text{on } \partial K, \qquad \left|\mathcal{L}^K_F(\phi)\right|_{\mathrm{W}^{1,\mathfrak{a}'}(K)} \leq C_{\mathcal{L}}\|\phi\|_{\mathrm{W}^{\frac{1}{\mathfrak{a}},\mathfrak{a}'}(F)} \qquad \forall \phi \in \mathrm{W}^{1,\mathfrak{a}'}(K). \tag{59}$$

For all F and K_F such that F belongs to $\mathcal{F}^K$, let ψ denote $\mathcal{L}_F^{K_F}(\varphi - \Pi_{k-1}^{0,\mathcal{F}_\mathrm{h}}\varphi)$. Hölder's inequality entails

$$\begin{aligned}
&\langle(\mathbf{w} - \mathbf{\Pi}_{k-1}^{\mathbf{RT},\mathcal{T}_\mathrm{h}}\mathbf{w})\cdot\mathbf{n}_K, \varphi\rangle_F \\
&\overset{(54)}{=} \langle(\mathbf{w} - \mathbf{\Pi}_{k-1}^{\mathbf{RT},\mathcal{T}_\mathrm{h}}\mathbf{w})\cdot\mathbf{n}_K, \varphi - \Pi_{k-1}^{0,\mathcal{F}_\mathrm{h}}\varphi\rangle_F \overset{(59)}{=} \langle(\mathbf{w} - \mathbf{\Pi}_{k-1}^{\mathbf{RT},\mathcal{T}_\mathrm{h}}\mathbf{w})\cdot\mathbf{n}_K, \psi\rangle_{\partial K_F} \\
&\overset{(\mathrm{IBP})}{=} \int_{K_F}(\mathbf{w} - \mathbf{\Pi}_{k-1}^{\mathbf{RT},\mathcal{T}_\mathrm{h}}\mathbf{w})\cdot\boldsymbol{\nabla}\psi\,\mathrm{d}\mathbf{x} + \int_{K_F}(\boldsymbol{\nabla}\cdot(\mathbf{w} - \mathbf{\Pi}_{k-1}^{\mathbf{RT},\mathcal{T}_\mathrm{h}}\mathbf{w}))\psi\,\mathrm{d}\mathbf{x} \\
&\overset{(3),(6),(53)}{\lesssim} \Big(\Big\|\mathbf{w} - \mathbf{\Pi}_{k-1}^{\mathbf{RT},\mathcal{T}_\mathrm{h}}\mathbf{w}\Big\|_{\mathbf{L}^{\mathfrak{a}}(K_F)} + \Big\|\boldsymbol{\nabla}\cdot\mathbf{w} - \Pi_{k-1}^{0,\mathcal{T}_\mathrm{h}}\boldsymbol{\nabla}\cdot\mathbf{w}\Big\|_{\mathrm{L}^{((\mathfrak{a}')^*)'}(K_F)}\Big)|\psi|_{\mathrm{W}^{1,\mathfrak{a}'}(K_F)} \\
&\overset{(59)}{\lesssim} \Big(\Big\|\mathbf{w} - \mathbf{\Pi}_{k-1}^{\mathbf{RT},\mathcal{T}_\mathrm{h}}\mathbf{w}\Big\|_{\mathbf{L}^{\mathfrak{a}}(K_F)} + \Big\|\boldsymbol{\nabla}\cdot\mathbf{w} - \Pi_{k-1}^{0,\mathcal{T}_\mathrm{h}}\boldsymbol{\nabla}\cdot\mathbf{w}\Big\|_{\mathrm{L}^{((\mathfrak{a}')^*)'}(K_F)}\Big)\|\varphi\|_{\mathrm{W}^{\frac{1}{\mathfrak{a}},\mathfrak{a}'}(F)}.
\end{aligned} \tag{60}$$

Combining (58) and (60), we deduce

$$\begin{aligned}
&\Big\|\mathbf{w}\cdot\mathbf{n}_K - \Pi_{k-1}^{0,\mathcal{F}_\mathrm{h}}(\mathbf{w}\cdot\mathbf{n}_K)\Big\|_{(\mathrm{W}^{\frac{1}{\mathfrak{a}},\mathfrak{a}'}(F))^*} \\
&\lesssim \Big\|\mathbf{w} - \mathbf{\Pi}_{k-1}^{\mathbf{RT},\mathcal{T}_\mathrm{h}}\mathbf{w}\Big\|_{\mathbf{L}^{\mathfrak{a}}(K_F)} + \Big\|\boldsymbol{\nabla}\cdot\mathbf{w} - \Pi_{k-1}^{0,\mathcal{T}_\mathrm{h}}\boldsymbol{\nabla}\cdot\mathbf{w}\Big\|_{\mathrm{L}^{((\mathfrak{a}')^*)'}(K_F)}.
\end{aligned} \tag{61}$$

Since

$$\frac{\mathfrak{a}}{((\mathfrak{a}')^*)'} = \frac{d+\mathfrak{a}}{d} > 1, \tag{62}$$

Jensen's inequality for sequences entails

$$\begin{aligned}
&\Big(\sum_{K\in\mathcal{T}_\mathrm{h}}\Big\|\boldsymbol{\nabla}\cdot\mathbf{w} - \Pi_{k-1}^{0,\mathcal{T}_\mathrm{h}}\boldsymbol{\nabla}\cdot\mathbf{w}\Big\|_{\mathrm{L}^{((\mathfrak{a}')^*)'}(K)}^{\mathfrak{a}}\Big)^{\frac{1}{\mathfrak{a}}} = \Big(\sum_{K\in\mathcal{T}_\mathrm{h}}\Big\|\boldsymbol{\nabla}\cdot\mathbf{w} - \Pi_{k-1}^{0,\mathcal{T}_\mathrm{h}}\boldsymbol{\nabla}\cdot\mathbf{w}\Big\|_{\mathrm{L}^{((\mathfrak{a}')^*)'}(K)}^{((\mathfrak{a}')^*)'\frac{\mathfrak{a}}{((\mathfrak{a}')^*)'}}\Big)^{\frac{1}{\mathfrak{a}}} \\
&\overset{(62)}{\leq} \Big(\sum_{K\in\mathcal{T}_\mathrm{h}}\Big\|\boldsymbol{\nabla}\cdot\mathbf{w} - \Pi_{k-1}^{0,\mathcal{T}_\mathrm{h}}\boldsymbol{\nabla}\cdot\mathbf{w}\Big\|_{\mathrm{L}^{((\mathfrak{a}')^*)'}(K)}^{((\mathfrak{a}')^*)'}\Big)^{\frac{1}{((\mathfrak{a}')^*)'}} = \Big\|\boldsymbol{\nabla}\cdot\mathbf{w} - \Pi_{k-1}^{0,\mathcal{T}_\mathrm{h}}\boldsymbol{\nabla}\cdot\mathbf{w}\Big\|_{\mathrm{L}^{((\mathfrak{a}')^*)'}(\Omega)}.
\end{aligned}$$

Combining the above display, (61), (56), and (57) yields

$$\int_\Omega \mathbf{c}_\mathrm{h}\cdot\boldsymbol{\nabla}_\mathrm{h}\,\mathrm{q}_\mathrm{h}\,\mathrm{d}\mathbf{x} \lesssim \Big(\Big\|\mathbf{w} - \mathbf{\Pi}_{k-1}^{\mathbf{RT},\mathcal{T}_\mathrm{h}}\mathbf{w}\Big\|_{\mathbf{L}^{\mathfrak{a}}(K)} + \Big\|\boldsymbol{\nabla}\cdot\mathbf{w} - \Pi_{k-1}^{0,\mathcal{T}_\mathrm{h}}\boldsymbol{\nabla}\cdot\mathbf{w}\Big\|_{\mathrm{L}^{((\mathfrak{a}')^*)'}(\Omega)}\Big)\|\boldsymbol{\nabla}_\mathrm{h}\,\mathrm{q}_\mathrm{h}\|_{\mathbf{L}^{\mathfrak{a}'}(\Omega)}. \tag{63}$$

The assertion follows from the inf-sup condition (42) and the fact that $\mathbf{c}_\mathrm{h}$ is selected in $\boldsymbol{\mathcal{D}}_\mathrm{h}^{k-1,\perp}$. □

We have strong convergence of several interpolation and projection operators in certain norms.

Lemma 5.2. *Let* $\mathbf{w}$ *be in* $\mathbf{L}^{\mathfrak{a}}(\Omega)$ *with* $\boldsymbol{\nabla}\cdot\mathbf{w}$ *in* $\mathrm{L}^{((\mathfrak{a}')^*)'}(\Omega)$, $\mathfrak{a}$ *larger than* 2, *and* q *in* $\mathrm{W}^{1,s'}(\Omega)$, s' *larger than* 1. *Given* $\mathbf{\Pi}_{k-1}^{0,\mathcal{T}_\mathrm{h}}$ *and* $\Pi_{k-1}^{0,\mathcal{T}_\mathrm{h}}$, $\mathbf{\Pi}_{k-1}^{\mathbf{RT},\mathcal{T}_\mathrm{h}}$, $\mathbf{P}_\mathrm{h}$, *and* $\mathcal{I}_k$ *as in* (23), (52)–(53)–(54), (51), *and* (48), *we have*

$$\lim_{\mathrm{h}\to0}\mathbf{\Pi}_{k-1}^{0,\mathcal{T}_\mathrm{h}}\mathbf{w} = \mathbf{w}, \qquad \lim_{\mathrm{h}\to0}\mathbf{\Pi}_{k-1}^{\mathbf{RT},\mathcal{T}_\mathrm{h}}\mathbf{w} = \mathbf{w}, \qquad \lim_{\mathrm{h}\to0}\mathbf{P}_\mathrm{h}(\mathbf{w}) = \mathbf{w}, \qquad \textit{in } \mathbf{L}^{\mathfrak{a}}(\Omega) \tag{64}$$

$$\lim_{\mathrm{h}\to0}\Pi_{k-1}^{0,\mathcal{T}_\mathrm{h}}\boldsymbol{\nabla}\cdot\mathbf{w} = \boldsymbol{\nabla}\cdot\mathbf{w}, \qquad \textit{in } \mathbf{L}^{((\mathfrak{a}')^*)'}(\Omega), \tag{65}$$

$$\lim_{\mathrm{h}\to0}\boldsymbol{\nabla}_\mathrm{h}\,\mathcal{I}_k\,\mathrm{q} = \boldsymbol{\nabla}\,\mathrm{q} \qquad \textit{in } \mathbf{L}^{s'}(\Omega). \tag{66}$$

Proof. The validity of (64) and (66) follows from a density argument and the stability of $\mathbf{\Pi}_{k-1}^{0,\mathcal{T}_\mathrm{h}}$ and $\mathcal{I}_k$ in the correct norms. The proof of (65) follows recalling that $\mathbf{P}_\mathrm{h}(\mathbf{w})$ is $\mathbf{\Pi}_{k-1}^{0,\mathcal{T}_\mathrm{h}}(\mathbf{w}) + \mathbf{c}_\mathrm{h}(\mathbf{w})$, and applying (64) to the first term, and Theorem 5.1 and standard polynomial approximation properties to the second term. □

Remark 3. In light of (46a) and (46b), $\mathbf{u}_\mathrm{h}$ and $\boldsymbol{\nabla}_\mathrm{h}\,\mathrm{p}_\mathrm{h}$ are uniformly bounded in $\mathbf{L}^{\alpha}(\Omega)$ and $\mathbf{L}^{\alpha'}(\Omega)$, respectively; hence, we deduce the weak convergence in $\mathbf{L}^{\alpha}(\Omega)$ of a subsequence of $\mathbf{u}_\mathrm{h}$ and in $\mathbf{L}^{\alpha'}(\Omega)$ of a subsequence of $\boldsymbol{\nabla}_\mathrm{h}\,\mathrm{p}_\mathrm{h}$. With an abuse of notation, we still denote these subsequences by $\mathbf{u}_\mathrm{h}$ and $\boldsymbol{\nabla}_\mathrm{h}\,\mathrm{p}_\mathrm{h}$. ■

We show the weak convergence in $\mathbf{L}^\alpha(\Omega)$ of $\mathbf{u}_\mathrm{h}$ to $\mathbf{u}$.

Lemma 5.3. *Let* $\mathbf{u}$ *and* $\mathbf{u}_\mathrm{h}$ *for a mesh* $\mathcal{T}_\mathrm{h}$ *be the solutions to* (16) *and* (45)*, respectively. Then, we have*

$$\lim_{\mathrm{h}\to 0} \mathbf{u}_\mathrm{h} = \mathbf{u} \qquad \textit{weakly in } \mathbf{L}^\alpha(\Omega).$$

Proof. Let $\widetilde{\mathbf{u}}$ denote the weak limit in $\mathbf{L}^\alpha(\Omega)$ of the subsequence $\{\mathbf{u}_\mathrm{h}\}$ in Remark 3. The assertion follows if we prove $\widetilde{\mathbf{u}} = \mathbf{u}$. Given $\mathbf{u}_\ell$ as in (14), we consider the splittings

$$\widetilde{\mathbf{u}} = (\widetilde{\mathbf{u}} - \mathbf{u}_\ell) + \mathbf{u}_\ell =: \widetilde{\mathbf{u}}_0 + \mathbf{u}_\ell. \qquad\qquad \mathbf{u}_\mathrm{h} = (\mathbf{u}_\mathrm{h} - \mathbf{P}_\mathrm{h}(\mathbf{u}_\ell)) + \mathbf{P}_\mathrm{h}(\mathbf{u}_\ell) =: \mathbf{u}_{\mathrm{h},0} + \mathbf{u}_{\mathrm{h},\ell}. \tag{67}$$

We preliminarily observe

$$\begin{aligned} 0 &\overset{(21a)}{\leq} \int_\Omega \big(\boldsymbol{\mathcal{A}}(\mathbf{u}_{\mathrm{h},0} + \mathbf{u}_{\mathrm{h},\ell}) - \boldsymbol{\mathcal{A}}(\mathbf{v}_\mathrm{h} + \mathbf{u}_{\mathrm{h},\ell})\big) \cdot (\mathbf{u}_{\mathrm{h},0} - \mathbf{v}_\mathrm{h})\,\mathrm{d}\mathbf{x} \\ &\overset{(45)}{=} \int_\Omega -\boldsymbol{\mathcal{A}}(\mathbf{v}_\mathrm{h} + \mathbf{u}_{\mathrm{h},\ell}) \cdot (\mathbf{u}_{\mathrm{h},0} - \mathbf{v}_\mathrm{h})\,\mathrm{d}\mathbf{x} \qquad \forall \mathbf{v}_\mathrm{h} \in \boldsymbol{\mathcal{V}}_\mathrm{h}^{k-1}. \end{aligned} \tag{68}$$

Now, let $\mathbf{v}$ be in $\boldsymbol{\mathcal{D}}$ and $\mathbf{v}_\mathrm{h} := \mathbf{P}_\mathrm{h}(\mathbf{v})$. We have

$$\begin{aligned} \|\boldsymbol{\mathcal{A}}(\mathbf{P}_\mathrm{h}(\mathbf{v}) + \mathbf{u}_{\mathrm{h},\ell}) - \boldsymbol{\mathcal{A}}(\mathbf{v} + \mathbf{u}_\ell)\|_{\mathbf{L}^{\alpha'}(\Omega)} &\overset{(20)}{\leq} |\Omega|^{\frac{1}{\alpha}} \Big[\frac{\mu}{\rho}\|\underline{\mathbf{K}}^{-1}\|_{\underline{\mathbf{L}}^{\frac{\alpha}{\alpha+2}}(\Omega)} + \mathrm{C_{BL}}\,\frac{\beta}{\rho}\cdot \\ &\cdot \big(\|\mathbf{P}_\mathrm{h}(\mathbf{v}) + \mathbf{u}_{\mathrm{h},\ell}\|_{\mathbf{L}^\alpha(\Omega)}^{\alpha-2} + \|\mathbf{v} + \mathbf{u}_\ell\|_{\mathbf{L}^\alpha(\Omega)}^{\alpha-2}\big)\Big] \big(\|(\mathbf{P}_\mathrm{h}(\mathbf{v}) - \mathbf{v}) + (\mathbf{u}_{\mathrm{h},\ell} - \mathbf{u}_\ell)\|_{\mathbf{L}^\alpha(\Omega)}\big). \end{aligned}$$

Using (65) and Remark 3 entails

$$\lim_{\mathrm{h}\to 0} \boldsymbol{\mathcal{A}}(\mathbf{P}_\mathrm{h}(\mathbf{v}) + \mathbf{u}_{\mathrm{h},\ell}) = \boldsymbol{\mathcal{A}}(\mathbf{v} + \mathbf{u}_\ell) \qquad \text{in } \mathbf{L}^{\alpha'}(\Omega). \tag{69}$$

The weak convergence of $\mathbf{u}_{\mathrm{h},0}$ to $\widetilde{\mathbf{u}}_0$, which is a consequence of the weak convergence of $\mathbf{u}_\mathrm{h}$ to $\widetilde{\mathbf{u}}$ and the strong convergence of $\mathbf{u}_{\mathrm{h},\ell}$ to $\widetilde{\mathbf{u}}_\ell$, and the strong convergence of $\mathbf{P}_\mathrm{h}(\mathbf{v})$ to $\mathbf{v}$ in $\mathbf{L}^\alpha(\Omega)$ entail

$$\lim_{\mathrm{h}\to 0} (\mathbf{u}_{\mathrm{h},0} - \mathbf{P}_\mathrm{h}(\mathbf{v})) = \widetilde{\mathbf{u}}_0 - \mathbf{v} \qquad \text{weakly in } \mathbf{L}^\alpha(\Omega). \tag{70}$$

Then, (69) and (70) allow for passing to the limit in (68) and obtain

$$\int_\Omega \boldsymbol{\mathcal{A}}(\mathbf{v} + \mathbf{u}_\ell) \cdot (\widetilde{\mathbf{u}}_0 - \mathbf{v})\,\mathrm{d}\mathbf{x} \leq 0 \qquad\qquad \forall \mathbf{v} \in \boldsymbol{\mathcal{D}}.$$

Given an arbitrary $\boldsymbol{\varphi}$ in $\boldsymbol{\mathcal{D}}$ and $\varepsilon > 0$, fixing $\mathbf{v}$ as $\widetilde{\mathbf{u}}_0 + \varepsilon\boldsymbol{\varphi}$ and as $\widetilde{\mathbf{u}}_0 - \varepsilon\boldsymbol{\varphi}$, the hemi-continuity (21c) yields

$$\int_\Omega \boldsymbol{\mathcal{A}}(\widetilde{\mathbf{u}}_0 + \mathbf{u}_\ell) \cdot \boldsymbol{\varphi}\,\mathrm{d}\mathbf{x} = 0 \qquad\qquad \forall \boldsymbol{\varphi} \in \boldsymbol{\mathcal{D}}.$$

The assertion follows from the uniqueness of the solution to (16). □

We prove an auxiliary result, which extends [23, Eq. (3.36)] to the general-order case.

Lemma 5.4. *Let* $(\mathbf{u}, \mathrm{p})$ *and* $(\mathbf{u}_\mathrm{h}, \mathrm{p}_\mathrm{h})$ *for a mesh* $\mathcal{T}_\mathrm{h}$ *be the solutions to* (10) *and* (41)*, and* $k > 1$*. Then, we have*

$$\int_\Omega (\boldsymbol{\mathcal{A}}(\mathbf{u}) - \boldsymbol{\mathcal{A}}(\mathbf{u}_\mathrm{h})) \cdot \mathbf{v}_\mathrm{h}\,\mathrm{d}\mathbf{x} = \int_\Omega (\mathrm{p} - \mathcal{I}_k\,\mathrm{p})(\boldsymbol{\nabla}_\mathrm{h} \cdot \mathbf{v}_\mathrm{h} - \Pi_{k-3}^{0,\mathcal{T}_\mathrm{h}}\,\boldsymbol{\nabla}_\mathrm{h} \cdot \mathbf{v}_\mathrm{h})\,\mathrm{d}\mathbf{x} \qquad \forall \mathbf{v}_\mathrm{h} \in \boldsymbol{\mathcal{D}}_\mathrm{h}^{k-1}. \tag{71}$$

If $k = 1$*, then we recover [23, Eq. (3.36)], i.e.,*

$$\int_\Omega (\boldsymbol{\mathcal{A}}(\mathbf{u}) - \boldsymbol{\mathcal{A}}(\mathbf{u}_\mathrm{h})) \cdot \mathbf{v}_\mathrm{h}\,\mathrm{d}\mathbf{x} = 0 \qquad\qquad \forall \mathbf{v}_\mathrm{h} \in \boldsymbol{\mathcal{D}}_\mathrm{h}^{0}. \tag{72}$$

Proof. Given $\mathbf{v}_\mathrm{h}$ in $\boldsymbol{\mathcal{D}}_\mathrm{h}^{k-1}$ and K in $\mathcal{T}_\mathrm{h}$, we have

$$\begin{aligned}
&\int_K (\mathrm{p} - \mathcal{I}_k\,\mathrm{p})(\boldsymbol{\nabla}\cdot\mathbf{v}_\mathrm{h} - \Pi_{k-3}^{0,\mathcal{T}_\mathrm{h}}\boldsymbol{\nabla}\cdot\mathbf{v}_\mathrm{h})\,\mathrm{d}\mathbf{x} \overset{(28b)}{=} \int_K (\mathrm{p} - \mathcal{I}_k\,\mathrm{p})\,\boldsymbol{\nabla}\cdot\mathbf{v}_\mathrm{h}\,\mathrm{d}\mathbf{x}\\
&\overset{(28a)}{=} \int_{\partial K} (\mathcal{I}_k\,\mathrm{p} - \mathrm{p})(\mathbf{v}_\mathrm{h}\cdot\mathbf{n}_K)\,\mathrm{d}s - \int_K (\mathcal{I}_k\,\mathrm{p} - \mathrm{p})\,\boldsymbol{\nabla}\cdot\mathbf{v}_\mathrm{h}\,\mathrm{d}\mathbf{x} = \int_K \boldsymbol{\nabla}(\mathcal{I}_k\,\mathrm{p} - \mathrm{p})\cdot\mathbf{v}_\mathrm{h}\,\mathrm{d}\mathbf{x}\\
&\overset{(\mathbf{v}_\mathrm{h}\in\boldsymbol{\mathcal{D}}_\mathrm{h}^{k-1})}{=} \int_K \boldsymbol{\nabla}(\mathcal{I}_k\,\mathrm{p} - \mathrm{p})\cdot\mathbf{v}_\mathrm{h}\,\mathrm{d}\mathbf{x} + \int_K \boldsymbol{\nabla}(\mathrm{p}_\mathrm{h} - \mathcal{I}_k\,\mathrm{p})\cdot\mathbf{v}_\mathrm{h}\,\mathrm{d}\mathbf{x} = \int_K \boldsymbol{\nabla}(\mathrm{p}_\mathrm{h} - \mathrm{p})\cdot\mathbf{v}_\mathrm{h}\,\mathrm{d}\mathbf{x}.
\end{aligned} \tag{73}$$

The assertion follows from summing over K in $\mathcal{T}_\mathrm{h}$, subtracting (10) to (41), and the above display. □

We now show the strong convergence in $\mathbf{L}^2(\Omega)$ of $\mathbf{u}_\mathrm{h}$ to $\mathbf{u}$.

Lemma 5.5. *Let* $\mathbf{u}$ *and* $\mathbf{u}_\mathrm{h}$ *for a mesh* $\mathcal{T}_\mathrm{h}$ *be the solutions to* (16) *and* (45)*, respectively. Then, we have*

$$\lim_{\mathrm{h}\to 0}\mathbf{u}_\mathrm{h} = \mathbf{u} \qquad \textit{in } \mathbf{L}^2(\Omega).$$

Proof. Since $\mathbf{u}_0$ belongs to $\boldsymbol{\mathcal{D}}$, we write

$$0 \overset{(11),(50)}{=} \int_\Omega \mathbf{c}_\mathrm{h}(\mathbf{u}_0)\cdot\boldsymbol{\nabla}_\mathrm{h}\,\mathrm{q}_\mathrm{h}\;\mathrm{d}\mathbf{x} \overset{(51)}{=} \int_\Omega \mathbf{P}_\mathrm{h}(\mathbf{u}_0)\cdot\boldsymbol{\nabla}_\mathrm{h}\,\mathrm{q}_\mathrm{h}\;\mathrm{d}\mathbf{x} - \int_\Omega \boldsymbol{\Pi}_{k-1}^{0,\mathcal{T}_\mathrm{h}}\mathbf{u}_0\cdot\boldsymbol{\nabla}_\mathrm{h}\,\mathrm{q}_\mathrm{h}\;\mathrm{d}\mathbf{x} \qquad \forall\,\mathrm{q}_\mathrm{h}\in\mathcal{Q}_{h,0}^k,$$

i.e., thanks to (67), $\mathbf{u}_{\mathrm{h},0}$ belongs to $\boldsymbol{\mathcal{D}}_\mathrm{h}^{k-1}$. Then, for $k>1$, we write

$$\begin{aligned}
\frac{\mu}{\rho}\lambda_{\min}\|\mathbf{u}_\mathrm{h} - \mathbf{P}_\mathrm{h}(\mathbf{u})\|^2_{\mathbf{L}^2(\Omega)} &\overset{(67)}{=} \frac{\mu}{\rho}\lambda_{\min}\|\mathbf{u}_{\mathrm{h},0} - \mathbf{P}_\mathrm{h}(\mathbf{u}_0)\|^2_{\mathbf{L}^2(\Omega)}\\
&\overset{(21a)}{\le} \int_\Omega (\boldsymbol{\mathcal{A}}(\mathbf{u}_{\mathrm{h},0} + \mathbf{u}_{\mathrm{h},\ell}) - \boldsymbol{\mathcal{A}}(\mathbf{P}_\mathrm{h}(\mathbf{u}_0) + \mathbf{u}_{\mathrm{h},\ell}))\cdot(\mathbf{u}_{\mathrm{h},0} - \mathbf{P}_\mathrm{h}(\mathbf{u}_0))\,\mathrm{d}\mathbf{x}\\
&\overset{(67),(71),(73)}{=} \int_\Omega (\boldsymbol{\mathcal{A}}(\mathbf{u}_0 + \mathbf{u}_\ell) - \boldsymbol{\mathcal{A}}(\mathbf{P}_\mathrm{h}(\mathbf{u}_0) + \mathbf{u}_{\mathrm{h},\ell}))\cdot(\mathbf{u}_{\mathrm{h},0} - \mathbf{P}_\mathrm{h}(\mathbf{u}_0))\,\mathrm{d}\mathbf{x}\\
&\qquad + \int_\Omega \boldsymbol{\nabla}_\mathrm{h}(\mathcal{I}_k\,\mathrm{p} - \mathrm{p})\cdot(\mathbf{u}_{\mathrm{h},0} - \mathbf{P}_\mathrm{h}(\mathbf{u}_0))\,\mathrm{d}\mathbf{x}.
\end{aligned} \tag{74}$$

Proceeding as in the proof of (69), $\boldsymbol{\mathcal{A}}(\mathbf{P}_\mathrm{h}(\mathbf{u}_0) + \mathbf{u}_{\mathrm{h},\ell})$ converges strongly in $\mathbf{L}^{\alpha'}(\Omega)$ to $\boldsymbol{\mathcal{A}}(\mathbf{u}_0 + \mathbf{u}_\ell)$; $\mathbf{u}_{\mathrm{h},0}$ converges weakly in $\mathbf{L}^\alpha(\Omega)$ to $\mathbf{u}_0$, cf. Lemma 5.3; $\mathbf{P}_\mathrm{h}\,\mathbf{u}_0$ converges strongly in $\mathbf{L}^\alpha(\Omega)$ to $\mathbf{u}_0$, cf. (64). Therefore, we can pass to the limit for h going to 0 in the first term on the right-hand side of (74) and get 0. On the other hand, $\mathbf{P}_\mathrm{h}(\mathbf{u}_0)$ converges strongly in $\mathbf{L}^\alpha(\Omega)$ to $\mathbf{u}_0$, cf. (64); $\boldsymbol{\nabla}_\mathrm{h}\,\mathcal{I}_k\,\mathrm{p}$ converges strongly in $\mathbf{L}^{\alpha'}(\Omega)$ to $\boldsymbol{\nabla}_\mathrm{h}\,\mathrm{p}$, cf. (66). Therefore, we can pass to the limit for h going to 0 in the second term on the right-hand side of (74) and get 0. Therefore, we can pass to the limit in (74) and the assertion follows for k larger than 1.

The case $k=1$ is dealt with analogously and no pressure term appears; cf. (72) and [23]. □

Define $\mathbf{w}_\mathrm{h}$ as

$$\mathbf{w}_\mathrm{h} := \boldsymbol{\nabla}_\mathrm{h}\,\mathrm{p}_\mathrm{h}\,. \tag{75}$$

We have that

- $\mathbf{w}_\mathrm{h}$ is uniformly bounded in $\mathbf{L}^{\alpha'}(\Omega)$ due to Proposition 4.3, whence there exists $\mathbf{w}$ in $\mathbf{L}^{\alpha'}(\Omega)$ such that
$$\lim_{\mathrm{h}\to 0}\mathbf{w}_\mathrm{h} = \mathbf{w} \qquad \text{weakly in } \mathbf{L}^{\alpha'}(\Omega); \tag{76}$$
- p_h is uniformly bounded in $\mathbf{L}^{(\alpha')^*}(\Omega)$ due to Corollary 3.3 and Proposition 4.3, whence there exists q in $\mathrm{L}^{(\alpha')^*}(\Omega)$ such that
$$\lim_{\mathrm{h}\to 0}\mathrm{p}_\mathrm{h} = \mathrm{q} \qquad \text{weakly in } \mathrm{L}^{(\alpha')^*}(\Omega). \tag{77}$$

We show the weak convergence in $\mathbf{L}^{\alpha'}(\Omega)$ of the gradient of the potential variable.

Proposition 5.6. *Let* $(\mathbf{u}, \mathrm{p})$ *and* $(\mathbf{u}_\mathrm{h}, \mathrm{p}_\mathrm{h})$ *for a mesh* $\mathcal{T}_\mathrm{h}$ *be the solutions to* (16) *and* (45)*, respectively, and let the* (47) *be valid. Then, for* $\mathbf{w}_\mathrm{h}$ *as in* (75)*, we have*

$$\lim_{\mathrm{h}\to 0} \mathbf{w}_\mathrm{h} = \boldsymbol{\nabla}\, \mathrm{p} \qquad \textit{weakly in } \mathbf{L}^{\alpha'}(\Omega).$$

Proof. We split the proof into two steps.

Step 1: proving that the limit is the gradient of a function q**.** An integration by parts yields

$$\int_\Omega \mathbf{w}_\mathrm{h} \cdot \boldsymbol{\varphi} \,\mathrm{d}\mathbf{x} \overset{(75)}{:=} \sum_{K\in\mathcal{T}_\mathrm{h}} \int_K \boldsymbol{\nabla}\, \mathrm{p}_\mathrm{h} \cdot \boldsymbol{\varphi} \,\mathrm{d}\mathbf{x} = \int_{\mathcal{F}_\mathrm{h}^I} [\![\mathrm{p}_\mathrm{h}]\!] \,(\boldsymbol{\varphi}\cdot \mathbf{n}_F) \,\mathrm{d}s - \int_\Omega \mathrm{p}_\mathrm{h}\, \boldsymbol{\nabla}\cdot \boldsymbol{\varphi} \,\mathrm{d}\mathbf{x} \qquad \forall \boldsymbol{\varphi} \in [\mathcal{C}_0^\infty(\Omega)]^2. \tag{78}$$

Standard polynomial approximation (PA) results yield

$$\Big| \int_{\mathcal{F}_\mathrm{h}^I} [\![\mathrm{p}_\mathrm{h}]\!] \,(\boldsymbol{\varphi}\cdot \mathbf{n}_F) \,\mathrm{d}s \Big| \overset{(\mathrm{IBP}),(50)}{=} \Big| \int_\Omega \mathbf{c}_\mathrm{h}(\boldsymbol{\varphi}) \cdot \boldsymbol{\nabla}_\mathrm{h}\, \mathrm{p}_\mathrm{h} \;\mathrm{d}\mathbf{x} \Big| \overset{(\mathrm{PA}),(63)}{\lesssim} \mathrm{h}\, |\boldsymbol{\varphi}|_{\mathbf{W}^{1,\alpha}(\Omega)} \|\boldsymbol{\nabla}_\mathrm{h}\, \mathrm{p}_\mathrm{h}\|_{\mathbf{L}^{\alpha'}(\Omega)}.$$

Hence, the left-hand side of the above display tends to zero when h goes to zero, which combined with (76) and (77) allows for passing to the limit in (78) and obtain

$$\int_\Omega \mathbf{w} \cdot \boldsymbol{\varphi} \,\mathrm{d}\mathbf{x} = -\int_\Omega \mathrm{q}\, \boldsymbol{\nabla}\cdot \boldsymbol{\varphi} \,\mathrm{d}\mathbf{x},$$

i.e., $\mathbf{w} = \boldsymbol{\nabla}\, \mathrm{q}$ and q belongs to $\mathrm{W}^{1,\alpha'}(\Omega)$.

Step 2: proving that q **equals** p**.** Given $\mathbf{v}$ in $\mathbf{L}^{\frac{2\alpha}{4-\alpha}}(\Omega)$, taking $\boldsymbol{\Pi}_{k-1}^{0,\mathcal{T}_\mathrm{h}} \mathbf{v}$ as a test function in (41a) gives

$$\begin{aligned} \int_\Omega \mathbf{w}_\mathrm{h} \cdot \boldsymbol{\Pi}_{k-1}^{0,\mathcal{T}_\mathrm{h}} \mathbf{v} \,\mathrm{d}\mathbf{x} &\overset{(75)}{:=} \int_{\mathcal{T}_\mathrm{h}} \boldsymbol{\nabla}_\mathrm{h}\, \mathrm{p}_\mathrm{h} \cdot \boldsymbol{\Pi}_{k-1}^{0,\mathcal{T}_\mathrm{h}} \mathbf{v} \,\mathrm{d}\mathbf{x} \overset{(41\mathrm{a})}{=} -\int_\Omega \boldsymbol{\mathcal{A}}(\mathbf{u}_\mathrm{h}) \cdot \boldsymbol{\Pi}_{k-1}^{0,\mathcal{T}_\mathrm{h}} \mathbf{v} \,\mathrm{d}\mathbf{x} \\ &= -\int_\Omega (\boldsymbol{\mathcal{A}}(\mathbf{u}_\mathrm{h}) - \boldsymbol{\mathcal{A}}(\mathbf{u})) \cdot \boldsymbol{\Pi}_{k-1}^{0,\mathcal{T}_\mathrm{h}} \mathbf{v} \,\mathrm{d}\mathbf{x} + \int_\Omega \boldsymbol{\mathcal{A}}(\mathbf{u}) \cdot \boldsymbol{\Pi}_{k-1}^{0,\mathcal{T}_\mathrm{h}} \mathbf{v} \,\mathrm{d}\mathbf{x} \\ &\overset{(19)}{=} -\int_\Omega (\boldsymbol{\mathcal{A}}(\mathbf{u}_\mathrm{h}) - \boldsymbol{\mathcal{A}}(\mathbf{u})) \cdot \boldsymbol{\Pi}_{k-1}^{0,\mathcal{T}_\mathrm{h}} \mathbf{v} \,\mathrm{d}\mathbf{x} + \int_\Omega \boldsymbol{\nabla}\, \mathrm{p} \cdot \boldsymbol{\Pi}_{k-1}^{0,\mathcal{T}_\mathrm{h}} \mathbf{v} \,\mathrm{d}\mathbf{x}. \end{aligned} \tag{79}$$

Using (20) in the above display together with Hölder's inequality applied twice with exponents $(\alpha/(\alpha-2), 2, 2\alpha/(4-\alpha))$, which is an admissible choice since α is in $(2,4)$ due to (47), give

$$\begin{aligned} \Big| \int_\Omega (\boldsymbol{\mathcal{A}}(\mathbf{u}_\mathrm{h}) - \boldsymbol{\mathcal{A}}(\mathbf{u})) \cdot \boldsymbol{\Pi}_{k-1}^{0,\mathcal{T}_\mathrm{h}} \mathbf{v} \,\mathrm{d}\mathbf{x} \Big| &\le \frac{\mu}{\rho} \|\underline{\mathbf{K}}^{-1}\|_{\underline{\mathbf{L}}^{\frac{\alpha}{\alpha-2}}(\Omega)} \|\mathbf{u} - \mathbf{u}_\mathrm{h}\|_{\mathbf{L}^2(\Omega)} \Big\| \boldsymbol{\Pi}_{k-1}^{0,\mathcal{T}_\mathrm{h}} \mathbf{v} \Big\|_{\mathbf{L}^{\frac{2\alpha}{4-\alpha}}(\Omega)} \\ + \mathrm{C}_{\mathrm{BL}} \frac{\beta}{\rho} \|\mathbf{u} - \mathbf{u}_\mathrm{h}\|_{\mathbf{L}^2(\Omega)} (\|\mathbf{u}_\mathrm{h}\|_{\mathbf{L}^\alpha(\Omega)}^{\alpha-2} &+ \|\mathbf{u}\|_{\mathbf{L}^\alpha(\Omega)}^{\alpha-2}) \Big\| \boldsymbol{\Pi}_{k-1}^{0,\mathcal{T}_\mathrm{h}} \mathbf{v} \Big\|_{\mathbf{L}^{\frac{2\alpha}{4-\alpha}}(\Omega)}. \end{aligned} \tag{80}$$

The strong convergence in $\mathbf{L}^2(\Omega)$ of $\mathbf{u}_\mathrm{h}$ to $\mathbf{u}$, cf. Lemma 5.5, and the strong convergence in $\mathbf{L}^{\frac{2\alpha}{4-\alpha}}(\Omega)$ of $\boldsymbol{\Pi}_{k-1}^{0,\mathcal{T}_\mathrm{h}} \mathbf{v}$ to $\mathbf{v}$, cf. (64), imply that the left-hand side of (80) tends to zero when h goes to zero. The assertion follows passing to the limit in (79) and using the uniqueness of the solution of (16). □

5.2 Strong convergence in the natural norms

Next, we show the strong convergence of $\mathbf{u}_\mathrm{h}$ in $\mathbf{L}^\alpha(\Omega)$.

Theorem 5.7. *Let* $(\mathbf{u}, p)$ *and* $(\mathbf{u}_\mathrm{h}, \mathrm{p}_\mathrm{h})$ *for a mesh* $\mathcal{T}_\mathrm{h}$ *be the solutions to* (10) *and* (41)*, respectively, and let* (47) *be valid. Assume that* $\underline{\mathbf{K}}^{-1}$ *is in* $\underline{\mathbf{L}}^{\frac{2\alpha}{\alpha-2}}(\Omega)$*. Then, we have*

$$\lim_{\mathrm{h}\to 0} \mathbf{u}_\mathrm{h} = \mathbf{u} \qquad \textit{in } \mathbf{L}^\alpha(\Omega).$$

Proof. We have

$$0 \overset{(41a)}{=} \frac{\mu}{\rho}\int_\Omega (\underline{\mathbf{K}}^{-1})\mathbf{u}_h \cdot \mathbf{u}_h \,\mathrm{d}\mathbf{x} + \frac{\beta}{\rho}\int_\Omega |\mathbf{u}_h|^\alpha \,\mathrm{d}\mathbf{x} + \int_\Omega \boldsymbol{\nabla}_h \,\mathrm{p}_h \cdot \mathbf{u}_h \,\mathrm{d}\mathbf{x}$$
$$\overset{(\mathbf{u}_{h,0}\in\boldsymbol{\mathcal{D}}_h^{k-1})}{=} \frac{\mu}{\rho}\int_\Omega (\underline{\mathbf{K}}^{-1})\mathbf{u}_h \cdot \mathbf{u}_h \,\mathrm{d}\mathbf{x} + \frac{\beta}{\rho}\int_\Omega |\mathbf{u}_h|^\alpha \,\mathrm{d}\mathbf{x} + \int_\Omega \boldsymbol{\nabla}_h \,\mathrm{p}_h \cdot \mathbf{u}_{h,\ell} \,\mathrm{d}\mathbf{x}.$$

Using the fact that $\underline{\mathbf{K}}^{-1}$ is in $\underline{\mathbf{L}}^{\frac{2\alpha}{\alpha-2}}(\Omega)$, the strong convergence of $\mathbf{u}_h$ to $\mathbf{u}$ in $\mathbf{L}^2(\Omega)$, see Lemma 5.5, and the weak convergence of $\mathbf{u}_h$ to $\mathbf{u}$ in $\mathbf{L}^\alpha(\Omega)$, see Lemma 5.3, for the first term on the left-hand side, the weak convergence of $\boldsymbol{\nabla}_h \,\mathrm{p}_h$ to $\nabla \mathrm{p}$ in $\mathbf{L}^{\alpha'}(\Omega)$, see Proposition 5.6, and the strong convergence of $\mathbf{u}_{h,\ell}$ to $\mathbf{u}_\ell$ in $\mathbf{L}^\alpha(\Omega)$, see Lemma 5.2, for the third term on the left-hand side, and passing to the limit h going to 0 entail

$$\frac{\mu}{\rho}\int_\Omega (\underline{\mathbf{K}}^{-1})\mathbf{u} \cdot \mathbf{u} \,\mathrm{d}\mathbf{x} + \lim_{h\to 0}\frac{\beta}{\rho}\int_\Omega |\mathbf{u}_h|^\alpha \,\mathrm{d}\mathbf{x} + \int_\Omega \boldsymbol{\nabla}\,\mathrm{p} \cdot \mathbf{u} \,\mathrm{d}\mathbf{x} = 0. \tag{81}$$

Taking $\mathbf{u} = \mathbf{u}_0 + \mathbf{u}_\ell$ as test function $\mathbf{v}$ in the continuous formulation (10a) gives

$$\frac{\mu}{\rho}\int_\Omega (\underline{\mathbf{K}}^{-1})\mathbf{u} \cdot \mathbf{u} \,\mathrm{d}\mathbf{x} + \frac{\beta}{\rho}\int_\Omega |\mathbf{u}|^\alpha \,\mathrm{d}\mathbf{x} + \int_\Omega \boldsymbol{\nabla}\,\mathrm{p} \cdot \mathbf{u} \,\mathrm{d}\mathbf{x} = 0 \tag{82}$$

Taking the difference of (81) and (82) yields

$$\lim_{h\to 0} \|\mathbf{u}_h\|^\alpha_{\mathbf{L}^\alpha(\Omega)} = \|\mathbf{u}\|^\alpha_{\mathbf{L}^\alpha(\Omega)}.$$

□

Next, we show the strong convergence of $\boldsymbol{\nabla}_h \,\mathrm{p}_h$ in $\mathbf{L}^{\alpha'}(\Omega)$.

Theorem 5.8. *Let* $(\mathbf{u}, \mathrm{p})$ *and* $(\mathbf{u}_h, \mathrm{p}_h)$ *for a mesh* $\mathcal{T}_h$ *be the solutions to* (10) *and* (41)*, respectively, and let* (47) *be valid. Assume that* $\underline{\mathbf{K}}^{-1}$ *is in* $\underline{\mathbf{L}}^{\frac{2\alpha}{\alpha-2}}(\Omega)$*. Then, we have*

$$\lim_{h\to 0} \boldsymbol{\nabla}_h \,\mathrm{p}_h = \boldsymbol{\nabla}\,\mathrm{p} \qquad \textit{in } \mathbf{L}^{\alpha'}(\Omega).$$

Proof. Subtracting (10a) and (41a), we have

$$\int_\Omega (\boldsymbol{\mathcal{A}}(\mathbf{u}) - \boldsymbol{\mathcal{A}}(\mathbf{u}_h)) \cdot \mathbf{v}_h \,\mathrm{d}\mathbf{x} = \int_\Omega \boldsymbol{\nabla}_h(\mathrm{p}_h - \mathrm{p}) \cdot \mathbf{v}_h \,\mathrm{d}\mathbf{x}$$
$$= \int_\Omega \boldsymbol{\nabla}_h(\mathrm{p}_h - \mathcal{I}_k\,\mathrm{p}) \cdot \mathbf{v}_h \,\mathrm{d}\mathbf{x} + \int_\Omega \boldsymbol{\nabla}_h(\mathcal{I}_k\,\mathrm{p} - \mathrm{p}) \cdot \mathbf{v}_h \,\mathrm{d}\mathbf{x} \qquad \forall \mathbf{v}_h \in \boldsymbol{\mathcal{V}}_h^{k-1}.$$

Using (20) in the above display together with triangle's inequality and Hölder's inequality with exponents $(\alpha/(\alpha-2), \alpha, \alpha)$ give

$$\begin{aligned}\left|\int_\Omega \boldsymbol{\nabla}_h(\mathrm{p}_h - \mathcal{I}_k\,\mathrm{p}) \cdot \mathbf{v}_h \,\mathrm{d}\mathbf{x}\right| &\le \left|\int_\Omega \boldsymbol{\nabla}_h(\mathrm{p} - \mathcal{I}_k\,\mathrm{p}) \cdot \mathbf{v}_h \,\mathrm{d}\mathbf{x}\right| + \left|\int_\Omega (\boldsymbol{\mathcal{A}}(\mathbf{u}) - \boldsymbol{\mathcal{A}}(\mathbf{u}_h)) \cdot \mathbf{v}_h \,\mathrm{d}\mathbf{x}\right| \\ &\le \left|\int_\Omega \boldsymbol{\nabla}_h(\mathrm{p} - \mathcal{I}_k\,\mathrm{p}) \cdot \mathbf{v}_h \,\mathrm{d}\mathbf{x}\right| + \frac{\mu}{\rho}\|\underline{\mathbf{K}}^{-1}\|_{\underline{\mathbf{L}}^{\frac{\alpha}{\alpha-2}}(\Omega)} \|\mathbf{u} - \mathbf{u}_h\|_{\mathbf{L}^\alpha(\Omega)} \|\mathbf{v}_h\|_{\mathbf{L}^\alpha(\Omega)} \\ &\quad + \mathrm{C}_{\mathrm{BL}}\frac{\beta}{\rho}\|\mathbf{u} - \mathbf{u}_h\|_{\mathbf{L}^\alpha(\Omega)} (\|\mathbf{u}_h\|^{\alpha-2}_{\mathbf{L}^\alpha(\Omega)} + \|\mathbf{u}\|^{\alpha-2}_{\mathbf{L}^\alpha(\Omega)}) \|\mathbf{v}_h\|_{\mathbf{L}^\alpha(\Omega)}.\end{aligned} \tag{83}$$

We deduce

$$\mathfrak{b}_h \|\boldsymbol{\nabla}_h(\mathrm{p}_h - \mathcal{I}_k\,\mathrm{p})\|_{\mathbf{L}^{\alpha'}(\Omega)} \overset{(42)}{\le} \sup_{\mathbf{v}_h \in \boldsymbol{\mathcal{V}}_h^{k-1}} \frac{\int_\Omega \mathbf{v}_h \cdot \boldsymbol{\nabla}_h(\mathrm{p}_h - \mathcal{I}_k\,\mathrm{p}) \,\mathrm{d}\mathbf{x}}{\|\mathbf{v}_h\|_{\mathbf{L}^\alpha(\Omega)}}$$
$$\overset{(83), \boldsymbol{\mathcal{V}}_h^{k-1} \subset \boldsymbol{\mathcal{V}}}{\le} \sup_{\mathbf{v} \in \boldsymbol{\mathcal{V}}} \frac{\int_\Omega \mathbf{v} \cdot \boldsymbol{\nabla}_h(\mathrm{p} - \mathcal{I}_k\,\mathrm{p}) \,\mathrm{d}\mathbf{x}}{\|\mathbf{v}\|_{\mathbf{L}^\alpha(\Omega)}} + \frac{\mu}{\rho}\|\underline{\mathbf{K}}^{-1}\|_{\underline{\mathbf{L}}^{\frac{\alpha}{\alpha-2}}(\Omega)} \|\mathbf{u} - \mathbf{u}_h\|_{\mathbf{L}^\alpha(\Omega)}$$
$$+ \mathrm{C}_{\mathrm{BL}}\frac{\beta}{\rho}\|\mathbf{u} - \mathbf{u}_h\|_{\mathbf{L}^\alpha(\Omega)} (\|\mathbf{u}_h\|^{\alpha-2}_{\mathbf{L}^\alpha(\Omega)} + \|\mathbf{u}\|^{\alpha-2}_{\mathbf{L}^\alpha(\Omega)}).$$

Triangle's inequality and the above estimate yield

$$\begin{aligned}\mathfrak{b}_{\mathrm{h}}\|\boldsymbol{\nabla}_{\mathrm{h}}(\mathrm{p}-\mathrm{p}_{\mathrm{h}})\|_{\mathbf{L}^{\alpha'}(\Omega)} &\leq \mathfrak{b}_{\mathrm{h}}\|\boldsymbol{\nabla}_{\mathrm{h}}(\mathrm{p}-\mathcal{I}_k\,\mathrm{p})\|_{\mathbf{L}^{\alpha'}(\Omega)} + \mathfrak{b}_{\mathrm{h}}\|\boldsymbol{\nabla}_{\mathrm{h}}(\mathrm{p}_{\mathrm{h}}-\mathcal{I}_k\,\mathrm{p}_{\mathrm{h}})\|_{\mathbf{L}^{\alpha'}(\Omega)}\\ &\leq (1+\mathfrak{b}_{\mathrm{h}})\|\boldsymbol{\nabla}_{\mathrm{h}}(\mathrm{p}-\mathcal{I}_k\,\mathrm{p})\|_{\mathbf{L}^{\alpha'}(\Omega)} + \frac{\mu}{\rho}\|\underline{\mathbf{K}}^{-1}\|_{\underline{\mathbf{L}}^{\frac{\alpha}{\alpha-2}}(\Omega)}\|\mathbf{u}-\mathbf{u}_{\mathrm{h}}\|_{\mathbf{L}^{\alpha}(\Omega)}\\ &\quad + \mathrm{C}_{\mathrm{BL}}\,\frac{\beta}{\rho}\|\mathbf{u}-\mathbf{u}_{\mathrm{h}}\|_{\mathbf{L}^{\alpha}(\Omega)}(\|\mathbf{u}_{\mathrm{h}}\|^{\alpha-2}_{\mathbf{L}^{\alpha}(\Omega)}+\|\mathbf{u}\|^{\alpha-2}_{\mathbf{L}^{\alpha}(\Omega)}).\end{aligned}$$

The assertion follows from combining the above estimate with the strong convergences in $\mathbf{L}^{\alpha}(\Omega)$ of $\mathbf{u}_{\mathrm{h}}$ to $\mathbf{u}$ (here we use that $\underline{\mathbf{K}}^{-1}$ is in $\underline{\mathbf{L}}^{\frac{2\alpha}{\alpha-2}}(\Omega)$), cf. Theorem 5.7, and in $\mathbf{L}^{\alpha'}(\Omega)$ of $\boldsymbol{\nabla}_{\mathrm{h}}\,\mathcal{I}_k\,\mathrm{p}$ to $\boldsymbol{\nabla}\,\mathrm{p}$, cf. (66). □

Due to the uniqueness of the solution $(\mathbf{u},\mathrm{p})$, we deduce the convergence of the whole sequence.

6 Error estimates

The goal of this section is to establish general-order error estimates for method (41).

Given an element K in $\mathcal{T}_{\mathrm{h}}$, a polynomial inverse estimate holds true: there exists a positive constant C^K_{inv} depending only on k and γ, such that

$$\|\boldsymbol{\nabla}\cdot\mathbf{q}_k\|_{\mathrm{L}^s(K)} \leq C^K_{\mathrm{inv}}\,\mathrm{h}_K^{-1}\,\|\mathbf{q}_k\|_{\mathrm{L}^s(K)} \qquad \forall\mathbf{q}_k\in\mathbf{P}_k(K),\,\forall K\in\mathcal{T}_{\mathrm{h}}. \tag{84}$$

We show an upper bound for the error in the L^2-norm of the flux variable.

Proposition 6.1. *Let* $(\mathbf{u},\mathrm{p})$ *and* $(\mathbf{u}_{\mathrm{h}},\mathrm{p}_{\mathrm{h}})$ *for a mesh* $\mathcal{T}_{\mathrm{h}}$ *be solutions to* (10) *and* (41)*, respectively. Assume that*

$$\begin{cases}\mathbf{u}\in\mathbf{L}^{4\alpha-8}(\Omega),\ \underline{\mathbf{K}}^{-1}\in\underline{\mathbf{L}}^{\infty}(\Omega) & \textit{if } \alpha>2\\ \mathbf{u}\in\mathbf{L}^{\frac{2\alpha}{4-\alpha}}(\Omega),\ \underline{\mathbf{K}}^{-1}\in\underline{\mathbf{L}}^{\frac{\alpha}{\alpha-2}}(\Omega) & \textit{only if } \alpha\in(2,4),\end{cases} \qquad \mathrm{p}\in\mathrm{H}^1(\Omega)\cap\mathcal{Q}_{g_D}.$$

Then, for all $\mathbf{w}_{\mathrm{h}}$ *in* $\boldsymbol{\mathcal{V}}^{k-1}_{\mathrm{h}}$*, we have*

$$\begin{aligned}\|\mathbf{u}-\mathbf{u}_{\mathrm{h}}\|_{\mathbf{L}^2(\Omega)} &\leq \mathfrak{E}(\underline{\mathbf{K}}^{-1},\mathbf{u},\mathbf{w}_{\mathrm{h}},\alpha)\\ &\quad+\frac{\beta}{\mu\lambda_{min}}(\alpha-1)\|\mathbf{u}-\mathbf{w}_{\mathrm{h}}\|_{\mathbf{L}^4(\Omega)}(\|\mathbf{u}\|^{\alpha-2}_{\mathbf{L}^{4\alpha-8}(\Omega)}+\|\mathbf{w}_{\mathrm{h}}\|^{\alpha-2}_{\mathbf{L}^{4\alpha-8}(\Omega)})\\ &\quad+\frac{\mu}{\rho\lambda_{min}}C_{\mathrm{SP}}\max_{K\in\mathcal{T}_{\mathrm{h}}}C^K_{inv}\|\boldsymbol{\nabla}_{\mathrm{h}}(\mathrm{p}-\mathcal{I}_k\,\mathrm{p})\|_{\mathbf{L}^2(\Omega)},\end{aligned} \tag{85}$$

where

$$\mathfrak{E}(\underline{\mathbf{K}}^{-1},\mathbf{u},\mathbf{w}_{\mathrm{h}},\alpha)=\begin{cases}\left(1+\frac{\|\underline{\mathbf{K}}^{-1}\|_{\underline{\mathbf{L}}^{\infty}(\Omega)}}{\lambda_{min}}\right)\|\mathbf{u}-\mathbf{w}_{\mathrm{h}}\|_{\mathbf{L}^2(\Omega)} & \textit{if } \alpha>2\\ \left(1+\frac{\|\underline{\mathbf{K}}^{-1}\|_{\underline{\mathbf{L}}^{\frac{\alpha}{\alpha-2}}(\Omega)}}{\lambda_{min}}\right)\|\mathbf{u}-\mathbf{w}_{\mathrm{h}}\|_{\mathbf{L}^{\frac{2\alpha}{4-\alpha}}(\Omega)} & \textit{only if } \alpha\in(2,4).\end{cases}$$

The last term on the right-hand side of (85) *drops if* $k=1$*; cf. [23, Theorem 8] and* (72).

Proof. We prove the assertion for $\underline{\mathbf{K}}^{-1}$ in $\underline{\mathbf{L}}^{\infty}(\Omega)$ as the other case follows analogously.

For a given $\mathbf{w}_{\mathrm{h}}$ in $\boldsymbol{\mathcal{V}}^{k-1}_{\mathrm{h}}$, triangle's inequality implies

$$\|\mathbf{u}-\mathbf{u}_{\mathrm{h}}\|_{\mathbf{L}^2(\Omega)} \leq \|\mathbf{u}-\mathbf{w}_{\mathrm{h}}\|_{\mathbf{L}^2(\Omega)}+\|\mathbf{u}_{\mathrm{h}}-\mathbf{w}_{\mathrm{h}}\|_{\mathbf{L}^2(\Omega)}. \tag{86}$$

Choosing $\mathbf{u}$ as $\mathbf{u}_{\ell}$ in (21a) and $\mathbf{u}_{\mathrm{h}}-\mathbf{w}_{\mathrm{h}}$ as $\mathbf{v}_{\mathrm{h}}$ in (71), applying inequality (20), Cauchy-Schwarz' inequality (if α is in $(2,4)$, then we use Hölder's inequality with exponents $(\alpha/(\alpha-2), 2\alpha/(4-\alpha), 2)$), and Hölder's inequality with exponents $(4,4,2)$, we have

$$\begin{aligned}
\frac{\mu}{\rho}\lambda_{\min}\|\mathbf{u}_{\mathrm{h}}-\mathbf{w}_{\mathrm{h}}\|^2_{\mathbf{L}^2(\Omega)} &\overset{(21a)}{\leq} \int_\Omega (\boldsymbol{\mathcal{A}}(\mathbf{u}_{\mathrm{h}})-\boldsymbol{\mathcal{A}}(\mathbf{w}_{\mathrm{h}}))\cdot(\mathbf{u}_{\mathrm{h}}-\mathbf{w}_{\mathrm{h}})\,\mathrm{d}\mathbf{x}\\
&\overset{(67),(71),(73)}{=} \int_\Omega (\boldsymbol{\mathcal{A}}(\mathbf{u})-\boldsymbol{\mathcal{A}}(\mathbf{w}_{\mathrm{h}}))\cdot(\mathbf{u}_{\mathrm{h}}-\mathbf{w}_{\mathrm{h}})\,\mathrm{d}\mathbf{x}\\
&\quad+\sum_{K\in\mathcal{T}_{\mathrm{h}}}\int_K(\mathcal{I}_k\,\mathrm{p}-\mathrm{p})(\boldsymbol{\nabla}\cdot(\mathbf{u}_{\mathrm{h}}-\mathbf{w}_{\mathrm{h}})-\Pi^{0,\mathcal{T}_{\mathrm{h}}}_{k-3}\,\boldsymbol{\nabla}\cdot(\mathbf{u}_{\mathrm{h}}-\mathbf{w}_{\mathrm{h}}))\,\mathrm{d}\mathbf{x}.\\
&\overset{(20)}{\leq}\frac{\mu}{\rho}\|\underline{\mathbf{K}}^{-1}\|_{\mathbf{L}^\infty(\Omega)}\|\mathbf{u}-\mathbf{w}_{\mathrm{h}}\|_{\mathbf{L}^2(\Omega)}\|\mathbf{u}_{\mathrm{h}}-\mathbf{w}_{\mathrm{h}}\|_{\mathbf{L}^2(\Omega)}\\
&\quad+\mathrm{C}_{\mathrm{BL}}\,\frac{\beta}{\rho}\|\mathbf{u}-\mathbf{w}_{\mathrm{h}}\|_{\mathbf{L}^4(\Omega)}\Big(\|\mathbf{u}\|^{\alpha-2}_{\mathbf{L}^{4\alpha-8}(\Omega)}+\|\mathbf{w}_{\mathrm{h}}\|^{\alpha-2}_{\mathbf{L}^{4\alpha-8}(\Omega)}\Big)\|\mathbf{u}_{\mathrm{h}}-\mathbf{w}_{\mathrm{h}}\|_{\mathbf{L}^2(\Omega)}\\
&\quad+\sum_{K\in\mathcal{T}_{\mathrm{h}}}\|\mathrm{p}-\mathcal{I}_k\,\mathrm{p}\|_{\mathrm{L}^2(K)}\|\boldsymbol{\nabla}\cdot(\mathbf{u}_{\mathrm{h}}-\mathbf{w}_{\mathrm{h}})\|_{\mathbf{L}^2(K)}.
\end{aligned}\tag{87}$$

Using that $\mathrm{p}-\mathcal{I}_k\,\mathrm{p}$ has zero average over ∂K for all K in $\mathcal{T}_{\mathrm{h}}$, the polynomial inverse estimate (84), Cauchy-Schwarz' inequality, and Poincaré-Steklov's inequality (6) imply

$$\begin{aligned}
\sum_{K\in\mathcal{T}_{\mathrm{h}}}\|\mathrm{p}-\mathcal{I}_k\,\mathrm{p}\|_{\mathrm{L}^2(K)}\|\boldsymbol{\nabla}\cdot(\mathbf{u}_{\mathrm{h}}-\mathbf{v}_{\mathrm{h}})\|_{\mathbf{L}^2(K)} &\overset{(84)}{\leq}\sum_{K\in\mathcal{T}_{\mathrm{h}}}\|\mathrm{p}-\mathcal{I}_k\,\mathrm{p}\|_{\mathrm{L}^2(K)}C^K_{\mathrm{inv}}\,\mathrm{h}_K^{-1}\,\|\mathbf{u}_{\mathrm{h}}-\mathbf{v}_{\mathrm{h}}\|_{\mathbf{L}^2(K)}\\
&\leq\Big((\max_{K\in\mathcal{T}_{\mathrm{h}}}C^K_{\mathrm{inv}})^2\sum_{K\in\mathcal{T}_{\mathrm{h}}}\mathrm{h}_K^{-2}\,\|\mathrm{p}-\mathcal{I}_k\,\mathrm{p}\|^2_{\mathrm{L}^2(K)}\Big)^{\frac12}\Big(\sum_{K\in\mathcal{T}_{\mathrm{h}}}\|\mathbf{u}_{\mathrm{h}}-\mathbf{v}_{\mathrm{h}}\|^2_{\mathbf{L}^2(K)}\Big)^{\frac12}\\
&\leq C_{\mathrm{SP}}\max_{K\in\mathcal{T}_{\mathrm{h}}}C^K_{\mathrm{inv}}\,\|\boldsymbol{\nabla}_{\mathrm{h}}(\mathrm{p}-\mathcal{I}_k\,\mathrm{p})\|_{\mathbf{L}^2(\Omega)}\|\mathbf{u}_{\mathrm{h}}-\mathbf{v}_{\mathrm{h}}\|_{\mathbf{L}^2(\Omega)}.
\end{aligned}$$

Combining the display above and (87) yields

$$\begin{aligned}
\|\mathbf{u}_{\mathrm{h}}-\mathbf{w}_{\mathrm{h}}\|_{\mathbf{L}^2(\Omega)}\leq{}&\frac{\|\underline{\mathbf{K}}^{-1}\|_{\mathbf{L}^\infty(\Omega)}}{\lambda_{\min}}\|\mathbf{u}-\mathbf{w}_{\mathrm{h}}\|_{\mathbf{L}^2(\Omega)}+\frac{\mu}{\rho\lambda_{\min}}\max_{K\in\mathcal{T}_{\mathrm{h}}}C_PC^K_{\mathrm{inv}}\|\boldsymbol{\nabla}_{\mathrm{h}}(\mathrm{p}-\mathcal{I}_k\,\mathrm{p})\|_{\mathbf{L}^2(\Omega)}\\
&+\mathrm{C}_{\mathrm{BL}}\,\frac{\beta}{\lambda_{\min}}\|\mathbf{u}-\mathbf{w}_{\mathrm{h}}\|_{\mathbf{L}^4(\Omega)}\Big(\|\mathbf{u}\|^{\alpha-2}_{\mathbf{L}^{4\alpha-8}(\Omega)}+\|\mathbf{w}_{\mathrm{h}}\|^{\alpha-2}_{\mathbf{L}^{4\alpha-8}(\Omega)}\Big).
\end{aligned}$$

Inserting the above display in (86), the assertion follows. □

We are now in the position to derive error estimates.

Theorem 6.2. *Let* $(\mathbf{u},\mathrm{p})$ *and* $(\mathbf{u}_{\mathrm{h}},\mathrm{p}_{\mathrm{h}})$ *be the solutions to* (10) *and* (41), *respectively. Given* s *in* $\mathbb{N}$, *assume that*

$$\begin{cases}\mathbf{u}\in\mathbf{W}^{s,4}(\Omega),\ \boldsymbol{\nabla}\cdot\mathbf{u}\in\mathrm{W}^{s,\frac43}(\Omega),\ \underline{\mathbf{K}}^{-1}\in\underline{\mathbf{L}}^\infty(\Omega) & \text{if } \alpha>2\\ \mathbf{u}\in\mathbf{W}^{s,\frac{2\alpha}{4-\alpha}}(\Omega),\ \boldsymbol{\nabla}\cdot\mathbf{u}\in\mathrm{W}^{s,\frac{\alpha}{2}}(\Omega),\ \underline{\mathbf{K}}^{-1}\in\underline{\mathbf{L}}^{\frac{\alpha}{\alpha-2}}(\Omega) & \text{only if } \alpha\in(2,4),\end{cases}\qquad \mathrm{p}\in\mathrm{W}^{s+1,2}(\Omega).$$

Denoting $\mathfrak{s}:=\min\{k,s\}$, *for hidden constants only depending on* k, Γ_D, Ω *through either* $\mathfrak{R}$ *or* $\mathfrak{N}$ *in* (1) *and* (2), γ, α, β, ρ, μ, *and* $\underline{\mathbf{K}}^{-1}$, *the following estimates hold true:*

$$\begin{cases}\|\mathbf{u}-\mathbf{u}_{\mathrm{h}}\|_{\mathbf{L}^2(\Omega)}\lesssim\mathrm{h}^{\mathfrak{s}}\left(\|\mathbf{u}\|_{\mathbf{W}^{\mathfrak{s},4}(\Omega)}+\|\boldsymbol{\nabla}\cdot\mathbf{u}\|_{\mathrm{W}^{\mathfrak{s},\frac43}(\Omega)}+\|\mathrm{p}\|_{\mathrm{W}^{\mathfrak{s}+1,2}(\Omega)}\right) & \text{if } \alpha>2\\ \|\mathbf{u}-\mathbf{u}_{\mathrm{h}}\|_{\mathbf{L}^2(\Omega)}\lesssim\mathrm{h}^{\mathfrak{s}}\left(\|\mathbf{u}\|_{\mathbf{W}^{\mathfrak{s},\frac{2\alpha}{4-\alpha}}(\Omega)}+\|\boldsymbol{\nabla}\cdot\mathbf{u}\|_{\mathrm{W}^{\mathfrak{s},\frac{\alpha}{2}}(\Omega)}+\|\mathrm{p}\|_{\mathrm{W}^{\mathfrak{s}+1,2}(\Omega)}\right) & \text{only if } \alpha\in(2,4)\end{cases}\tag{88}$$

and

$$\begin{cases}\|\boldsymbol{\nabla}_{\mathrm{h}}(\mathrm{p}-\mathrm{p}_{\mathrm{h}})\|_{\mathbf{L}^{\alpha'}(\Omega)}\lesssim\mathrm{h}^{\mathfrak{s}}\left(\|\mathbf{u}\|_{\mathbf{W}^{\mathfrak{s},4}(\Omega)}+\|\boldsymbol{\nabla}\cdot\mathbf{u}\|_{\mathrm{W}^{\mathfrak{s},\frac43}(\Omega)}+\|\mathrm{p}\|_{\mathrm{W}^{\mathfrak{s}+1,2}(\Omega)}\right) & \text{if } \alpha>2\\ \|\boldsymbol{\nabla}_{\mathrm{h}}(\mathrm{p}-\mathrm{p}_{\mathrm{h}})\|_{\mathbf{L}^{\alpha'}(\Omega)}\lesssim\mathrm{h}^{\mathfrak{s}}\left(\|\mathbf{u}\|_{\mathbf{W}^{\mathfrak{s},\frac{2\alpha}{4-\alpha}}(\Omega)}+\|\boldsymbol{\nabla}\cdot\mathbf{u}\|_{\mathrm{W}^{\mathfrak{s},\frac{\alpha}{2}}(\Omega)}+\|\mathrm{p}\|_{\mathrm{W}^{\mathfrak{s}+1,2}(\Omega)}\right) & \text{only if } \alpha\in(2,4).\end{cases}\tag{89}$$

Proof. We prove the assertion for $\underline{\mathbf{K}}^{-1}$ in $\underline{\mathbf{L}}^\infty(\Omega)$; the other case follows analogously as in Proposition 6.1 using different Sobolev embeddings and noting that $\alpha/2=(((2\alpha/(4-\alpha))')^*)'$.

Flux error estimates. Given $\mathbf{c}_\mathrm{h} = \mathbf{c}_\mathrm{h}(\mathbf{u})$ solution to (50) with $\mathbf{u}$ as in (10), we pick $\mathbf{w}_\mathrm{h}$ equal to $\mathbf{\Pi}^{0,\mathcal{T}_\mathrm{h}}_{k-1}(\mathbf{u}) + \mathbf{c}_\mathrm{h}(\mathbf{u})$ in (85) and get

$$\begin{aligned}
\|\mathbf{u}-\mathbf{u}_\mathrm{h}\|_{\mathbf{L}^2(\Omega)} &\lesssim \Big(\Big\|\mathbf{u}-\mathbf{\Pi}^{0,\mathcal{T}_\mathrm{h}}_{k-1}\mathbf{u}\Big\|_{\mathbf{L}^2(\Omega)} + \|\mathbf{c}_\mathrm{h}(\mathbf{u})\|_{\mathbf{L}^2(\Omega)}\Big)\\
&+\Big(\Big\|\mathbf{u}-\mathbf{\Pi}^{0,\mathcal{T}_\mathrm{h}}_{k-1}\mathbf{u}\Big\|_{\mathbf{L}^4(\Omega)} + \|\mathbf{c}_\mathrm{h}(\mathbf{u})\|_{\mathbf{L}^4(\Omega)}\Big)\Big(\|\mathbf{u}\|^{\alpha-2}_{\mathbf{L}^{4\alpha-8}(\Omega)} + \Big\|\mathbf{\Pi}^{0,\mathcal{T}_\mathrm{h}}_{k-1}(\mathbf{u})+\mathbf{c}_\mathrm{h}(\mathbf{u})\Big\|^{\alpha-2}_{\mathbf{L}^{4\alpha-8}(\Omega)}\Big)\\
&+\|\boldsymbol{\nabla}_\mathrm{h}(\mathrm{p}-\mathcal{I}_k\,\mathrm{p})\|_{\mathbf{L}^2(\Omega)} =: T_1 + T_2\cdot T_3 + T_4.
\end{aligned}$$

Standard polynomial approximation properties and (55) with $\mathfrak{a} = 2,\, 4$, and $4\alpha-8$ imply

$$\begin{aligned}
&T_1 \lesssim \mathrm{h}^{\mathfrak{s}}(\|\mathbf{u}\|_{\mathbf{W}^{s,2}(\Omega)} + \|\boldsymbol{\nabla}\cdot\mathbf{u}\|_{\mathbf{W}^{s,1}(\Omega)}), \qquad T_2 \lesssim \mathrm{h}^{\mathfrak{s}}(\|\mathbf{u}\|_{\mathbf{W}^{s,4}(\Omega)} + \|\boldsymbol{\nabla}\cdot\mathbf{u}\|_{\mathbf{W}^{s,\frac{4}{3}}(\Omega)}),\\
&T_3 \lesssim \|\mathbf{u}\|^{\alpha-2}_{\mathbf{L}^{4\alpha-8}(\Omega)} + \|\boldsymbol{\nabla}\cdot\mathbf{u}\|^{\alpha-2}_{\mathbf{L}^{(((4\alpha-8)')^*)'}(\Omega)}.
\end{aligned}$$

Using the interpolation estimates (49), we further obtain

$$T_4 \lesssim \mathrm{h}^{\mathfrak{s}}\,\|\mathrm{p}\|_{\mathrm{W}^{s+1,2}(\Omega)}.$$

Estimate (88) follows combining the above bounds.

Potential error estimates. Subtracting (41a) from (10a), we have

$$\begin{aligned}
-\int_\Omega(\boldsymbol{\mathcal{A}}(\mathbf{u}_\mathrm{h})-\boldsymbol{\mathcal{A}}(\mathbf{u}))\cdot\mathbf{v}_\mathrm{h}\,\mathrm{d}\mathbf{x} &= \int_\Omega \boldsymbol{\nabla}_\mathrm{h}(\mathrm{p}_\mathrm{h}-\mathrm{p})\cdot\mathbf{v}_\mathrm{h}\,\mathrm{d}\mathbf{x}\\
&= \int_\Omega \boldsymbol{\nabla}_\mathrm{h}(\mathrm{p}_\mathrm{h}-\mathcal{I}_k\,\mathrm{p})\cdot\mathbf{v}_\mathrm{h}\,\mathrm{d}\mathbf{x} + \int_\Omega \boldsymbol{\nabla}_\mathrm{h}(\mathcal{I}_k\,\mathrm{p}-\mathrm{p})\cdot\mathbf{v}_\mathrm{h}\,\mathrm{d}\mathbf{x} \qquad \forall \mathbf{v}_\mathrm{h}\in\boldsymbol{\mathcal{V}}^{k-1}_\mathrm{h}.
\end{aligned}$$

Using (20) in the above display together with triangle's inequality, Cauchy-Schwarz' inequality (if $\underline{\mathbf{K}}^{-1}$ is in $\underline{\mathbf{L}}^{\frac{\alpha}{\alpha-2}}(\Omega)$ we rather use Hölder's inequality with exponents $(2\alpha/(\alpha-2), 2, \alpha)$), and Hölder's inequality with exponents $(2, 2\alpha/(\alpha-2), \alpha)$ give

$$\begin{aligned}
\left|\int_\Omega \mathbf{v}_\mathrm{h}\cdot\boldsymbol{\nabla}_\mathrm{h}(\mathrm{p}_\mathrm{h}-\mathcal{I}_k\,\mathrm{p})\,\mathrm{d}\mathbf{x}\right| &\le \left|\int_\Omega \mathbf{v}_\mathrm{h}\cdot\boldsymbol{\nabla}_\mathrm{h}(\mathrm{p}-\mathcal{I}_k\,\mathrm{p})\,\mathrm{d}\mathbf{x}\right| + \left|\int_\Omega(\boldsymbol{\mathcal{A}}(\mathbf{u}_\mathrm{h})-\boldsymbol{\mathcal{A}}(\mathbf{u}))\cdot\mathbf{v}_\mathrm{h}\,\mathrm{d}\mathbf{x}\right|\\
&\le \left|\int_\Omega \mathbf{v}_\mathrm{h}\cdot\boldsymbol{\nabla}_\mathrm{h}(\mathrm{p}-\mathcal{I}_k\,\mathrm{p})\,\mathrm{d}\mathbf{x}\right| + \frac{\mu}{\rho}\big\|\underline{\mathbf{K}}^{-1}\big\|_{\underline{\mathbf{L}}^\infty(\Omega)}\|\mathbf{u}-\mathbf{u}_\mathrm{h}\|_{\mathbf{L}^2(\Omega)}\|\mathbf{v}_\mathrm{h}\|_{\mathbf{L}^2(\Omega)}\\
&\quad + \mathrm{C}_{\mathrm{BL}}\,\frac{\beta}{\rho}\|\mathbf{u}-\mathbf{u}_\mathrm{h}\|_{\mathbf{L}^2(\Omega)}(\|\mathbf{u}_\mathrm{h}\|^{\alpha-2}_{\mathbf{L}^{2\alpha}(\Omega)} + \|\mathbf{u}\|^{\alpha-2}_{\mathbf{L}^{2\alpha}(\Omega)})\|\mathbf{v}_\mathrm{h}\|_{\mathbf{L}^\alpha(\Omega)}.
\end{aligned} \tag{90}$$

We deduce

$$\begin{aligned}
\mathfrak{b}_\mathrm{h}\|\boldsymbol{\nabla}_\mathrm{h}(\mathrm{p}_\mathrm{h}-\mathcal{I}_k\,\mathrm{p})\|_{\mathbf{L}^{\alpha'}(\Omega)} &\overset{(42)}{\le} \sup_{\mathbf{v}_\mathrm{h}\in\boldsymbol{\mathcal{V}}^{k-1}_\mathrm{h}} \frac{\int_\Omega \mathbf{v}_\mathrm{h}\cdot\boldsymbol{\nabla}_\mathrm{h}(\mathrm{p}_\mathrm{h}-\mathcal{I}_k\,\mathrm{p})\,\mathrm{d}\mathbf{x}}{\|\mathbf{v}_\mathrm{h}\|_{\mathbf{L}^\alpha(\Omega)}}\\
&\overset{(90),\boldsymbol{\mathcal{V}}^{k-1}_\mathrm{h}\subset\boldsymbol{\mathcal{V}}}{\le} \sup_{\mathbf{v}\in\boldsymbol{\mathcal{V}}} \frac{\int_\Omega \mathbf{v}\cdot\boldsymbol{\nabla}(\mathrm{p}-\mathcal{I}_k\,\mathrm{p})\,\mathrm{d}\mathbf{x}}{\|\mathbf{v}\|_{\mathbf{L}^\alpha(\Omega)}} + \frac{\mu}{\rho}\big\|\underline{\mathbf{K}}^{-1}\big\|_{\underline{\mathbf{L}}^\infty(\Omega)}\|\mathbf{u}-\mathbf{u}_\mathrm{h}\|_{\mathbf{L}^2(\Omega)}\\
&\qquad + \mathrm{C}_{\mathrm{BL}}\,\frac{\beta}{\rho}\|\mathbf{u}-\mathbf{u}_\mathrm{h}\|_{\mathbf{L}^2(\Omega)}(\|\mathbf{u}_\mathrm{h}\|^{\alpha-2}_{\mathbf{L}^{2\alpha}(\Omega)} + \|\mathbf{u}\|^{\alpha-2}_{\mathbf{L}^{2\alpha}(\Omega)}).
\end{aligned}$$

Triangle's inequality, Hölder's inequality, and the above estimate yield

$$\begin{aligned}
\mathfrak{b}_\mathrm{h}\|\boldsymbol{\nabla}_\mathrm{h}(\mathrm{p}-\mathrm{p}_\mathrm{h})\|_{\mathbf{L}^{\alpha'}(\Omega)} &\le \mathfrak{b}_\mathrm{h}\|\boldsymbol{\nabla}_\mathrm{h}(\mathrm{p}-\mathcal{I}_k\,\mathrm{p})\|_{\mathbf{L}^{\alpha'}(\Omega)} + \mathfrak{b}_\mathrm{h}\|\boldsymbol{\nabla}_\mathrm{h}(\mathrm{p}_\mathrm{h}-\mathcal{I}_k\,\mathrm{p})\|_{\mathbf{L}^{\alpha'}(\Omega)}\\
&\le (1+\mathfrak{b}_\mathrm{h})\|\boldsymbol{\nabla}_\mathrm{h}(\mathrm{p}-\mathcal{I}_k\,\mathrm{p})\|_{\mathbf{L}^{\alpha'}(\Omega)} + \frac{\mu}{\rho}\big\|\underline{\mathbf{K}}^{-1}\big\|_{\underline{\mathbf{L}}^\infty(\Omega)}\|\mathbf{u}-\mathbf{u}_\mathrm{h}\|_{\mathbf{L}^2(\Omega)}\\
&\quad + \mathrm{C}_{\mathrm{BL}}\,\frac{\beta}{\rho}\|\mathbf{u}-\mathbf{u}_\mathrm{h}\|_{\mathbf{L}^2(\Omega)}(\|\mathbf{u}_\mathrm{h}\|^{\alpha-2}_{\mathbf{L}^{2\alpha}(\Omega)} + \|\mathbf{u}\|^{\alpha-2}_{\mathbf{L}^{2\alpha}(\Omega)}).
\end{aligned} \tag{91}$$

We now show that $\mathbf{u}_\mathrm{h}$ is bounded in $\mathbf{L}^{2\alpha}(\Omega)$ for fixed order k. Triangle's inequality, an $\mathbf{L}^{2\alpha}-\mathbf{L}^2$ polynomial inverse inequality, and the stability of the projection imply

$$\|\mathbf{u}_\mathrm{h}\|_{\mathbf{L}^{2\alpha}(\Omega)} \le \Big\|\mathbf{u}_\mathrm{h}-\mathbf{\Pi}^{0,\mathcal{T}_\mathrm{h}}_{k-1}\mathbf{u}\Big\|_{\mathbf{L}^{2\alpha}(\Omega)} + \Big\|\mathbf{\Pi}^{0,\mathcal{T}_\mathrm{h}}_{k-1}\mathbf{u}\Big\|_{\mathbf{L}^{2\alpha}(\Omega)} \lesssim \mathrm{h}^{\frac{\alpha-1}{\alpha}}\,\|\mathbf{u}-\mathbf{u}_\mathrm{h}\|_{\mathbf{L}^2(\Omega)} + \|\mathbf{u}\|_{\mathbf{L}^{2\alpha}(\Omega)}.$$

Since the Sobolev embedding $\mathbf{W}^{1,4}(\Omega)$ in $\mathbf{L}^{2\alpha}(\Omega)$ holds true, estimate (89) gives

$$\|\mathbf{u}\|_{\mathbf{L}^{2\alpha}(\Omega)} \lesssim \|\mathbf{u}\|_{\mathbf{W}^{1,4}(\Omega)} \qquad \Longrightarrow \qquad \mathbf{u}_{\mathrm{h}} \in \mathbf{L}^{2\alpha}(\Omega). \tag{92}$$

The assertion follows inserting (49), (85), and (92) in (91), and noting that α' is smaller than 2. □

Remark 4. In the lowest-order counterpart of Theorem 6.1; see [23, Prop. 8], the error estimate on the fluxes is decoupled from the potential. Indeed, for $k = 1$ the right-hand side of (71) vanishes and a Galerkin orthogonality property for the mapping $\boldsymbol{\mathcal{A}}$ holds true; thus, in (87) the term involving the pressure does not longer appear. This fact is confirmed on the numerical level as well; see Figure 6 below. ■

7 Numerical experiments

Here, we assess the numerical performance of method (41); to this aim, we consider two iterative schemes in order to cope with the nonlinearity. In what follows, we consider a slight generalization of problem (7), where the first equation admits an inhomogeneous right-hand side $\mathbf{f}$.

Iterative scheme 1. We consider a *standard* fixed point iterative scheme. We initialize the scheme constructing an initial guess $(\mathbf{u}_{\mathrm{h}}^0, \mathrm{p}_{\mathrm{h}}^0)$ in $\boldsymbol{\mathcal{V}}_{\mathrm{h}}^{k-1} \times \mathcal{Q}_{h,g_D}^k$, which is solution to the linear Darcy model problem

$$\frac{\mu}{\rho}\int_\Omega (\underline{\mathbf{K}}^{-1})\mathbf{u}_{\mathrm{h}}^0 \cdot \mathbf{v}_{\mathrm{h}}\,\mathrm{d}\mathbf{x} + \int_\Omega \boldsymbol{\nabla}_{\mathrm{h}}\, \mathrm{p}_{\mathrm{h}}^0 \cdot \mathbf{v}_{\mathrm{h}}\,\mathrm{d}\mathbf{x} = \int_\Omega \mathbf{f}\cdot \mathbf{v}_{\mathrm{h}}\,\mathrm{d}\mathbf{x} \qquad \forall\, \mathbf{v}_{\mathrm{h}} \in \boldsymbol{\mathcal{V}}_{\mathrm{h}}^{k-1} \tag{93a}$$

$$\int_\Omega \boldsymbol{\nabla}\, \mathrm{q}_{\mathrm{h}} \cdot \mathbf{u}_{\mathrm{h}}^0\,\mathrm{d}\mathbf{x} = -\int_\Omega b\, \mathrm{q}_{\mathrm{h}}\,\mathrm{d}\mathbf{x} + \int_{\Gamma_N} g_N\, \mathrm{q}_{\mathrm{h}}\,\mathrm{d}s \qquad \forall\, \mathrm{q}_{\mathrm{h}} \in \mathcal{Q}_{h,0}^k. \tag{93b}$$

Then, for all $\mathrm{n} \ge 1$, given the solution $(\mathbf{u}_{\mathrm{h}}^{\mathrm{n}-1}, \mathrm{p}_{\mathrm{h}}^{\mathrm{n}-1})$ at the $(\mathrm{n}-1)$-th step of the iterative scheme, we solve: find $(\mathbf{u}_{\mathrm{h}}^{\mathrm{n}}, \mathrm{p}_{\mathrm{h}}^{\mathrm{n}})$ in $\boldsymbol{\mathcal{V}}_{\mathrm{h}}^{k-1} \times \mathcal{Q}_{h,g_D}^k$ such that

$$\frac{\mu}{\rho}\int_\Omega (\underline{\mathbf{K}}^{-1})\mathbf{u}_{\mathrm{h}}^{\mathrm{n}} \cdot \mathbf{v}_{\mathrm{h}}\,\mathrm{d}\mathbf{x} + \frac{\beta}{\rho}\int_\Omega \left|\mathbf{u}_{\mathrm{h}}^{\mathrm{n}-1}\right|^{\alpha-2}\mathbf{u}_{\mathrm{h}}^{\mathrm{n}} \cdot \mathbf{v}_{\mathrm{h}}\,\mathrm{d}\mathbf{x} + \int_\Omega \boldsymbol{\nabla}\, \mathrm{p}_{\mathrm{h}}^{\mathrm{n}} \cdot \mathbf{v}_{\mathrm{h}}\,\mathrm{d}\mathbf{x} = \int_\Omega \mathbf{f}\cdot \mathbf{v}_{\mathrm{h}}\,\mathrm{d}\mathbf{x} \quad \forall\, \mathbf{v}_{\mathrm{h}} \in \boldsymbol{\mathcal{V}}_{\mathrm{h}}^{k-1} \tag{94a}$$

$$\int_\Omega \boldsymbol{\nabla}\, \mathrm{q}_{\mathrm{h}} \cdot \mathbf{u}_{\mathrm{h}}^{\mathrm{n}}\,\mathrm{d}\mathbf{x} = -\int_\Omega b\, \mathrm{q}_{\mathrm{h}}\,\mathrm{d}\mathbf{x} + \int_{\Gamma_N} g_N\, \mathrm{q}_{\mathrm{h}}\,\mathrm{d}s \quad \forall\, \mathrm{q}_{\mathrm{h}} \in \mathcal{Q}_{h,0}^k. \tag{94b}$$

With obvious notation for the matrices $\underline{\mathbf{M}}$, $\underline{\mathbf{N}}^{\mathrm{n}-1}$, and $\underline{\mathbf{B}}$, and for the vectors $\mathbf{f}$, $\mathbf{b}$, and $\mathbf{g}$, we set

$$\underline{\mathbf{A}}^{\mathrm{n}} := \begin{pmatrix} \underline{\mathbf{M}} + \underline{\mathbf{N}}^{\mathrm{n}-1} & \underline{\mathbf{B}}^T \\ \underline{\mathbf{B}} & \mathbf{0} \end{pmatrix} \qquad \mathbf{r} := \begin{pmatrix} \mathbf{f} \\ -\mathbf{b} + \mathbf{g} \end{pmatrix}.$$

In matrix form, (94) reads

$$\underline{\mathbf{A}}^{\mathrm{n}} \begin{pmatrix} \mathbf{u}_{\mathrm{h}}^{\mathrm{n}} \\ \mathbf{p}_{\mathrm{h}}^{\mathrm{n}} \end{pmatrix} = \mathbf{r}.$$

Iterative scheme 2. We further consider a *relaxed* (also known in the literature as *damped* or *Mann*'s) fixed point iterative scheme; see, e.g., [8, Sect. 1.2, Ch. 4]. The initial guess $(\widetilde{\mathbf{u}}_{\mathrm{h}}^0, \widetilde{\mathrm{p}}_{\mathrm{h}}^0) = (\mathbf{u}_{\mathrm{h}}^0, \mathrm{p}_{\mathrm{h}}^0)$ is the solution to (93). Then, for all $\mathrm{n} \ge 1$, given $(\widetilde{\mathbf{u}}_{\mathrm{h}}^{\mathrm{n}-1}, \widetilde{\mathrm{p}}_{\mathrm{h}}^{\mathrm{n}-1})$, we proceed as follows: (i) find $(\mathbf{u}_{\mathrm{h}}^{\mathrm{n}}, \mathrm{p}_{\mathrm{h}}^{\mathrm{n}})$ solution to (94) where the term $\left|\mathbf{u}_{\mathrm{h}}^{\mathrm{n}-1}\right|^{\alpha-2}$ is replaced by $\left|\widetilde{\mathbf{u}}_{\mathrm{h}}^{\mathrm{n}-1}\right|^{\alpha-2}$; ($ii$) given a relaxation parameter ω in $(0, 1]$, set

$$\widetilde{\mathbf{u}}_{\mathrm{h}}^{\mathrm{n}} := \omega \mathbf{u}_{\mathrm{h}}^{\mathrm{n}} + (1-\omega)\widetilde{\mathbf{u}}_{\mathrm{h}}^{\mathrm{n}-1}, \qquad \widetilde{\mathrm{p}}_{\mathrm{h}}^{\mathrm{n}} = \mathrm{p}_{\mathrm{h}}^{\mathrm{n}}. \tag{95}$$

When no confusion occurs, we shall denote either $(\mathbf{u}_{\mathrm{h}}^{\mathrm{n}}, \mathrm{p}_{\mathrm{h}}^{\mathrm{n}})$ or $(\widetilde{\mathbf{u}}_{\mathrm{h}}^{\mathrm{n}}, \widetilde{\mathrm{p}}_{\mathrm{h}}^{\mathrm{n}})$ by $\mathbf{s}_{\mathrm{h}}^{\mathrm{n}}$.

Meshes. We consider sequences of shape-regular, quasi-uniform, unstructured simplicial meshes with decreasing diameter.

Parameters. Given $\underline{\mathbf{N}}$ the matrix associated with $\frac{\beta}{\rho}\int_\Omega |\mathbf{u}_\mathrm{h}^\mathrm{n}|^{\alpha-2}\mathbf{u}_\mathrm{h}^\mathrm{n}\cdot\mathbf{v}_\mathrm{h}\,\mathrm{d}\mathbf{x}$, we set

$$\underline{\mathbf{A}} := \begin{pmatrix} \underline{\mathbf{M}}+\underline{\mathbf{N}} & \underline{\mathbf{B}}^T \\ \underline{\mathbf{B}} & \mathbf{0} \end{pmatrix}.$$

We consider the following stopping criterion for the iterative scheme:

$$\|\underline{\mathbf{A}}\mathbf{s}_\mathrm{h}^\mathrm{n} - \mathbf{r}\|_{\mathrm{L}^2(\Omega)} \le \mathrm{TOL}. \tag{96}$$

In all experiments below, TOL is set to 10^{-8}. We also consider a maximum number of iterations $n_{\max}$ equal to 2500. We set $\underline{\mathbf{K}} = \underline{\mathbf{I}}$, and $\mu = \rho = 1$. We consider full Neumann boundary conditions, i.e., set $\Gamma_N = \Gamma$, and impose the zero-mean condition for the potential as a Lagrange multiplier.

Test case 1. On the domain $\Omega := (-1,1)^2$, we consider the following exact flux and potential:

$$\mathbf{u}(x,y) = \begin{pmatrix} \sin(\pi x) \\ \cos(\pi y) \end{pmatrix} \qquad\qquad \mathrm{p}(x,y) = \cos\left(\frac{\pi}{2}x\right)\sin\left(\frac{\pi}{2}y\right). \tag{97}$$

The corresponding data are computed accordingly: the source term is given by

$$\mathbf{f}(x,y) = \begin{pmatrix} \sin(\pi x) - \frac{\pi}{2}\sin\left(\frac{\pi}{2}x\right)\sin\left(\frac{\pi}{2}y\right) + \beta\big(\sin(\pi x)^2 + \cos(\pi y)^2\big)^{\frac{\alpha-2}{2}}\sin(\pi x) \\ \cos(\pi y) - \frac{\pi}{2}\cos\left(\frac{\pi}{2}x\right)\cos\left(\frac{\pi}{2}y\right) + \beta\big(\sin(\pi x)^2 + \cos(\pi y)^2\big)^{\frac{\alpha-2}{2}}\cos(\pi y) \end{pmatrix};$$

the divergence constraint is given by $b(x,y) = -2\pi\sin(\pi x)\sin(\pi y)$; the Neumann boundary datum g_N is 0 on the left and right facets; 1 on the bottom facet; -1 on the top facet.

Test case 2. On the domain $\Omega := (-1,1)^2$, we consider the following exact flux and potential:

$$\mathbf{u}(x,y) = \begin{pmatrix} 1 \\ -1 \end{pmatrix} \qquad \text{and} \qquad \mathrm{p}(x,y) = x^3 + y^3. \tag{98}$$

The corresponding data are computed accordingly: the source term is given by

$$\mathbf{f}(x,y) = \begin{pmatrix} 1 + 2^{\frac{\alpha-2}{2}}\beta + 3x^2 \\ -1 - 2^{\frac{\alpha-2}{2}}\beta + 3y^2 \end{pmatrix};$$

the divergence constraint is given by $b(x,y) = 0$; the Neumann boundary datum g_N is 1 on the right and bottom facets; -1 on the left and top facets.

Error measures. In what follows, for a fixed order k, we compute the following error measures:

$$E^{\mathbf{u}}_{k-1,n} := \frac{\|\mathbf{u} - \mathbf{u}_\mathrm{h}^\mathrm{n}\|_{\mathbf{L}^2(\Omega)}}{\|\mathbf{u}\|_{\mathbf{L}^2(\Omega)}} \qquad \text{and} \qquad E^{\mathrm{p}}_{k,n} := \frac{\|\boldsymbol{\nabla}_\mathrm{h}(\mathrm{p} - \mathrm{p}_\mathrm{h}^\mathrm{n})\|_{\mathbf{L}^{\alpha'}(\Omega)}}{\|\boldsymbol{\nabla}\,\mathrm{p}\|_{\mathbf{L}^{\alpha'}(\Omega)}}. \tag{99}$$

The same error measures are considered when $\mathbf{u}_\mathrm{h}^\mathrm{n}$ is replaced by $\widetilde{\mathbf{u}}_\mathrm{h}^\mathrm{n}$.

Numerical results: varying the order of accuracy; fixed point scheme. In Figure 1, we display the errors in (99) under mesh refinements for the iterative scheme (94). We consider orders of accuracy k in $\{1,2,3,4\}$, $\alpha = 3$, and $\beta = 10$. In Table 1, we report the number of iterations needed to meet the stopping criterion (96). The number of iterations seems stable with respect to the order of accuracy k (with the exception of the lowest order case) and to the mesh size h.

Numerical results: varying the coefficient β of the nonlinear term; fixed point scheme. In Figure 2, we display the errors in (99) under mesh refinements for the iterative scheme (94). We consider β in $\{1,10,50,100\}$, $k = 2$, and $\alpha = 3$. In Table 2, we report the number of iterations needed to meet the stopping criterion (96). The number of iterations grows linearly with the value of β.

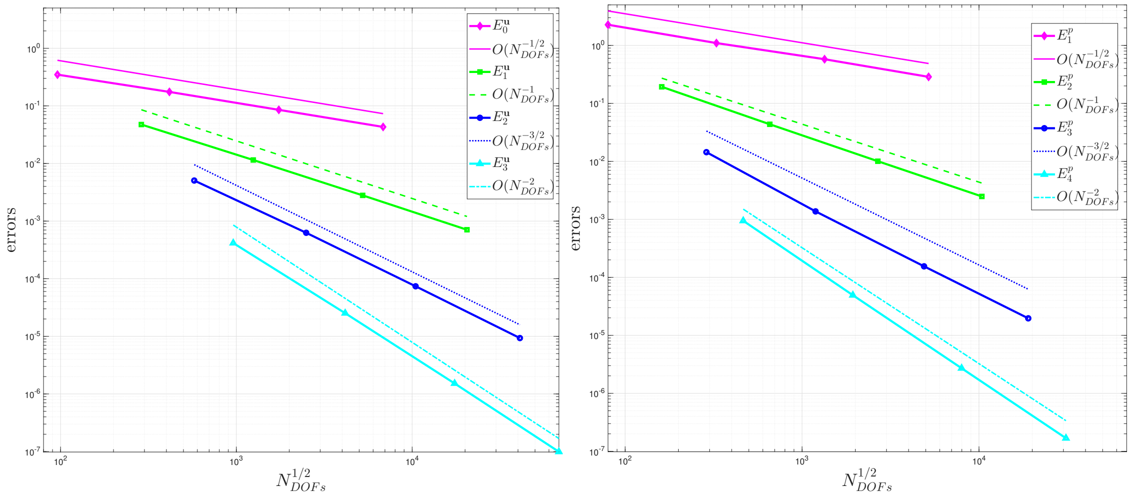

Figure 1: Exact solution in (97); h-convergence of the flux (*left-panel*) and the potential (*right-panel*) for k in $\{1, 2, 3, 4\}$, $\alpha = 3$, and $\beta = 10$. Standard fixed point iterative scheme (94).

	h=0.5	h=0.3	h=0.15	h=0.08
$k = 1$	85	122	145	160
$k = 2$	202	170	162	160
$k = 3$	162	167	166	166
$k = 4$	162	167	166	166

Table 1: Exact solution in (97): iterations needed to meet the stopping criterion (96) for different values of k, $\alpha = 3$, and $\beta = 10$. Standard fixed point iterative scheme (94).

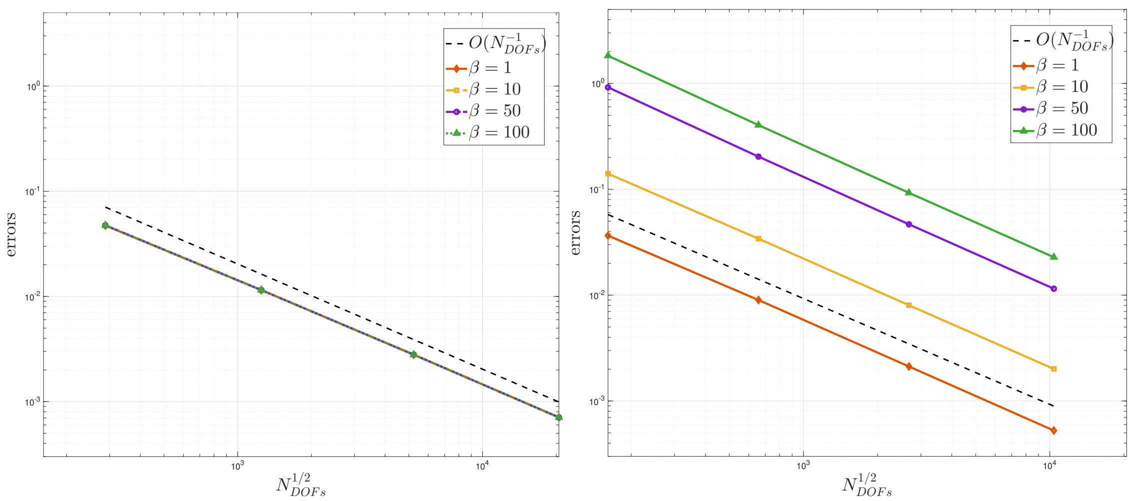

Figure 2: Exact solution in (97); h-convergence of the flux (*left-panel*) and the potential (*right-panel*) for β in $\{1, 10, 50, 100\}$, $k = 2$, and $\alpha = 3$. Standard fixed point iterative scheme (94).

	h=0.5	h=0.3	h=0.15	h=0.08
$\beta = 1$	23	22	22	21
$\beta = 10$	202	170	162	160
$\beta = 50$	913	753	770	745
$\beta = 100$	1604	1382	1464	1450

Table 2: Exact solution in (97): iterations needed to meet the stopping criterion (96) for different values of β, $k = 2$, and $\alpha = 3$. Standard fixed point iterative scheme (94).

Numerical results: varying the exponent α of the nonlinear term; $2 < \alpha < 3$; fixed point scheme. In Figure 3, we display the errors in (99) under mesh refinements for the iterative scheme (94). We consider α in $\{2.2, 2.4, 2.6, 2.8\}$, $k = 2$, and $\beta = 10$. In Table 3, we report the number of iterations needed to meet the stopping criterion (96). The number of iterations grows

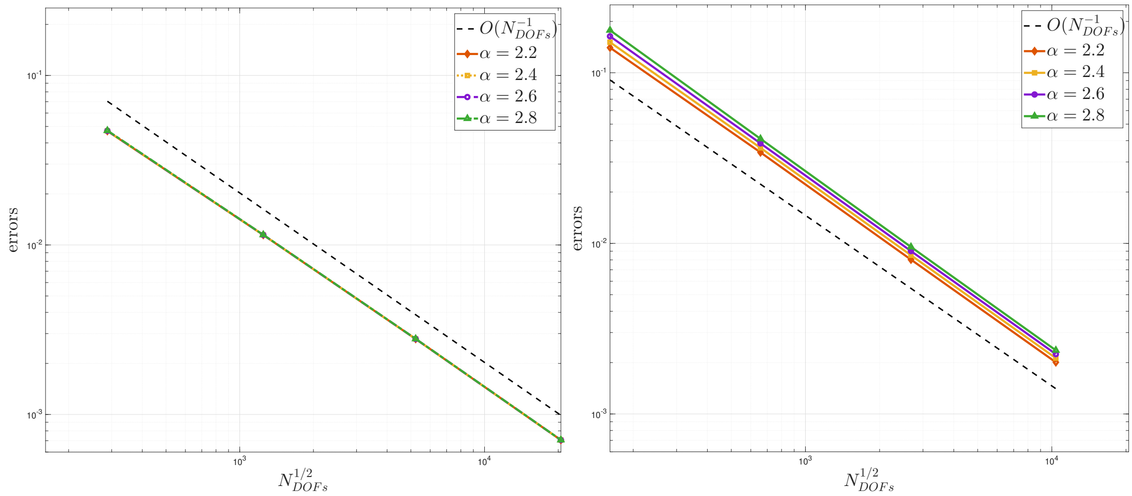

Figure 3: Exact solution in (97); h-convergence of the flux (*left-panel*) and the potential (*right-panel*) for α in $\{2.2, 2.4, 2.6, 2.8\}$, $k = 2$, and $\beta = 10$. Standard fixed point iterative scheme (94).

	h=0.5	h=0.3	h=0.15	h=0.08
$\alpha = 2.2$	11	11	11	11
$\alpha = 2.4$	17	18	18	19
$\alpha = 2.6$	28	28	28	28
$\alpha = 2.8$	52	52	52	51

Table 3: Exact solution in (97): iterations needed to meet the stopping criterion (96) for values of α smaller than 3, $k = 2$, and $\beta = 10$. Standard fixed point iterative scheme (94).

with α. Similar results were obtained using higher order methods.

For α larger than 3, the standard fixed point algorithm (94) fails to reach the prescribed tolerance within the prescribed maximum number of iterations; we do not report the results here for the sake of conciseness. Thus, in the next paragraphs, we employ the relaxed iterative scheme (95) for such values of α.

Numerical results: varying the exponent α of the nonlinear term; $2 < \alpha \leq 4$; relaxed scheme. In Figure 4, we display the errors in (99) under mesh refinements for the relaxed scheme (95). We consider α in $\{2.2, 2.4, 2.6, 2.8, 3.2, 3.4, 3.6, 3.8, 4\}$, $k = 2$, $\beta = 10$, and relaxation parameter $\omega = 0.5$. The corresponding number of iterations is reported in Table 4. The number of iterations remains essentially stable as α increases; for values of α smaller than 3, this was instead not the case for scheme (94); cf. Table 3. For values of α close to 2, the relaxed version requires more iterations.

Numerical results: varying the exponent α of the nonlinear term; $\alpha > 4$; relaxed scheme. In Figure 5, we display the errors in (99) under mesh refinements for the relaxed scheme (95). We consider α in $\{4.2, 4.4, 4.6, 4.8, 5, 5.1\}$, $k = 2$, $\beta = 10$, and relaxation parameter $\omega = 0.5$. The corresponding number of iterations is reported in Table 5. The number of iterations grows with α, differently from what was reported in Table 4; optimal convergence rates are observed. Convergence is not achieved for α larger than or equal to 5.2 within the prescribed maximum number of iterations.

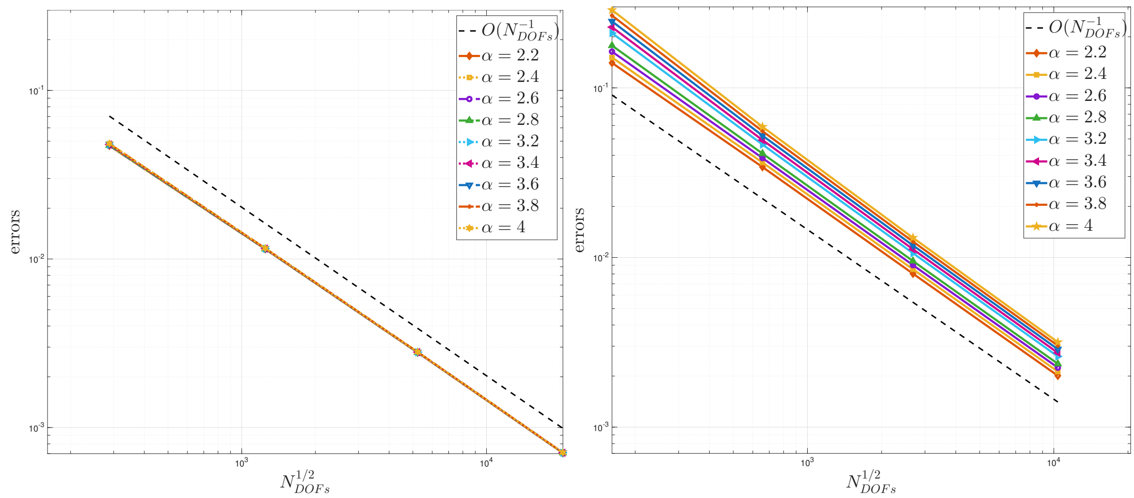

Figure 4: Exact solution in (97); h-convergence of the flux (*left-panel*) and the potential (*right-panel*) for α in $\{2.2, 2.4, 2.6, 2.8, 3.2, 3.4, 3.6, 3.8, 4\}$, $k = 2$, and $\beta = 10$. Relaxed fixed point iterative scheme (95) with $\omega = 0.5$.

	h=0.5	h=0.3	h=0.15	h=0.08
$\alpha = 2.2$	23	22	22	22
$\alpha = 2.4$	22	22	22	22
$\alpha = 2.6$	22	22	22	22
$\alpha = 2.8$	22	22	22	22
$\alpha = 3.2$	23	22	22	22
$\alpha = 3.4$	22	22	22	22
$\alpha = 3.6$	22	22	22	22
$\alpha = 3.8$	23	23	23	23
$\alpha = 4$	23	23	23	23

Table 4: Exact solution in (97): iterations needed to meet the stopping criterion (96) for values of α between 2 and 4, $k = 2$, and $\beta = 10$. Relaxed fixed point iterative scheme (95) with $\omega = 0.5$.

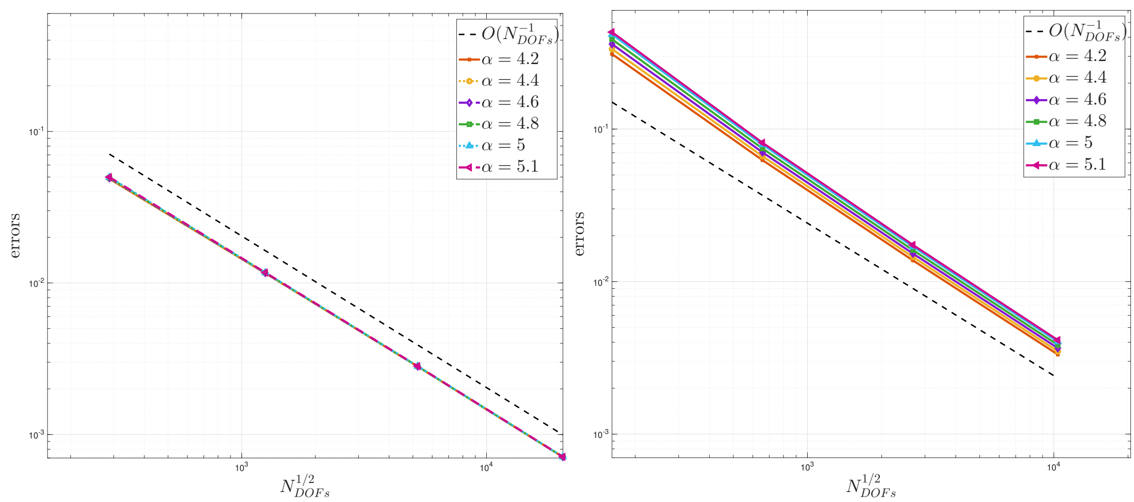

Figure 5: Exact solution in (97); h-convergence of the flux (*left-panel*) and the potential (*right-panel*) for α in $\{4.2, 4.4, 4.6, 4.8, 5, 5.1\}$, $k = 2$, and $\beta = 10$. Relaxed fixed point iterative scheme (95) with $\omega = 0.5$.

	h=0.5	h=0.3	h=0.15	h=0.08
$\alpha = 4.2$	25	25	25	25
$\alpha = 4.4$	33	33	33	33
$\alpha = 4.6$	50	45	47	47
$\alpha = 4.8$	85	73	77	77
$\alpha = 5$	224	172	187	186
$\alpha = 5.1$	934	715	774	2051

Table 5: Exact solution in (97): iterations needed to meet the stopping criterion (96) for values of α larger than 4, $k = 2$, and $\beta = 10$. Relaxed fixed point iterative scheme (95) with $\omega = 0.5$.

Numerical results: varying the relaxation parameter ω; $\alpha > 4$; relaxed scheme. As a first attempt to address the lack of convergence for large α observed in the previous paragraph, we consider different choices of the relaxation parameter ω. We consider ω in $\{0.1, 0.2, 0.3, 0.4, 0.5, 0.6, 0.8\}$, α in $\{4.6, 5.1, 6\}$, $k = 2$, and $\beta = 10$. In Table 6, we report the number of iterations under mesh refinements for the relaxed scheme (95). The results suggest that a careful choice of the relaxation

	h=0.5	h=0.3	h=0.15	h=0.08
$\omega = 0.1$	145	143	140	139
$\omega = 0.2$	69	68	67	67
$\omega = 0.3$	44	43	43	43
$\omega = 0.4$	31	31	31	32
$\omega = 0.5$	50	45	47	47
$\omega = 0.6$	$n_{\max}$	$n_{\max}$	$n_{\max}$	$n_{\max}$
$\omega = 0.8$	$n_{\max}$	$n_{\max}$	$n_{\max}$	$n_{\max}$

(a) $\alpha = 4.6$

	h=0.5	h=0.3	h=0.15	h=0.08
$\omega = 0.1$	148	146	142	141
$\omega = 0.2$	71	70	68	68
$\omega = 0.3$	45	44	44	44
$\omega = 0.4$	33	32	32	33
$\omega = 0.5$	$n_{\max}$	$n_{\max}$	$n_{\max}$	$n_{\max}$
$\omega = 0.6$	$n_{\max}$	$n_{\max}$	$n_{\max}$	$n_{\max}$
$\omega = 0.8$	$n_{\max}$	$n_{\max}$	$n_{\max}$	$n_{\max}$

(b) $\alpha = 5.1$

	h=0.5	h=0.3	h=0.15	h=0.08
$\omega = 0.1$	154	154	146	146
$\omega = 0.2$	73	73	70	70
$\omega = 0.3$	47	47	45	46
$\omega = 0.4$	274	227	245	243
$\omega = 0.5$	$n_{\max}$	$n_{\max}$	$n_{\max}$	$n_{\max}$
$\omega = 0.6$	$n_{\max}$	$n_{\max}$	$n_{\max}$	$n_{\max}$
$\omega = 0.8$	$n_{\max}$	$n_{\max}$	$n_{\max}$	$n_{\max}$

(c) $\alpha = 6$

Table 6: Exact solution in (97): iterations for different values of ω, $k = 2$, $\beta = 10$, and $\alpha = 4.6$ (*top-left panel*), $\alpha = 5.1$ (*top-right panel*), and $\alpha = 6$ (*bottom panel*). Relaxed fixed point iterative scheme (95). The entry $n_{\max}$ stands for "maximum number of iterations is reached".

parameter may affect the performance of the method, not only by possibly optimizing the number of iterations, but also by determining whether the method converges or not; the optimal value of ω may depend on the exponent of the nonlinear term α. More sophisticated iterative schemes should be used in order to avoid such a dependence and to cope with larger α.

Lack of consistency for higher order methods. In Figure 6, we display the errors in (99) under mesh refinements for the iterative scheme (94). We consider $k = 1, 2$, $\alpha = 3$, and $\beta = 10$. As detailed in Remark 4, the error estimates for the lowest order discretization of (41) are decoupled whence the error of the fluxes is zero up to machine precision. This is instead not the case for higher polynomial degrees; cf. also Proposition 6.1.

8 Conclusions

In this work, we presented and analyzed a general-order dual mixed nonconforming discretization for a generalized Darcy–Forchheimer problem. Our approach extends the framework in [23], along

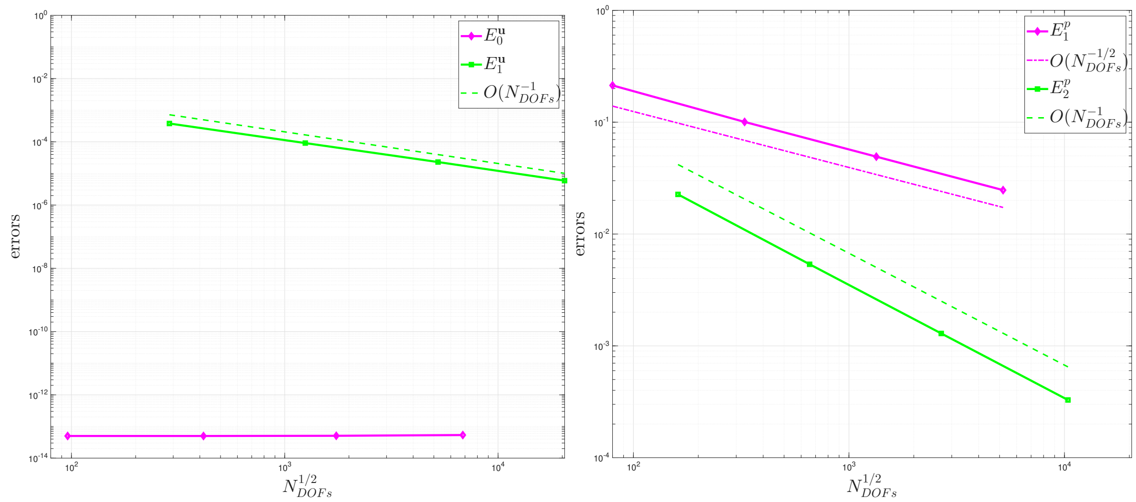

Figure 6: Exact solution u_2 in (98); h-convergence of the flux (*left-panel*) and the potential (*right-panel*) for $k = 1, 2$, $\alpha = 3$, and $\beta = 10$. Standard fixed point iterative scheme (94).

different directions:

- (α-2)-type Forchheimer nonlinearities are allowed, moving beyond the standard quadratic model;
- the proposed method accommodates mixed, inhomogeneous boundary conditions, and permits permeability tensors with lower Lebesgue regularity;
- we developed general-order schemes based on piecewise-polynomial spaces of order $k-1$ for the fluxes paired with Crouzeix-Raviart elements of order k for the potentials;
- based on novel Sobolev-trace inequalities for broken spaces with constants independent of the polynomial degree, we established convergence to the exact solution under low-regularity assumptions;
- we further derived general-order error estimates assuming additional regularity of the exact solution and data.

The theoretical findings were supported by numerical experiments that assessed the performance of two iterative schemes for different nonlinearity parameters α, orders k, and parameters of the model. While a standard fixed point scheme does not converge for large nonlinearity parameters α, a relaxed version may reach convergence by suitably tuning the relaxation parameter.

The framework introduced in this work lays the essential mathematical groundwork for our future objective: the prospective development of *hp*-adaptive strategies to efficiently discretize complex generalized Darcy–Forchheimer models.

Acknowledgments. MB and LM have been partially funded by the European Union (ERC, NEMESIS, project number 101115663); views and opinions expressed are however those of the authors only and do not necessarily reflect those of the EU or the ERC Executive Agency. MB and LM have been partially supported by the INdAM-GNCS project CUP E53C25002010001. The authors are members of the Gruppo Nazionale Calcolo Scientifico-Istituto Nazionale di Alta Matematica (GNCS-INdAM).

References

[1] M. Ainsworth and R. Rankin. Fully computable bounds for the error in nonconforming finite element approximations of arbitrary order on triangular elements. *SIAM J. Numer. Anal.*, 46(6):3207–3232, 2008.

[2] J. A. Almonacid, H. S. Díaz, G. N. Gatica, and A. Márquez. A fully mixed finite element method for the coupling of the Stokes and Darcy-Forchheimer problems. *IMA J. Numer. Anal.*, 40(2):1454–1502, 2020.

[3] D. Amigo, F. Lepe, E. Otárola, and G. Rivera. A virtual element method for a convective Brinkman-Forchheimer problem coupled with a heat equation. *Comput. Math. Appl.*, 191:1–23, 2025.

[4] S. Badia, C. Carstensen, A. F. Martin, R. Ruiz-Baier, and S. Villa-Fuentes. A velocity-vorticity-pressure formulation for the steady Navier-Stokes-Brinkman-Forchheimer problem. *Comput. Methods Appl. Mech. Engrg.*, 447:Paper No. 118343, 27, 2025.

[5] A. Kh. Balci, Ch. Ortner, and J. Storn. Crouzeix-Raviart finite element method for non-autonomous variational problems with Lavrentiev gap. *Numer. Math.*, 151(4):779–805, 2022.

[6] Á. Baran and G. Stoyan. Gauss-Legendre elements: a stable, higher order non-conforming finite element family. *Computing*, 79(1):1–21, 2007.

[7] J. W. Barrett and W. B. Liu. Finite element approximation of the p-Laplacian. *Math. Comp.*, 61(204):523–537, 1993.

[8] V. Berinde. *Iterative Approximation of Fixed Points*, volume 1912 of *Lecture Notes in Mathematics*. Springer, Berlin, second edition, 2007.

[9] S. Bonetti, M. Botti, and P. F. Antonietti. Conforming and discontinuous discretizations of non-isothermal Darcy-Forchheimer flows. `http://arxiv.org/abs/2508.21630`, 2025.

[10] M. Botti and L. Mascotto. Trace inequalities for piecewise $W^{1,p}$ functions over general polytopic meshes. `http://arxiv.org/abs/2512.09752`, 2025.

[11] M. Botti and L. Mascotto. Sobolev-Poincaré inequalities for piecewise $W^{1,p}$ functions over general polytopic meshes. *Accepted on SIAM J. Numer. Anal.*, 2026.

[12] S. C. Brenner and L. R. Scott. *The Mathematical Theory of Finite Element Methods*, volume 15 of *Texts in Applied Mathematics*. Springer, New York, third edition, 2008.

[13] A. Bressan, L. Mascotto, and M. Mosconi. New Crouzeix-Raviart elements of even degree: theoretical aspects, numerical performance, and applications to the Stokes' equations. *IMA J. Numer. Anal*, 2026. `https://doi.org/10.1093/imanum/draf091`.

[14] E. Burman and P. Hansbo. Stabilized Crouzeix-Raviart element for the Darcy-Stokes problem. *Numer. Methods Partial Differential Equations*, 21(5):986–997, 2005.

[15] C. Carstensen and S. A. Sauter. Critical functions and inf-sup stability of Crouzeix-Raviart elements. *Comput. Math. Appl.*, 108:12–23, 2022.

[16] S. Caucao, G. N. Gatica, and L. F. Gatica. A Banach spaces-based mixed finite element method for the stationary convective Brinkman-Forchheimer problem. *Calcolo*, 60(4):Paper No. 51, 32, 2023.

[17] S. Caucao, G. N. Gatica, and F. Sandoval. A fully-mixed finite element method for the coupling of the Navier-Stokes and Darcy-Forchheimer equations. *Numer. Methods Partial Differential Equations*, 37(3):2550–2587, 2021.

[18] M. Crouzeix and P.-A. Raviart. Conforming and nonconforming finite element methods for solving the stationary Stokes equations. I. *Rev. Fran¸ Automat. Informat. Rech. Opér. Sér. Rouge*, 7:33–75, 1973.

[19] J. Douglas, Jr., P. J. Paes-Leme, and T. Giorgi. Generalized Forchheimer flow in porous media. In *Boundary value problems for partial differential equations and applications*, volume 29 of *RMA Res. Notes Appl. Math.*, pages 99–111. Masson, Paris, 1993.

[20] A. Ern and J.-L. Guermond. *Finite Elements I: Approximation and Interpolation*, volume 72. Springer Nature, 2021.

[21] P. H. Forchheimer. Wasserbewegung durch Boden. *Z. Ver. Deutsch. Ing.*, 45:1782–1788, 1901.

[22] M. Fortin and M. Soulie. A nonconforming piecewise quadratic finite element on triangles. *Internat. J. Numer. Methods Engrg.*, 19(4):505–520, 1983.

[23] V. Girault and M. F. Wheeler. Numerical discretization of a Darcy-Forchheimer model. *Numer. Math.*, 110(2):161–198, 2008.

[24] M.-Y. Kim and E.-J. Park. Fully discrete mixed finite element approximations for non-Darcy flows in porous media. *Comput. Math. Appl.*, 38(11-12):113–129, 1999.

[25] H. López, B. Molina, and J. J. Salas. Comparison between different numerical discretizations for a Darcy-Forchheimer model. *Electron. Trans. Numer. Anal.*, 34:187–203, 2008/09.

[26] E.-J. Park. Mixed finite element methods for generalized Forchheimer flow in porous media. *Numer. Methods Partial Differential Equations*, 21(2):213–228, 2005.

[27] P.-A. Raviart and J. M. Thomas. Primal hybrid finite element methods for 2nd order elliptic equations. *Math. Comp.*, 31(138):391–413, 1977.

[28] H. Rui and H. Pan. A block-centered finite difference method for the Darcy-Forchheimer model. *SIAM J. Numer. Anal.*, 50(5):2612–2631, 2012.

[29] H. Rui and H. Pan. A block-centered finite difference method for slightly compressible Darcy-Forchheimer flow in porous media. *J. Sci. Comput.*, 73(1):70–92, 2017.

[30] J. J. Salas, H. López, and B. Molina. An analysis of a mixed finite element method for a Darcy-Forchheimer model. *Math. Comput. Modelling*, 57(9-10):2325–2338, 2013.

[31] T. Sayah, G. Semaan, and F. Triki. Finite element methods for the Darcy-Forchheimer problem coupled with the convection-diffusion-reaction problem. *ESAIM Math. Model. Numer. Anal.*, 55(6):2643–2678, 2021.

[32] R. E. Showalter. *Monotone Operators in Banach Space and Nonlinear Partial Differential Equations*, volume 49 of *Mathematical Surveys and Monographs*. American Mathematical Society, Providence, RI, 1997.

[33] G. Stoyan and Á. Baran. Crouzeix-Velte decompositions for higher-order finite elements. *Comput. Math. Appl.*, 51(6-7):967–986, 2006.

[34] F. Triki, T. Sayah, and G. Semaan. A posteriori error estimates for Darcy-Forchheimer's problem coupled with the convection-diffusion-reaction equation. *Int. J. Numer. Anal. Model.*, 21(1):65–103, 2024.

[35] Y. Wang and H. Rui. Stabilized Crouzeix-Raviart element for Darcy-Forchheimer model. *Numer. Methods Partial Differential Equations*, 31(5):1568–1588, 2015.

[36] J. Zhang and H. Rui. A stabilized Crouzeix-Raviart element method for coupling Stokes and Darcy-Forchheimer flows. *Numer. Methods Partial Differential Equations*, 33(4):1070–1094, 2017.

[37] L. Zhao, E. T. Chung, E.-J. Park, and G. Zhou. Staggered DG method for coupling of the Stokes and Darcy-Forchheimer problems. *SIAM J. Numer. Anal.*, 59(1):1–31, 2021.

A Properties of the nonlinear operator

This section is devoted with showing three properties of $\boldsymbol{\mathcal{A}}(\cdot)$:

1. monotonicity, in Section A.1;
2. coercivity, in Section A.2;
3. hemi-continuity, in Section A.3.

A.1 Monotonicity

Here, we show that $\boldsymbol{\mathcal{A}}(\cdot)$ is monotone.

Proposition A.1. *Let $\mathbf{y}$ be in $\boldsymbol{\mathcal{V}}$. Then, recalling that λ_{min} is the smallest eigenvalue of $\underline{\mathbf{K}}^{-1}$, the following estimate holds true:*

$$\frac{\mu}{\rho}\lambda_{min}\|\mathbf{w}-\mathbf{v}\|_{\mathbf{L}^2(\Omega)} \leq \int_\Omega (\boldsymbol{\mathcal{A}}(\mathbf{w}+\mathbf{y}) - \boldsymbol{\mathcal{A}}(\mathbf{v}+\mathbf{y}))\cdot(\mathbf{w}-\mathbf{v})\,\mathrm{d}\mathbf{x} \qquad \forall\, \mathbf{w},\mathbf{v}\in\boldsymbol{\mathcal{V}}.$$

Proof. We define $\mathcal{J}:\mathbf{L}^\alpha(\Omega)\to\mathbb{R}$ as

$$\mathcal{J}(\mathbf{v}) := \frac{1}{2}\frac{\mu}{\rho}\int_\Omega(\underline{\mathbf{K}}^{-1})\mathbf{v}\cdot\mathbf{v}\,\mathrm{d}\mathbf{x} + \frac{1}{\alpha}\frac{\beta}{\rho}\int_\Omega|\mathbf{v}|^\alpha\,\mathrm{d}\mathbf{x} \qquad \forall\,\mathbf{v}\in\mathbf{L}^\alpha(\Omega).$$

The first Gateaux derivative $\mathcal{J}'(\mathbf{v}):\mathbf{L}^\alpha(\Omega)\to\mathbf{L}^{\alpha'}(\Omega)$ reads

$$\langle\mathcal{J}'(\mathbf{v}),\mathbf{w}\rangle = \frac{\mu}{\rho}\int_\Omega(\underline{\mathbf{K}}^{-1})\mathbf{v}\cdot\mathbf{w}\,\mathrm{d}\mathbf{x} + \frac{\beta}{\rho}\int_\Omega|\mathbf{v}|^{\alpha-2}\mathbf{v}\cdot\mathbf{w}\,\mathrm{d}\mathbf{x} \qquad \forall\,\mathbf{v},\,\mathbf{w}\in\mathbf{L}^\alpha(\Omega). \tag{100}$$

The second Gateaux derivative $\mathcal{J}''(\mathbf{v})\mathbf{w}:\mathbf{L}^\alpha(\Omega)\to\mathbf{L}^{\alpha'}(\Omega)$ reads

$$\begin{aligned}\langle\mathcal{J}''(\mathbf{v})\mathbf{z},\mathbf{w}\rangle &= \frac{\mu}{\rho}\int_\Omega(\underline{\mathbf{K}}^{-1})\mathbf{z}\cdot\mathbf{w}\,\mathrm{d}\mathbf{x}\\ &\quad+\frac{\beta}{\rho}\int_\Omega(\alpha-2)|\mathbf{v}|^{\alpha-4}(\mathbf{v}\cdot\mathbf{z})(\mathbf{v}\cdot\mathbf{w}) + |\mathbf{v}|^{\alpha-2}\mathbf{z}\cdot\mathbf{w}\,\mathrm{d}\mathbf{x}\quad\forall\,\mathbf{v}\neq\mathbf{0},\mathbf{w},\mathbf{z}\in\mathbf{L}^\alpha(\Omega).\end{aligned} \tag{101}$$

with

$$\langle\mathcal{J}''(\mathbf{0})\mathbf{w},\mathbf{z}\rangle = \frac{\mu}{\rho}\int_\Omega(\underline{\mathbf{K}}^{-1})\mathbf{z}\cdot\mathbf{w}\,\mathrm{d}\mathbf{x} \qquad \forall\,\mathbf{w},\mathbf{z}\in\mathbf{L}^\alpha(\Omega).$$

Let $\mathbf{y}$ be fixed in $\mathbf{L}^\alpha(\Omega)$, and $\mathbf{v}$ and $\mathbf{w}$ be in $\mathbf{L}^\alpha(\Omega)$. Define $\widetilde{\mathbf{v}}:=\mathbf{v}+\mathbf{y}$ and $\widetilde{\mathbf{w}}:=\mathbf{w}+\mathbf{y}$; $\widetilde{\mathbf{w}}-\widetilde{\mathbf{v}}$ coincides with $\mathbf{w}-\mathbf{v}$. Hence, we use the fundamental theorem of calculus and get

$$\begin{aligned}\int_\Omega(\boldsymbol{\mathcal{A}}(\widetilde{\mathbf{w}})-\boldsymbol{\mathcal{A}}(\widetilde{\mathbf{v}}))\cdot(\mathbf{w}-\mathbf{v})\,\mathrm{d}\mathbf{x} &= \int_\Omega(\boldsymbol{\mathcal{A}}(\widetilde{\mathbf{w}})-\boldsymbol{\mathcal{A}}(\widetilde{\mathbf{v}})\cdot(\widetilde{\mathbf{w}}-\widetilde{\mathbf{v}}))\,\mathrm{d}\mathbf{x}\\ &\overset{(17),(100)}{=}\langle\mathcal{J}'(\widetilde{\mathbf{w}})-\mathcal{J}'(\widetilde{\mathbf{v}}),\widetilde{\mathbf{w}}-\widetilde{\mathbf{v}}\rangle = \int_0^1\langle\mathcal{J}''(\widetilde{\mathbf{v}}+\theta(\widetilde{\mathbf{w}}-\widetilde{\mathbf{v}}))(\widetilde{\mathbf{w}}-\widetilde{\mathbf{v}}),\widetilde{\mathbf{w}}-\widetilde{\mathbf{v}}\rangle\,\mathrm{d}\theta.\end{aligned}$$

The integral on the right-hand side is well-defined for all $\alpha > 2$ since

$$|\mathbf{v}|^{\alpha-4}(\mathbf{v}\cdot\mathbf{z})(\mathbf{v}\cdot\mathbf{w}) \leq |\mathbf{v}|^{\alpha-2}|\mathbf{z}||\mathbf{w}|.$$

For all $\mathbf{v}$ and $\mathbf{w}$ in $\mathbf{L}^\alpha(\Omega)$

$$\langle \mathcal{J}''(\mathbf{v})\mathbf{w},\mathbf{w}\rangle = \frac{\mu}{\rho}\int_\Omega (\underline{\mathbf{K}}^{-1}\mathbf{w})\cdot\mathbf{w}\,\mathrm{d}\mathbf{x} + \frac{\beta}{\rho}\int_\Omega (\alpha-2)|\mathbf{v}|^{\alpha-4}|\mathbf{v}\cdot\mathbf{w}|^2 + |\mathbf{v}|^{\alpha-2}|\mathbf{w}|\,\mathrm{d}\mathbf{x} \geq \frac{\mu}{\rho}\lambda_{\min}\|\mathbf{w}\|^2_{\mathrm{L}^2(\Omega)}.$$

In particular, we deduce

$$\int_\Omega (\boldsymbol{\mathcal{A}}(\widetilde{\mathbf{w}}) - \boldsymbol{\mathcal{A}}(\widetilde{\mathbf{v}}))\cdot(\mathbf{w}-\mathbf{v})\,\mathrm{d}\mathbf{x} \geq \frac{\mu}{\rho}\lambda_{\min}\|\widetilde{\mathbf{w}}-\widetilde{\mathbf{v}}\|_{\mathrm{L}^2(\Omega)} = \frac{\mu}{\rho}\lambda_{\min}\|\mathbf{w}-\mathbf{v}\|_{\mathrm{L}^2(\Omega)}.$$

□

A.2 Coercivity

Here, we show that $\boldsymbol{\mathcal{A}}(\cdot)$ is coercive.

Proposition A.2. *Let* $\mathbf{y}$ *be in* $\boldsymbol{\mathcal{V}}$*. We have*

$$\lim_{\|\mathbf{v}\|_{\mathbf{L}^\alpha(\Omega)}\to+\infty}\Big(\frac{1}{\|\mathbf{v}\|_{\mathbf{L}^\alpha(\Omega)}}\int_\Omega \boldsymbol{\mathcal{A}}(\mathbf{v}+\mathbf{y})\cdot\mathbf{v}\Big) = +\infty.$$

Proof. Let $\mathbf{v}$ and $\mathbf{w}$ be in $\boldsymbol{\mathcal{V}}$; define $\widetilde{\mathbf{v}} := \mathbf{v}+\mathbf{y}$. The definition of $\widetilde{\mathbf{v}}$ yields

$$\int_\Omega \boldsymbol{\mathcal{A}}(\widetilde{\mathbf{v}})\cdot\mathbf{v}\,\mathrm{d}\mathbf{x} = \int_\Omega \boldsymbol{\mathcal{A}}(\widetilde{\mathbf{v}})\cdot\widetilde{\mathbf{v}}\,\mathrm{d}\mathbf{x} - \int_\Omega \boldsymbol{\mathcal{A}}(\widetilde{\mathbf{v}})\cdot\mathbf{y}\,\mathrm{d}\mathbf{x} \overset{(17),(100)}{=} \langle\mathcal{J}'(\widetilde{\mathbf{v}}),\widetilde{\mathbf{v}}\rangle - \int_\Omega \boldsymbol{\mathcal{A}}(\widetilde{\mathbf{v}})\cdot\mathbf{y}\,\mathrm{d}\mathbf{x}. \quad (102)$$

We manipulate the two terms on the right-hand side separately. As for the former, we have

$$\langle\mathcal{J}'(\widetilde{\mathbf{v}}),\widetilde{\mathbf{v}}\rangle = \frac{\mu}{\rho}\int_\Omega(\underline{\mathbf{K}}^{-1}\widetilde{\mathbf{v}})\cdot\widetilde{\mathbf{v}}\,\mathrm{d}\mathbf{x} + \frac{\beta}{\rho}\int_\Omega|\widetilde{\mathbf{v}}|^{\alpha+2}\,\mathrm{d}\mathbf{x} \geq \frac{\mu}{\rho}\lambda_{\min}\|\widetilde{\mathbf{v}}\|^2_{\mathbf{L}^2(\Omega)} + \frac{\beta}{\rho}\|\widetilde{\mathbf{v}}\|^\alpha_{\mathbf{L}^\alpha(\Omega)}. \quad (103)$$

As for the latter, Hölder's inequality twice entails

$$\int_\Omega \boldsymbol{\mathcal{A}}(\widetilde{\mathbf{v}})\cdot\mathbf{y}\,\mathrm{d}\mathbf{x} \leq \frac{\mu}{\rho}\|\underline{\mathbf{K}}^{-1}\|_{\underline{\mathbf{L}}^{\frac{\alpha}{\alpha-2}}(\Omega)}\|\widetilde{\mathbf{v}}\|_{\mathrm{L}^\alpha(\Omega)}\|\mathbf{y}\|_{\mathrm{L}^\alpha(\Omega)} + \frac{\beta}{\rho}\|\widetilde{\mathbf{v}}\|^{\alpha-1}_{\mathbf{L}^\alpha(\Omega)}\|\mathbf{y}\|_{\mathbf{L}^\alpha(\Omega)}. \quad (104)$$

Inserting (103) and (104) in (102) we have

$$\begin{aligned}\int_\Omega \boldsymbol{\mathcal{A}}(\widetilde{\mathbf{v}})\cdot\mathbf{y}\,\mathrm{d}\mathbf{x} &\geq \frac{\mu}{\rho}\lambda_{\min}\|\widetilde{\mathbf{v}}\|^2_{\mathbf{L}^2(\Omega)} \\ &\quad + \frac{\beta}{\rho}\|\widetilde{\mathbf{v}}\|^{\alpha-1}_{\mathbf{L}^\alpha(\Omega)}\Big(\|\widetilde{\mathbf{v}}\|_{\mathbf{L}^\alpha(\Omega)} - \|\mathbf{y}\|_{\mathbf{L}^\alpha(\Omega)} - \frac{\mu}{\beta}\|\underline{\mathbf{K}}^{-1}\|_{\underline{\mathbf{L}}^{\frac{\alpha}{\alpha-2}}(\Omega)}\frac{\|\mathbf{y}\|_{\mathbf{L}^\alpha(\Omega)}}{\|\widetilde{\mathbf{v}}\|^{\alpha-2}_{\mathbf{L}^\alpha(\Omega)}}\Big) \\ &\geq \frac{\beta}{\rho}\|\widetilde{\mathbf{v}}\|^{\alpha-1}_{\mathbf{L}^\alpha(\Omega)}\Big(\|\widetilde{\mathbf{v}}\|_{\mathbf{L}^\alpha(\Omega)} - \|\mathbf{y}\|_{\mathbf{L}^\alpha(\Omega)} - \frac{\mu}{\beta}\|\underline{\mathbf{K}}^{-1}\|_{\underline{\mathbf{L}}^{\frac{\alpha}{\alpha-2}}(\Omega)}\frac{\|\mathbf{y}\|_{\mathbf{L}^\alpha(\Omega)}}{\|\widetilde{\mathbf{v}}\|^{\alpha-2}_{\mathbf{L}^\alpha(\Omega)}}\Big).\end{aligned} \quad (105)$$

Since $\frac{\|\widetilde{\mathbf{v}}\|_{\mathbf{L}^\alpha(\Omega)}}{\|\mathbf{v}\|_{\mathbf{L}^\alpha(\Omega)}} \to 1$ when $\|\mathbf{v}\|_{\mathbf{L}^\alpha(\Omega)} \to \infty$, we have, for $\|\widetilde{\mathbf{v}}\|^{\alpha-2}_{\mathbf{L}^\alpha(\Omega)}$ sufficiently large,

$$\frac{1}{\|\mathbf{v}\|_{\mathbf{L}^\alpha(\Omega)}}\int_\Omega \boldsymbol{\mathcal{A}}(\widetilde{\mathbf{v}})\cdot\mathbf{v}\,\mathrm{d}\mathbf{x} \gtrsim \frac{\beta}{\rho}\|\widetilde{\mathbf{v}}\|^{\alpha-2}_{\mathbf{L}^\alpha(\Omega)}\Big(\|\widetilde{\mathbf{v}}\|_{\mathbf{L}^\alpha(\Omega)} - \|\mathbf{y}\|_{\mathbf{L}^\alpha(\Omega)}\Big(1 - \frac{\mu}{\rho}\frac{\|\underline{\mathbf{K}}^{-1}\|_{\underline{\mathbf{L}}^{\frac{\alpha}{\alpha-2}}}}{\|\widetilde{\mathbf{v}}\|^{\alpha-2}_{\mathbf{L}^\alpha(\Omega)}}\Big)\Big) \gtrsim \|\widetilde{\mathbf{v}}\|^{\alpha-2}_{\mathbf{L}^\alpha(\Omega)}.$$

□

A.3 Hemi-continuity

Here, we show that the mapping $\boldsymbol{\mathcal{A}}(\cdot)$ is hemi-continuous.

Proposition A.3. *Given* $\mathbf{y}$*,* $\mathbf{v}$*, and* $\mathbf{w}$ *in* $\boldsymbol{\mathcal{V}}$*, the mapping*

$$t \to \int_\Omega \boldsymbol{\mathcal{A}}(\mathbf{y} + \mathbf{v} + t\,\mathbf{w}) \cdot \mathbf{w}\,\mathrm{d}\mathbf{x}$$

is continuous from $\mathbb{R}$ *into* $\mathbb{R}$*.*

Proof. Given $\mathbf{y}$, $\mathbf{v}$, and $\mathbf{w}$ in $\mathbf{L}^\alpha(\Omega)$, and defining $\widetilde{\mathbf{v}} := \mathbf{v} + \mathbf{y}$, for all t and t_0 in $\mathbb{R}$, the fundamental theorem of calculus gives

$$\begin{aligned}\int_\Omega (\boldsymbol{\mathcal{A}}(\widetilde{\mathbf{v}} + t_0\mathbf{v}) - \boldsymbol{\mathcal{A}}(\widetilde{\mathbf{v}} + t\mathbf{v})) \cdot \mathbf{v}\,\mathrm{d}\mathbf{x} &\overset{(17),(100)}{=} \langle \mathcal{J}'(\widetilde{\mathbf{v}} + t_0\mathbf{v}) - \mathcal{J}'(\widetilde{\mathbf{v}} + t\mathbf{v}), \mathbf{v}\rangle \\ &= -(t - t_0) \int_0^1 \langle \mathcal{J}''(\widetilde{\mathbf{v}} - t\mathbf{v} - \theta(t - t_0)\mathbf{v})\mathbf{v}, \mathbf{v}\rangle\,\mathrm{d}\theta.\end{aligned}$$

Hölder's inequality in (101), the fact that $\widetilde{\mathbf{v}} - t\mathbf{v} - \theta(t - t_0)\mathbf{v}$ belongs to $\mathbf{L}^\alpha(\Omega)$, and the fact that $\mathcal{J}''(\mathbf{v})\mathbf{w} : \mathbf{L}^\alpha(\Omega) \to \mathbf{L}^{\alpha'}(\Omega)$ yield that the right-hand side of the above display tends to zero as t goes to t_0. The assertion follows. □

MOX Technical Reports, last issues

Dipartimento di Matematica
Politecnico di Milano, Via Bonardi 9 - 20133 Milano (Italy)

35/2026 Caon, B.; Corti, M.; Bonizzoni, F.; Antonietti, P.F.
High-fidelity and Network-based Spatio-temporal Mathematical Models of Alzheimer's Disease Progression and their Validation Against PET-SUVR Imaging Data

34/2026 Mancinelli, F. M.; Torzoni, M.; Maisto, D.; Donnarumma, F.; Corigliano, A.; Pezzulo, G.; Manzoni, A.
Multi-Agent Digital Twins for strategic decision-making using Active Inference

33/2026 Franzoni, G.; Mirabella, S.; Dabek, A.; Ferro, N.; Antona, A.; Carlessi, M.; Cinquemani, S.; Matteucci, M.; Cocetta, G.; Perotto, S.
Integrating Environmental Control and Hyperspectral Imaging to Assess Light and Nutrient Effects on Lettuce Post-Harvest Quality in Vertical Farming

Franzoni, G.; Mirabella, S.; Dabek, A.; Ferro, N.; Antona, A.; Carlessi, M.; Cinquemani, S.; Matteucci, M.; Cocetta, G.; Perotto, S.
ntegrating Environmental Control and Hyperspectral Imaging to Assess Light and Nutrient Effects on Lettuce Post-Harvest Quality in Vertical Farming

32/2026 Antonietti, P.F.; Bonizzoni, F.; Perugia, I.; Verani, M.
A Multilevel Monte Carlo Virtual Element Method for Uncertainty Quantification of Elliptic Partial Differential Equations

31/2026 Guastamacchia, C.; Piersanti, R; Giardini, F.; Coppini, R.; Ferrantini C.; Dede' L.; Sacconi L.; Regazzoni F.
The functional impact of myofiber macroscopic organization and disarray in computational models of the murine heart

30/2026 Regazzoni, F.
The internal law of a material can be discovered from its boundary

28/2026 Daniele, F.; Leimer Saglio, C. B.; Pagani, S.; Antonietti, P. F.
Mathematical and numerical modeling of coupled oxygen dynamics and neuronal electrophysiology

27/2026 Antonietti, P. F.; Abdalla, O. M. O.; Garroni, M. G.; Mazzieri, I.; Parolini, N.
A hybrid reduced-order and high-fidelity discontinuous Galerkin Spectral Element framework for large-scale PMUT array simulations

23/2026 Ballini, E.; Muscarnera, L.; Fumagalli, A.; Scotti, A.; Regazzoni, F.
Elimination-compensation pruning for fully-connected neural networks